METABOLIC ENGINEERING OF *BACILLUS* FOR ENHANCED PRODUCT AND CELLULAR YIELDS

by

Zhiwei Pan

B.E. in Fermentation Engineering, Wuxi University of Light Industry, 1995

M.S. in Biochemical Engineering, East China University of Science & Technology, 2000

Submitted to the Graduate Faculty of

the School of Engineering in partial fulfillment

of the requirements for the degree of

Doctor of Philosophy

University of Pittsburgh

2007

UNIVERSITY OF PITTSBURGH

SCHOOL OF ENGINEERING

This dissertation was presented

by

Zhiwei Pan

It was defended on

May 29, 2007

and approved by

Michael M. Domach, Professor, Chemical Engineering Department, CMU

Richard Koepsel, Associate Professor, Chemical and Petroleum Engineering Department

Götz Veser, Assistant professor, Chemical and Petroleum Engineering Department

Dissertation Director: Mohammad Ataai, Professor, Chemical and Petroleum Engineering

Department

METABOLIC ENGINEERING OF *BACILLUS* FOR ENHANCED PRODUCT AND CELLULAR YIELDS

Zhiwei Pan, PhD

University of Pittsburgh, 2007

Microbial cultures usually produce a significant amount of acidic byproducts which can repress cell growth and product synthesis. In addition, the production of acids is a waste of carbon source thereby reducing the product yield and productivity.

Metabolic engineering provides a powerful approach to optimize the cellular activities and improve product yields by genetically manipulating specific metabolic pathways. Previous work has identified mutation of pyruvate kinase (PYK) as an efficient way to reduce acid production; however, complete abolishment of PYK in *Bacillus subtilis* resulted in dramatically reduced cell growth rate. In this study, an inducible PYK (iPYK) mutant of *B. subtilis* was constructed and extensively characterized. The results demonstrate that good cell growth rate and low acetate formation can be attained at an appropriate PYK expression level. In addition, mutation of phosphofructokinase (PFK) in the glycolysis pathway also provides an alternative approach to reduce acetate formation.

Two outcomes of the *pyk* mutant of *B. subtilis*, high phosphoenolpyruvate (PEP) pool and low acetate concentration, prompted us to investigate the employment of the *pyk* mutation as an efficient way to improve folic acid and recombinant protein production. The high intracellular PEP and glucose-6-phosphate (G6P) concentrations in the *pyk* mutant led to higher folic acid production by providing abundant synthetic precursors. Additional mutations in the folic acid synthesis pathway, along with the *pyk* mutation, resulted in an 8-fold increase in folic acid

production. Recombinant protein was improved two-fold by the *pyk* mutation due to low acetate formation and longer production time in the *pyk* mutant. In addition, using glycerol instead of glucose as the carbon source reduced acetate production and improved protein production by 60%.

The effect of citrate on acetate production in *Bacillus thuringiensis* (*Bt*) cultures was investigated and the continuous culture results show that citrate is very effective at reducing acetate formation. These results indicate that *pyk* may be a potential mutation target for reducing acetate formation in *Bt*.

DESCRIPTORS

Acetate	*Bacillus subtilis*
Bacillus thuringiensis	Byproduct
Folic Acid	Glucose-6-phosphate
Glycolysis	Metabolic Engineering
Phosphoenolpyruvate	Phosphofructokinase
Pyruvate Kinase	Recombinant Protein

TABLE OF CONTENTS

LIST OF TABLES

LIST OF FIGURES

NOMENCLATURE

Abbreviations

3PG	3-phosphoglycerate
aa	amino acids
AcCoA	acetyl-CoA
CIT	citrate
E4P	erythrose-4-phosphate
F6P	fructose-6-phosphate
G6P	glucose-6-phosphate
GABA	4-aminobutanote
GAP	glyceraldehyde-3-phosphate
ISOCIT	isoCitrate
KG	α-ketoglutarate
na	nucleic acids
OAA	oxaloacetate
PEP	phosphoenolpyruvate
PFK	phosphofructokinase
PYK	pyruvate kinase
R5P	ribose-5-phosphate
Succ	succinate

ACKNOWLEDGEMENTS

1.0   INTRODUCTION

Microbes have been used for the production of a variety of products including proteins and chemicals that are impossible or difficult to make by chemical synthesis because of the complexity of their structure. The rising energy costs and the favorable consideration of sustainable development have paved the way for the biological manufacturing route which employs an environmentally benign process and utilizes renewable raw materials. However, biosynthetic processes are often economically uncompetitive due to their low product concentrations in the living organisms. To make biosynthetic processes more competitive, the production levels of target products in microorganisms need to be significantly improved. Traditional strain improvement efforts have focused on random mutagenesis and screening (Beppu, 2000). Recent advances in gene sequencing and genetic engineering have allowed us to modify specific biochemical reactions in microorganisms to dramatically improve product yields. One of the most powerful technologies for strain improvement is metabolic engineering (Bailey, 1991).

Metabolic engineering is directed improvement of product formation or cellular properties through the modification of specific biochemical reactions or introduction of new ones to host strains using recombinant DNA technology (Stephanopoulos, 1999). The metabolic engineering process typically involves identifying the target reaction(s) based on careful analysis of cellular function, designing and genetically modifying the corresponding gene(s) using

established molecular biological techniques, followed by comprehensive evaluation and analysis of the genetically modified strains (Nielsen, 2001). Typically, additional genetic engineering steps are necessary to attain expected goal.

With the advances in molecular biological techniques and metabolic pathway analysis as well as the availability of genome sequences of most common microorganisms such as *Bacillus subtilis* (Kunst et al., 1997) and *E. coli* (Blattner et al., 1997; Hayashi et al., 2001) and more recently *Bacillus thuringiensis* (Han et al., 2004), metabolic engineering has gained increasing applications. Nielsen (2001) recently classified the applications of metabolic engineering into seven groups: (1) To produce heterogonous proteins, such as producing pharmaceutical proteins and novel enzymes from other sources in the production host; (2) To extend substrate range for the applied microorganism in order to have a more efficient utilization of the raw materials in industrial processes; (3) To introduce pathways leading to new product in the host strain; (4) To either introduce pathways from other organisms or engineer existing pathways for degradation of environmental pollutant; (5) To engineer cellular physiology for process improvement, such as making the cells tolerant to high glucose concentrations or low oxygen concentrations; (6) To eliminate or reduce by-product formation; (7) To improve the yield or productivity of target product. A few recent successful stories include engineering yeast for improved ethanol tolerance and production (Alper et al., 2006), engineering a mevalonate pathway in *Escherichia coli* for the production of terpenoids (Pitera et al., 2006; Martin et al., 2003), and metabolic engineering *E. coli* for the microbial production of 1, 3-propanidiol (Nakamura and Whited, 2003) which has been commercialized by DuPont in 2006.

This thesis will be focused on applying metabolic engineering to reduce acidic by-products formation and improve biomass yield, enhance heterogonous protein (GFP+ as a model

product in this study) production in *B. sutbilis*, and improve the yield and productivity of native metabolites (folic acid as a model product in this study) synthesized by microorganisms. Building upon the achievements we have made with *B. subtilis*, this thesis will also explore the feasibility of applying our successful approaches to reduce acetate formation in an agricultural important bacterium: *Bacillus thuringiensis* (*Bt*).

1.1   REDUCE ACETATE FORMATION IN MICROBIAL FERMENTATION

1.1.1   Central Carbon Metabolism and Acetate Formation

Cell metabolism represents a complex network of several thousand reactions taking place at any instance of time. The central carbon metabolism pathway, which consists of glycolysis pathway, hexose monophosphate pathway (HMP) and tricarboxylic acid (TCA) cycle, is the most important pathway in a living organism as it provides key precursors and energy for the synthesis of cell mass components and target products (Figure 1.1) (Gottschalk, 1985). Glycolysis or Embden-Meyerhof-Parnas (EMP) pathway is the sequence of ten-step catabolic reactions that convert glucose into pyruvate with the concomitant production of a relatively small amount of adenosine triphosphate (ATP), the energy currency of the cell. The overall reaction in glycolysis pathway can be summarized as the following equation:

$$glu\cos e + 2ADP + 2NAD^+ + 2Pi \rightarrow 2\,pyruvate + 2ATP + 2NADH + 2H^+$$
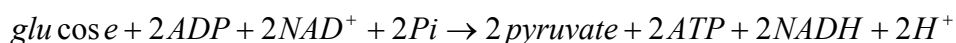
where NAD represents nicotinamide adenine dinucleotide and ADP represents adenosine diphosphate. TCA cycle, also known as citric acid cycle or Krebs cycle, starts with the condense reaction of four carbon compound oxaloacetic acid and two carbon acetyl CoA to form citrate

and contains the final oxidation reactions, coupled to the electron transport chain, which produces the majority of the ATP . The overall reaction of TCA cycle is:

$$Acetyl - CoA + 3NAD^+ + FAD + GDP + Pi + 2H_2O \rightarrow CoA + 3NADH + 3H^+ + FADH_2 + GTP + 2CO_2$$
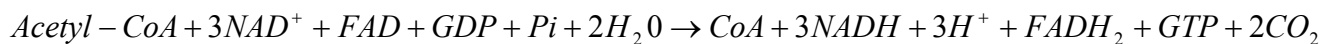
where FAD represents flavin adenine dinucleotide and GDP represents guanosine diphosphate. The HMP pathway or pentose-phosphate pathway begins with glucose-6-phosphate dehydrogenase (G6PDH) which generates NADPH (Nicotine Adenine Dinucleotide Phosphate, reduced form), and it is very important for the aromatic amino acid synthesis.

Bacteria may be grown under feast or famine condition. When there is an excess supply of nutrients such as glucose, bacteria tend to produce a significant amount of by-products. One of the key by-products is acetate. Acetate accumulates in the medium of most bacterial cultures when glucose is employed as the main carbon source and available in high concentrations. The acetate production in *E. coli* and *B. subtilis* is generally regarded as a result of mismatch between excessive glycolytic flux and limited tricarboxylic acid (TCA) cycle capacities (Majewski and Domach, 1990). An overflow of glycolystic flux will steer the carbon flow to the production of acidic by-products. The overflow of glycolysis could be caused by a limited TCA cycle flux (Han et al., 1992) or a limited capacity of the electron transport chain reactions through the cytochrome chain (Ingledew and Poole, 1984; Andersen and Meyenburg, 1980). While the high cell growth rate is desirable for high productivity, the overflow of glycolytic flux and formation of acetate are more serious problems at high growth rate as some enzymes of the TCA cycle are repressed at high growth rates, which further lowers the TCA flux (Fisher and Magasanik, 1984; Hanson and Cox, 1967; Grey et al., 1966; Oh and Liao, 2000). Doelle et al. (1982) observed that an increase in specific growth rate and an increase in glucose feed concentration in continuous culture experiments caused a repression of NADH oxidase activity, which resulted in the

4

accumulation of NADH. Accumulated NADH can repress the enzymes of TCA cycle and thus turn excess glycolytic flux to acid by-products. Vemuri et al. (2006) also reported that several genes involved in the tricarboxylic acid (TCA) cycle and respiration were repressed as the glucose consumption rate increased, and over-expression of NADH oxidase resulted in reduced NADH/NAD ratio and eliminated acetate formation (Vemuri et al., 2007).
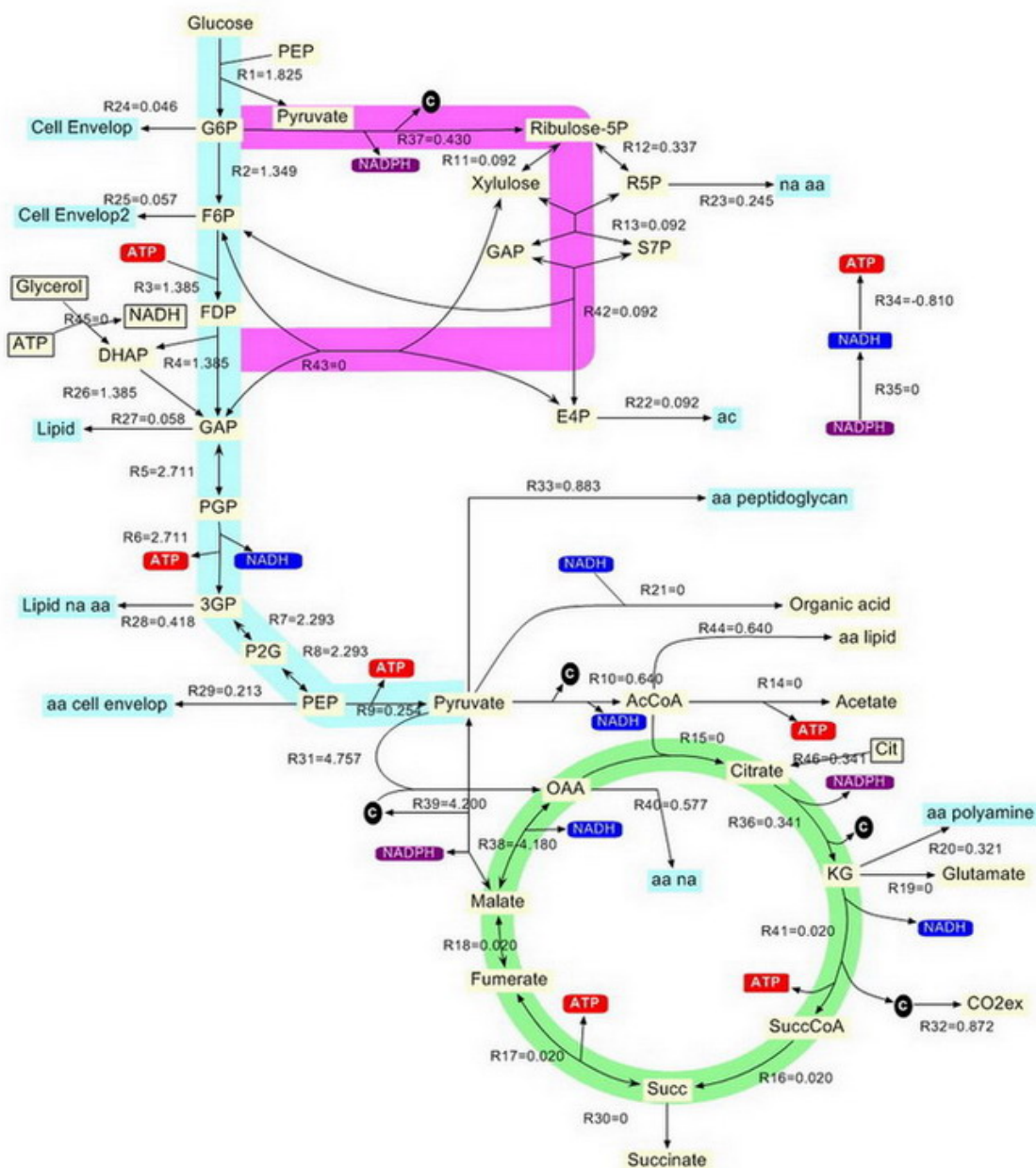
Figure 1.1. Central carbon metabolism of *B. subtilis*.

Abbreviations: aa (amino acids); na (nucleic acids); G6P (glucose-6-phosphate); F6P (fructose-6-phosphate); FDP (Fructose-1,3-bisphosphate); DHAP (Dihydroxyacetone-phosphate); R5P (ribose-5-phosphate); E4P (erythrose-4-phosphate); S7P (sedoheptulose-7-phosphate); GAP (Glyceraldehyde-3-phosphate); PGP (1,3-bisphosphoglycerate); 3GP (3-phosphoglycerate); P2G (2-phosphoglycerate); PEP (phosphoenolpyruvate); AcCoA (acetyl-CoA); Cit (Citrate); KG (α-ketoglutarate); Succ (succinate); OAA (oxaloacetate).

1.1.2 Overall Deleterious Effects of Acetate and Its Toxicity Mechanism

The acetate is regarded as a toxic by-product of glucose metabolism and its accumulation in the culture medium can repress cell growth and inhibit product synthesis in many bacterial cultures (Gerigk et al., 2002; van de Walle and Shiloach, 1998; Cierheller et al., 1995; Goel et al., 1993). Furthermore, acetate formation results in a loss of carbon, affecting the overall yield of biomass and/or a desired product on raw materials (Fieschko and Ritch, 1986). For example, in early days, it was thought impossible to grow *E. coli* to cell densities above 20 g/L as we now know it is because of the buildup of toxic metabolic by-products (primarily acetate) that inhibit cell growth (Shuler and Kargi, 1992). Nowadays, high-density *E. coli* cultures of 100 g/L can be attained with rational strain design and strict process control. Therefore, reducing acetate accumulation during microbial fermentation has become a vital issue for obtaining high cell density and productivity.

A common explanation of the toxicity of acetate lies in the uncoupling of the proton motive force (specifically pH) resulted from the accumulation of acetate in the culture medium. Acetate exists in both the ionized (CH_3COO^-) and protonated (CH_3COOH) states at neutral pH. The lipophilic protonated form can pass through the lipid membrane to the interior of the cell where dissociates to CH_3COO^- and $H+$, thereby decreases the intracellular pH (Luli and Strohl, 1990). Recently, some researchers showed that high glucose concentration which corresponds to acetate-forming conditions also activated the methyl glycoxalate pathway in bacteria such as *E. coli* (Weber et al., 2005). The methyl glyoxalate pathway, which converts dihydroxyacetone phosphate (DHAP) to pyruvate via methylglyoxal and D-lactate, may short-cut the glycolysis pathway and lead to limited energy (ATP) supply for biosynthesis. In addition, methyl glyoxalate

7

itself is a highly toxic compound and may adversely react with deoxyribonucleic acid (DNA), ribonucleic acid (RNA) and proteins (Lo et al., 1994; Papoulis et al., 1995).

1.1.3   A Review of Previous Efforts to Reduce Acetate Production

Since acetate accumulation is highly detrimental to microbial fermentation process, a variety of strategies have been investigated in an attempt to reduce problematic acetate formation in the past decades. The approaches can be divided into two general categories: (1) controlling process conditions or (2) genetic manipulations of the host strain. Process control solutions include removing the toxic byproduct as it accumulates (Landwall and Holme, 1977) and keeping the cell growth rate below a critical value where acetate production commences (Johnston et al., 2003; Luli and Strohl, 1990). For example, a fed-batch process with controlled feeding of glucose successfully reduced the acetate formation (Yoon et al., 1994; Paalme et al., 1990). However, these techniques can be challenging to implement in practice because of the limited availability of direct process measurements. In addition, controlling the growth rate below threshold is limited to low growth rates, which increases the process cycle time and thereby limits process throughput.

The genetic manipulation approach involves the application of metabolic engineering to reduce carbon flow to the acetate-producing pathways. One strategy is to abolish the activities of acetate kinase (ack) and acetyl phosphotransferase (pta), the enzymes catalyze the synthesis of acetate (Diaz-Ricci et al., 1991).

$$Acetyl - CoA + P_i \xrightarrow{\text{pta}} Acetyl - P + CoA - SH$$

$$Acetyl-P + ADP \xrightarrow{\text{ack}} Acetate + ATP$$
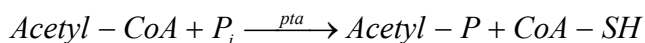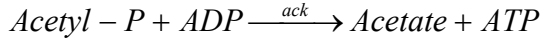
This approach reduced acetate formation in the mutant compared to the parent strain, but resulted in significant accumulation of other undesirable by-products such as pyruvate and lactate (Diaz-Ricci et al., 1991; Yang et al., 1999).

Another strategy is to divert excess glucose to products that are less toxic than acetate, for example, engineering *E. coli* to overproduce glycogen (Dedhia et al., 1994).

$$Glu\cos e + PEP \xrightarrow{\text{phosphotransferase}} Glu\cos e - 6 - Phosphate + Pyruvate$$

$$Glu\cos e - 6 - Phosphate \xrightarrow{\text{Phosphoglucomutase}} Glu\cos e - 1 - Phosphate$$

$$Glu\cos e - 1 - Phosphate + UTP + H_2O \xrightarrow{\text{UDPG phosphorylase}} UDP - Glu\cos e + 2Pi$$

$$UDP - Glu\cos e + (1,4\text{-}\alpha\text{-}D\text{-}glucosyl)_n \xrightarrow{\text{GLucogenSynthetase}} UDP + (1,4\text{-}\alpha\text{-}D\text{-}glucosyl)_n$$
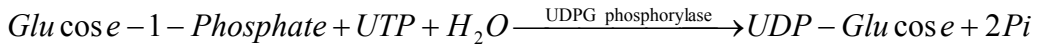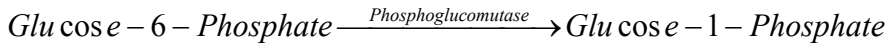
where PEP is phosphoenolpyruvate, and UTP is Uridine triphosphate. While glycogen levels increased several fold, the acetate production remained unchanged.

In a third approach, the *ptsG* gene encoding an enzyme in the glucose transferase system was mutated.

$$Glu\cos e + PEP \xrightarrow{\text{pts}} Glu\cos e - 6 - Phosphate + Pyruvate$$

The mutation resulted in reduced acetate yield, as well as lower growth rate (Chou et al., 1994; Chen et al., 1997). Another strategy to manipulate glucose transport is to over-express galactose permease to provide an alternate slower route for glucose uptake which resulted in lower glucose uptake rate and reduced acetate accumulation and improved recombinant protein production (De Anda et al., 2006).

Finally, increasd metabolic flux of two anaplerotic pathways through phosphoenolpyruvate carboxylase reaction and glyoxylate bypass was examined in *E. coli*.

$$PEP + H_2O + CO_2 \xrightarrow{ppc} OAA + Pi$$

$$Isocitrate \xleftrightarrow{IsocitrateLysate} Succinate + Glyoxylate$$

$$Acetyl - CoA + H_2O + Glyoxylate \xrightarrow{MalateSynthase} S - malate + CoA$$
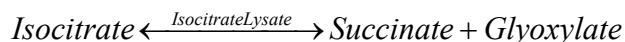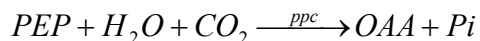
where OAA is oxaloacetate, and ppc represents phosphoenolpyruvate carboxylase. This approach reduced acetate production by four fold (Farmer and Liao, 1997); however, there was no increase in cell density indicating the possibility of glucose conversion to other metabolic by-products. In addition, this mutation is specific to *E. coli* since not all microorganisms (for example, *B. subtilis*) possess the enzyme ppc.

1.1.4 A Review of the Approaches in Our Group

An alternative approach was found in investigating the possible effect of some TCA cycle metabolites on the central carbon metabolism (Goel et al., 1995). It was observed that the glycolytic flux remarkably decreased and the acetate formation was eliminated when a small amount of citrate was fed into glucose minimal medium in *B. subtilis* continuous cultures. The effectiveness of citrate is rather due to glycolytic inhibition than just serving as a supplement of TCA cycle metabolites since adding other metabolites such as glutamine does not have similar effect as citrate. It was proposed that the effect of citrate is to attenuate the activities of pyruvate

kinase (PYK) and phosphofructose kinase (PFK), which are known to exert significant control over glycolysis (Goel et al., 1996). This hypothesis was both supported by experimental measurements and metabolic modeling analysis. Metabolic fluxes, pools, and enzyme measurements (Goel et al., 1999), as well as NMR experiments results (Phalakornkule et al., 2000), indicated PYK as a site of citrate-mediated glycolytic flux attenuation. Flux alternatives generated from linear programming analysis indicate that the fluxes through glycolysis, the TCA cycle, and hexose monophosphate pathway that maximize carbon use also correspond to minimized PYK flux (Lee et al., 1997).

A major shortcoming of this approach was that simultaneous utilization of glucose and citrate was only attainable in steady state continuous cultures where residual glucose concentration is low. The strategy was not applicable to batch cultures due to high initial glucose concentrations limiting citrate transport in batch cultures. The low transport of citrate in high glucose cultures is consistent with catabolite repression regulation of citrate transport in *B. subtilis* (Warner et al., 2000; Willecke and Pardee, 1971; Yamamoto et al., 2000). Since biotechnological processes aimed at production of proteins, metabolites, or other products are almost entirely based on batch or fed-batch cultures, design of a robust strain that will produce low levels of acidic byproduct in batch cultures is extremely desirable. It is likely that a PYK mutant of *B. subtilis* may display reduced acid formation without relying on citrate transport and such a strategy should also work for batch cultures with high glucose concentration in the feed.

To directly test the effect of attenuating the PYK-catalyzed flux, both *E. coli* (Zhu et al., 2001) and *B. subtilis* (Fry et al., 2000) bearing interrupted *pyk* were characterized. The results showed substantial reduction in acid formation for both mutants, where both the total amount of acetate and the fraction of glucose converted to acetate were reduced. The *B. subtilis pyk* mutant

grew significantly slower than the wild-type and displayed substantially higher intracellular concentrations of PEP and glucose-6-phospahte (Fry et al., 2000) than the wild type. The growth rate of *E. coli pyk* mutant was comparable to the wild-type (Zhu et al., 2001). Unlike *B. subtilis*, intracellular concentrations of PEP and glucose-6-phospahte of the wild type and *pyk* mutant of *E. coli* were similar. The difference between the anaplerotic pathways used by *B. subtilis* and *E. coli* to produce oxaloacetate (OAA) may explain the substantially elevated PEP pool in *B. subtilis pyk* mutant. Phosphoenolpyruvate carboxylase (PPC) converts phosphoenolpyruvate (PEP) to OAA in *E. coli*, whereas in *B. subtilis*, OAA is formed via the pyruvate carboxylase–catalyzed conversion of pyruvate (Figure 1.2). Thus, PEP in *B. subtilis pyk* mutant accumulates but not in *E. coli pyk* mutant.

We hypothesized that a pyruvate kinase knockout of *B. subtilis* mutant may be experiencing glucose transport limitation and/or global regulatory changes in response to an excess of PEP/G-6-P. It was felt that control of *pyk* expression at a small value may still maintain low acid production and prevent accumulation of PEP and glucose-6-P to levels that will not substantially reduce cell's growth rate.

Glucose

|
PTS
↓

Glucose-6-P

↓

Phosphoenolpyruvate

PPC   PCK   PYK | PTS

Pyruvate

PYC

Acetyl-CoA

Oxaloacetate   Citrate

KREBS cycle
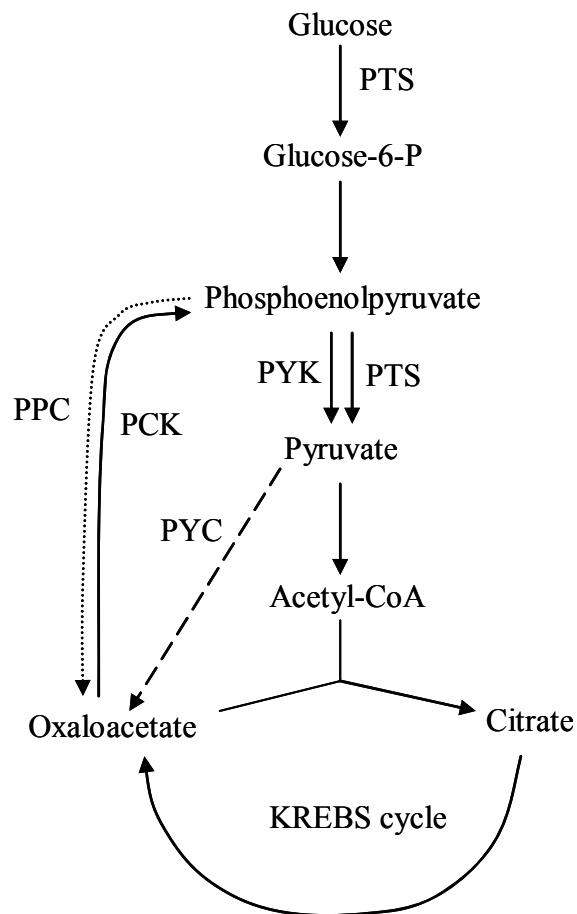
Figure 1.2. Reaction network of *B. subtilis* and *E. coli* central carbon metabolism.

PTS (PEP:sugar phosphotransferase systems) operates in both *E. coli* and *B. subtilis*. PYC (pyruvate carboxylase) catalyzed reaction (dashed line) is present only in *B. subtilis*. PPC (PEP carboxylase) catalyzed reaction (dotted line) is present only in *E. coli*. PCK (PEP carboxykinase) is the gluconeogenesis enzyme which may operate in reverse direction in *B. subtilis pyk* mutant.

1.1.5   Proposed Strategies to Improve Cellular Metabolism.

1.1.5.1 Inducible Pyruvate Kinase

Based on above experimental results and analysis, both the high level expression of pyruvate kinase in the wild-type *B. subtilis* strain and nil pyruvate kinase activity in the *pyk* knockout mutant may not attained good balance of glycolysis and TCA cycle fluxes, resulted in acetate production and slow growth rate, respectively. The complete knockout of *pyk* resulted in high PEP concentration which indirectly lowers the glucose uptake rate. The high PEP concentration could be alleviated by controlling the expression of the *pyk* gene, and thereafter possibly restores the cell growth rate of the mutant back to the wild-type level. Therefore, an inducible *pyk* mutant of *B. subtilis* is to be constructed by replacing the original promoter (a DNA sequence that controls the expression of gene) with an inducible one (Pspac, which can be induced by IPTG). The expression of PYK can be controlled by the concentration of IPTG.

1.1.5.2 Inducible Phosphofructokinase

Phosphofrucokinase (PFK) catalyzes the ATP-dependent phosphorylation of fructose 6-phosphate to fructose 1,6-biphosphate. As previously described, the attenuation of pyruvate kinase resulted in elevated PEP concentration. PEP is a strong inhibitor of PFK (Blangy et al., 1968; Evans and Hudson, 1979; Doelle et al., 1982), and high PEP concentration will reduce PFK activity, causing reduced glycolytic flux. Therefore, manipulating *pfk* expression will directly affect glycolysis flux. An inducible *pfk* mutant of *B. subtilis* will be constructed and the effect of *pfk* expression level on cell growth rate and acetate production will be studied.

1.2   FOLIC ACID

1.2.1   Introduction

Folic acid is an important member of B class vitamins. Mammals can not produce folic acid by themselves, yet it is an important dietary supplement. Food supplements and microbial production in the digestive track are the main sources of folic acid for mammals and birds.

A number of developments in diseases related to folic acid deficiency have raised the demand for folic acid. A few recent research results have shown that increased folic acid intake has been linked with reduced heart disease and lessened incidence of neutral spinal defects in newborns. Several other studies have associated diets low in folate with increased risk of breast, pancreatic and colon cancer (Giovannucci et al., 1998). These findings have accelerated an already booming nutrition industry, and providing abundant and cheap folic acid by improving its manufacture process will benefit all the people.

Folic acid is now primarily produced via chemical synthesis due to the low yields of folic acid produced by current bacterial strains (Miyata et al., 1999; Iwai et al., 1970). However, several reasons have prompted new exploration into using microbes for the commercial production of folic acid. First, the glutamated and reduced form of the natural vitamin, which many bacteria produce (Hintze and Farmer, 1975), is what the digestive system is "designed" to process. Unlike synthetic folic acid, the "natural" B vitamin does not require reduction prior to being used by the body. Secondly, a single step fermentation route could prove to be more environmentally benign than a multi-stage chemical process, if an effective production strain can

15

be developed. Finally, the metabolic capacity of *B. subtilis* for folic acid production is as high as 0.161 mole folic acid/mole glucose (Sauer et al., 1998), and the microorganism can be engineered to greatly improve the productivity of folic acid.

1.2.2 Biosynthesis of Folic Acid

The complete biosynthesis of folic acid in microbes involves many steps and complex regulation mechanism. Phosphoenolpyruvate (PEP), glutamate, erthyrose-4-phosphate (E4P) and guanosine triphosphate (GTP) are the four precursors of folic acid (Figure 1.3). *B. subtilis* mutant deficient in the enzyme PYK has been found to possess significantly increased PEP and glucose-6-phosphate pools (Fry et al., 2000; Pan et al., 2006). Both metabolites can fuel folic acid synthesis, where PEP is a direct folic acid precursor and glucose-6-phosphate reacts to form the precursor E4P. Therefore it is conceivable that a mutation in PYK may potentially increase folic acid production. This also offers a good start strain to be further engineered for enhanced folic acid production.

PEP   E4P   GTP

$\downarrow$ *mtrA/folE*

aroH

DAHP   *folA*

Phe

Tyr   Chorismate   *folK*

Trp $\downarrow$ **pabA, pabB, pabC**

PABA H_2 –Pterin – CH_2OPP

Sul

Dihydropteroate   Glutamate

folC

Dihydrofolate

dfr
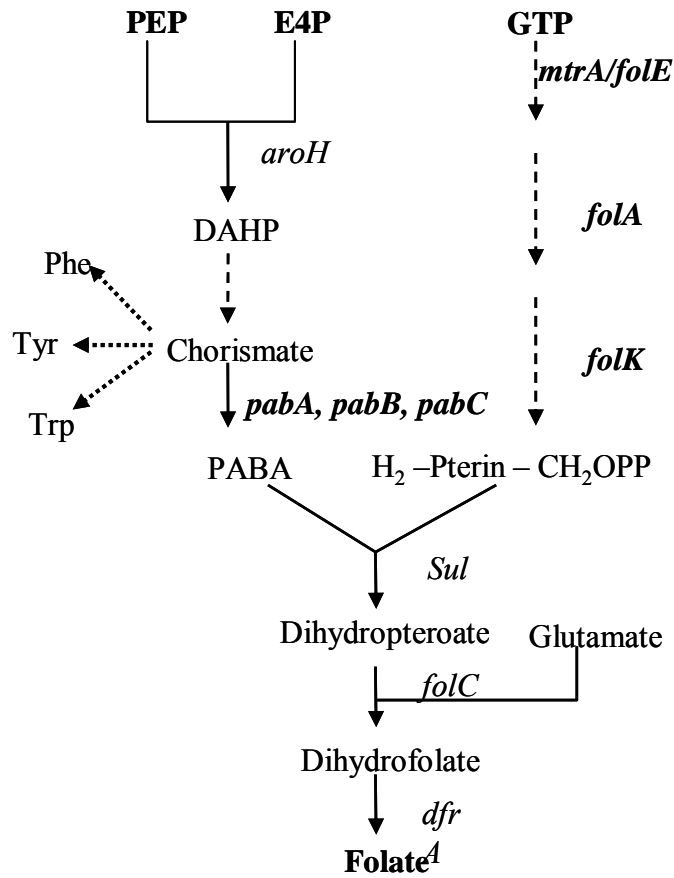
Folate[A]

Figure 1.3. Biosynthesis pathway of folic acid.

The schematic graph shows the flow of metabolites and the genes that encode the enzymes involved in folate. The abbreviation for the metabolites are PEP (phosphoenolpyruvate); E4P (erythrose-4-phosphate), DAHP (3-deoxy-D-arabino-heptulosonate-7-phosphate), PABA (para-aminobenzoic acid), Phe (phenylalanine), Tyr (tyrosine), Trp (tryptophan) and GTP (guanosine triphosphate).

1.2.3 Review of Efforts to Increase Folic Acid Production in Microbes

In the past decade, relatively limited efforts have been put on enhancing folic acid production in microorganisms. A few genetic engineering approaches have been investigated to enhance folic acid production by amplifying the expression of genes involved in folic acid biosynthesis. One study shows that over-expression of *folk* which encodes the first enzyme GTP cyclohydrolase I in the folate biosynthesis pathway in *Lactococcus lactis* increased extracellular folate production by 800% (Sybesma et al., 2003). It was shown that *folK* might encode the rate-limiting enzyme (Pyrophosphokinase) in *B. subtilis* strains that over-express each of the five genes (*sul, folA, folK, mtrA, and folC*) (Eichler et al., 1997). However, it is conceivable that amplifying all five genes could further elevate folic acid production. Another study with a few bacteria including one *B. subtilis* strain indicated that para-aminobenzoic acid (PABA) pathway may be rate limiting based on the experimental results that addition of PABA in the medium dramatically increased folic acid production (Miyata et al., 1999). Recent work in our group showed that a combination of mutations in over-expressing *aroH̱*, disrupting *mtrB* and *trpC2*, and down-regulating *pyk*, resulted in 8-fold increase in folic acid production as compared to *B. subtilis* 168 (Zhu et al., 2005). *mtrB* encodes the tryptophan RNA-binding attenuation protein (TRAP) which has been found to terminate the transcription and translation of the folate operon.

.

1.3 RECOMBINANT PROTEIN PRODUCTION

1.3.1 *B. subtilis* as a Host for Recombinant Protein Production

The gram-positive bacterium *B. subtilis* has been extensively used in the food industry due to its safety (generally recognized as safe by the FDA) and high secretion capacity of native enzymes. The majority of commercial available enzymes are produced by *B. subtilis* (Westers et. al., 2004), however, *E. coli* is still currently the most commonly used bacterial host for industrial production of heterogeneous pharmaceutical proteins as it is the best characterized bacterial strain and the availability of various expression vectors facilitates high levels of protein production in *E. coli*. The application of *B. subtilis* for heterogeneous protein production is limited by its low productivity due to increased proteolysis and eventual sporulation. A few recent developments, however, have made *B. subtilis* an attractive host for heterologous protein production. First, the availability of protease-deficient strains of *B. subtilis* has greatly improved the productivity and stability of secreted proteins (Wong et al., 1995; Wu et al., 1991 and 2002). Second, asporogenous strains are now available (Oh et al., 1995; Pierce et al., 1992), which further improves the productivity of desired products. Third, the complete genome sequence of *B. subtilis* is known (Kunst et al., 1997) and the host strain can be optimized for hetorologous proteins production using modern genetic engineering techniques. Furthermore, the recently developed high throughput analysis technologies such as DNA microarry and 2-D gel electrophoresis have greatly sped up developmental work in *B. subtilis*.

1.3.2   Detrimental Effect of Acetate on Recombinant Protein Production

As being addressed previously, most bacteria including *B. subtilis* produces a significant amount of acetate when the common carbon source glucose is employed. The accumulation of acetate not only inhibits cell growth (Luli and Stohl, 1990), it was also reported to have detrimental effect on recombinant protein production (George et al., 1992; Jensen and Carlsen, 1990; Hahm et al., 1994). Many acetate-reduction strategies have been found to confer increases in heterologous protein production (Bauer et al., 1990; De Anda et al., 2006; Kim and Cha, 2003; San et al., 1994; Vemuri et al., 2006). The majority of these efforts have been focusing on the gram negative *E . coli* and many approaches have achieved reduced acetate production as well as enhanced recombinant protein production (De Anda et al., 2006; March et al., 2002; Vemuri et al., 2006), however, less information is available for *B. subtilis*.

1.3.3   Effect of *pyk* Expression on Recombinant Protein Production

Our previous study with *B. subtilis* showed that down-regulating *pyk* significantly reduced the acetate production and a good balance of fluxes between glycolysis and the TCA cycle can be attained at an appropriate *pyk* expression level (Fry et al., 2000; Pan et al., 2006). Therefore, we hypothesize that a strain with lower *pyk* expression may be beneficial to recombinant protein expression in *B. subtilis* based on our following attained observations: (1) down-regulating *pyk* significantly reduced formation of toxic by-products (Fry et al., 2000; Pan et al., 2006), and   (2) production of recombinant protein was dramatically enhanced in continuous culture of *B. subtilis* with dual feeding of glucose and citrate (Vierheller et al., 1995)

20

which corresponds to a low pyruvate kinase status (Goel et a., 1995; Lee et al, 1997; Phalakornkule et al., 2000). In this study, we will investigate how *pyk* mutation will affect recombinant protein production in *B. subtilis*. GFP+ (Scholz et al., 2000) will be selected as a model protein due to its brightness (130-fold brighter than wild type GFP) and ease of detection by fluorescence spectrometry. In addition, GFP+ is very stable, which can minimize the effect of degradation.

2.0   MATERIALS AND METHODS

2.1   CELL CULTURING

2.1.1   Strains

B. subtilis 168 (wild-type or WT), 1A96, 1A99, 1A92, 1A330 were obtained from Bacillus Genomic Stock Center (BGSC, Columbus, OH). Competent *Escherichia coli* strain DH5a was purchased from Invitrogen (Carlsbad, CA), and used for the construction of plasmids throughout this work. The construction of inducible *pyk* mutant of *B. subtilis* (iPYK mutant) was briefly described elsewhere (Zhu et al., 2003) and in section 2.3 in detail. The construction of inducible *pfk* was described in section 2.3. The construction of GFP+ production strains WTpGFP+ (WT bearing plasmid pGFP10) and MTpGFP+ (iPYK mutant bearing plasmid pGFP10) was also described in section 2.3. *B. thuringiensis* was obtained from American Type Culture Collection (ATCC No. 35646). All the strains and plasmids used in this work were listed in Table 1.

Table 1. Strains and plasmids used in this work

Strains and plasmids	Description	Source or reference
Strains		
B. subtilis 168	*trpC2*	BGSC*
B. subtilis 1A96	*trpC2 pheA*	BGSC
B. subtilis 168 + iPYK	*trpC2 pyk (inducible), Erm^r*	Zhu et al., 2005
B. subtilis 168 + iPFK	*trpC2 pfk (inducible), Erm^r*	This study
B. subtilis 168 + pGFP10	*trpC2 gfp+, Kan^r*	This study
B. subtilis 168 + iPYK + pGFP10	*trpC2 pyk (inducible) gfp+, Erm^r Kan^r*	This study
BSTZ 0408	*trpC2 mtrB::erm*	Zhu et al., 2005
BSTZ 0410	*trpC2 aroH*	Zhu et al., 2005
BSTZ 0412	*trpC2 aroH tktA*	Zhu et al., 2005
BSTZ 0419	*trpC2 mtrB::cm pyk(Ind)*	Zhu et al., 2005
BSTZ 0425	*trpC2 aroH pyk(Ind)*	Zhu et al., 2005
BSTZ 0437	*trpC2 pyk(Ind)*	Zhu et al., 2005
B. subtilis 1A99	*ilvA3 trpC2 odhA1*	BGSC
B. subtilis 1A92	*arg(GH)2 aroG932 bioB141 sacA321*	BGSC
B. subtilis 1A330	*aroG932 bioB141*	BGSC
E.coli DH5a	Cloning strain	Invitrogen
B. thuringiensis Berliner	35646	ATCC **
Plasmids		
pMutin4	*Amp^r Erm^r*	BGSC
pRB374	*Amp^r Kan^r*	Brückner, 1992
pMTPYK	*Amp^r Erm^r;*	Zhu et al., 2005
pMTPFK	*Amp^r Erm^r*	This study
pMN402	*Amp^{r}Hyg^r*	BGSC
pGFP10	*Amp^r Kan^r*	This study
pRA1	*Amp^r Kan^r, aroH*	Zhu et al., 2005
pRAT2	*Amp^r Kan^r, aroH tktA*	Zhu et al., 2005
pVp2	*Amp^r Erm^r*, contains Erm^r cassette between 5' and 3' fragments of *mtrB*	Yang et al., 1995

*BGSC: Bacillus Genomic Stock Center (Columbus, OH).
**ATCC: American Type Culture Collection (Manassas, VA)

2.1.2 Media

Luria-Burtani (LB) Lennox Medium is a rich medium used for culturing bacteria. 25 g/L LB medium contains 10 g/L Tryptone, 5 g/L yeast extract and 10 g/L sodium chloride.

Glucose minimal medium was used as the basic culture medium for both *B. subtilis* and *B. thuringiensis*. 1 liter of glucose minimal medium contains: 1 g NH_4Cl, 1.0g KH_2PO_4, 2.72 g K_2HPO_4, 0.284 g Na_2SO_4, 0.17g $NaNO_3$, 0.15 g KCl, 0.049 g $MgCl_2 \cdot 6H_2O$, 2.16 mg $FeCl_3 \cdot 6H_2O$, 0.015 $MnCl_2 \cdot 4H_2O$, 0.022 g $CaCl_2 \cdot 6H_2O$. The concentration of glucose and citrate used in each experiment were noted in the text. In bioreactor cultures, 2 mL/L 10% antifoam B was added to control the foaming.

C medium is a buffered minimal medium used to culture *B. subtilis* (Aymerich, et al., 1986). 1 liter of C medium contains: 16 g $K_2HPO_4 \cdot 3H_2O$, 4.1 g KH_2PO_4, 3.3 g $(NH_4)_2SO_4$, 0.12 g $MgSO_4 \cdot 7H_2O$, 1.7 mg $MnSO_4 \cdot H_2O$, 22 mg $C_6H_{11}FeNO_7$, 1 mL trace element solution, and 0.1 g L-Tryptophan. The culture medium was supplemented with a carbon source of glucose or glycerol, and the amount of carbon source was described in the text. Trace element solution was prepared by adding the following salts to 1 L of 1 M HCl: 4.87 g $FeSO_4 \cdot 7H_2O$, 4.12 g $CaCl_2 \cdot 2H_2O$, 1.50 g $MnCl_2 \cdot 4H_2O$, 1.05 g $ZnSO_4 \cdot 7H_2O$, 0.30 g H_3BO_3, 0.25 g $Na_2MoO_4 \cdot 2H_2O$, 0.15 g $CuCl_2 \cdot 2H_2O$, and 0.84 g $Na_2EDTA \cdot 2H_2O$ (Bühler, et al., 2002).

Semi-rich media were prepared by adding appropriate amount of LB medium to either glucose minimal medium or C medium. The amount of LB medium, glucose, citrate, and glycerol were described in the text.

The culture media may contain appropriate antibiotics for the culture of recombinant strains which have resistance to specific antibiotic(s). Antibiotics were supplemented in the media at the following concentrations: ampicillin, 100 mg/L; chloramphenicol, 5 mg/L; kanamycin, 10 mg/L; and erythromycin, 0.5 mg/L.

2.1.3   Batch Cultures

Batch cultures were conducted in either baffled 300 ml shake flasks or 1 L bioreactors. The cultivation temperature is 37 $^{\circ}$C for *B. subtilis* and *E. coli*, and 30 $^{\circ}$C for *B. thuringiensis*. Aeration is 1.0 ~ 2.0 L/min. The shaking speed with shake flask culture is 200 rpm, and the agitation speed with bioreactor culture is 500 rpm**.**

2.1.4   Reactor Setup and Continuous Cultures

1-L Fermentation vessel (Applikon, Foster City, CA), with a working volume of 500 mL, was used throughout this study. The reactor setup for continuous culture is briefly shown in Figure 2.1. Initially, the bioreactor was operated batch-wise until the cells reached mid-exponential growth. Thereafter, fresh medium was fed into the bioreactor at the selected feed rate with a peristaltic pump. The culture was assumed to reach steady-state after more than five retention times when no variations in optical density and residue glucose were observed. The air flow rate was set at 2 L/min, and the pH was controlled between 6.5 and 7.0 by adding 1N KOH with a Chemcadet PH Meter/Controller (Cole-Parmer, Chicago, IL). The temperature was maintained at 37 ºC for *B. subtilis* and 30 ºC for *B. thuringiensis* by using a water circulator

(HAAKE, Austin, TX). Inocula were grown in LB broth overnight, and the inoculation size was

2.5% of the working volume.

Steady state:

$dX/dt = dS/dt = dP/dt = 0$

$D = \mu$

$D = F / V$
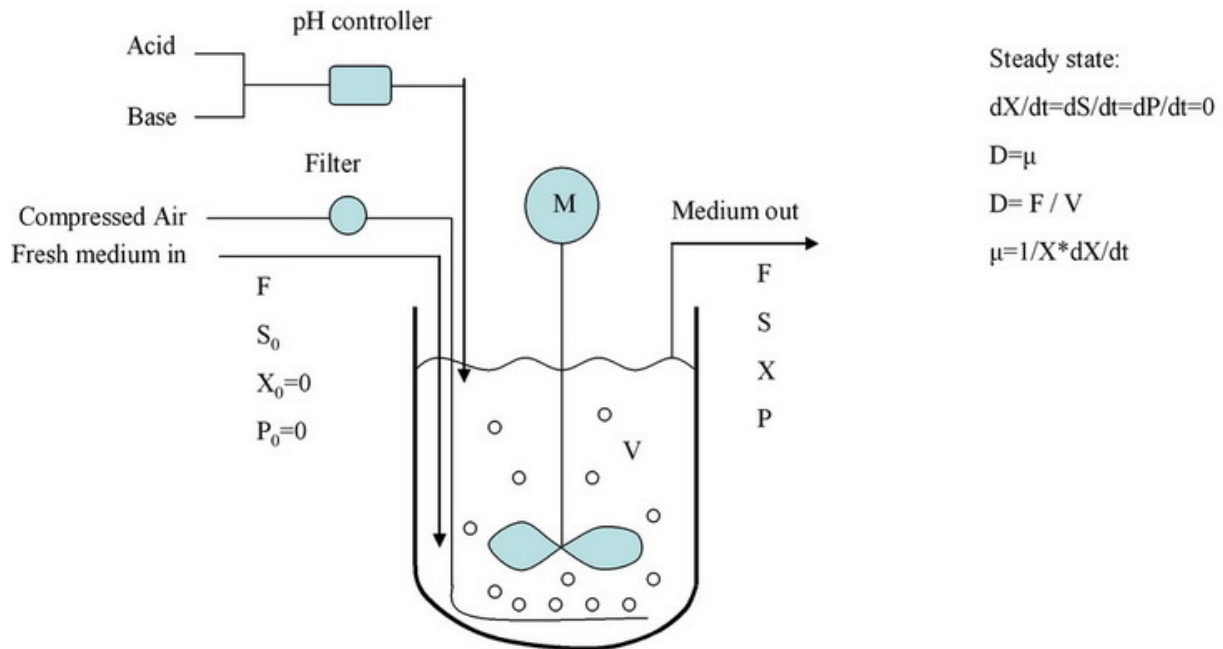
$\mu = 1/X * dX/dt$

Figure 2.1. Schematic diagram of continuous culture system.

D: dilution rate (D = F/V), μ: specific growth rate ($\mu = (1/X)*dX/dt$), F: flow rate, V: volume, X: cell density, P:

product concentration. When the culture reaches steady state, D = μ.

2.2   ASSAYS

2.2.1   Measurement of Cell Density

Samples were taken from the shake flask or bioreactor cultures at intervals. Cell density was determined by means of optical density (OD), based on their proportional relationship (1 OD_{660} = 0.35 g cell dry weight/L). Optical density was measured off-line at 660 nm using a Lambda-6 UV/Vis Perkin Elmer spectrophotometer (Perkin Elmer, Norwalk, CT). The optical density measurements are linear within the range of OD_{660} = 0.05 to 0.5, therefore, samples with higher cell densities were diluted in water before the measurement.

2.2.2   Enzymatic Assay of Glucose

Glucose concentration was assayed using a Glucose (HK) Assay Kit (Sigma GAHK20), which is based on the principle of an end-point assay.

$$Glu\cos e + ATP \xrightarrow{\quad Hexokinase \quad} Glu\cos e - 6 - Phosphate + ADP$$

$$G - 6 - P + NAD \xrightarrow{\quad G6PDH \quad} 6 - Phosphogluconate + NADH$$
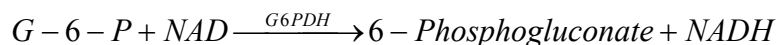
Glucose is phosphorylated by adenosine triphosphate (ATP) in the reaction catalyzed by hexokinase. Glucose-6-phosphate (G6P) is then oxidized to 6-phosphogluconate in the presence of oxidized nicotinamide adenine dinucleotide (NAD) in a reaction catalyzed by glucose-6-phosphate dehydrogenase (G6PDH). During this oxidation, an equal-molar amount of NAD is reduced to NADH. The consequent increase in absorbance at 340 nm is directly proportional to glucose concentration. In the process of culture, a glucometer Elite (Byer, Elkhart, IN)) was frequently used to quick monitor the glucose utilization.

2.2.3 Organic Acids

Organic acids were measured using HPLC or enzymatic assay kits. A 1 mL sample of culture medium was collected and cells were immediately removed using 0.45 μm syringe filter. Acetate and pyruvate were measured using a Waters HPLC equipped with UV/Vis monitor (Waters, Milford, MA) after being eluted from an organic acid analysis column (Bio-Rad, Richmond, CA) with 5mM H_2SO_4. The column was maintained at 50 °C and the isocratic flow rate was 0.7 ml/min. Acetate, as well as other acids, were detected by absorbance at 210 nm. Acid concentrations were calculated from comparing the peak area of corresponding acid with respect to the standard curves. Citrate and lactate were measured by enzymatic assay kits (r-Biopharm Inc., SouthMarshall, MI).

2.2.4 Enzyme Activities

Cell extract was prepared according the procedure used by Fisher & Magasanik (1984) with some minor modifications. Samples were taken during the mid-exponential phase for the batch cultures. Cells were harvested by centrifugation at 4 °C for 3 minutes at 14000 g. The pellet was washed twice with PBS (no calcium) buffer, and then disrupted via incubation in lysis buffer (20 mM Tris HCl pH 8.0, 10 mM EDTA pH8.0, 100 mM KCl, 20 g/L sucrose, 400 mg/L lysozyme, and 100 mg/L Dnase) for 10 ~ 20 minutes. The debris was then removed by centrifugation at 4 °C for 10 minutes at 14000 g, and the supernatant was used for total protein and enzyme assay.

The total protein was determined by Pierce BCA protein assay kit according to the protocol provided by the provider. For pyruvate kinase assay, the standard assay mixture

contains in a final volume of 1 mL: 31 mM K_2HPO_4 (pH = 7.5), 6.7 mM $MgSO_4$, 2 mM ADP, 0.24 mM NADH, 22 unit of crystalline lactate dehydrogenase, 10 mM Phosphoenolpyruvate tricyclohexylammonium salt, and 100 µL of crude cell extract. Pyruvate kinase was assayed at room temperature by determining the decrease of OD at 340 nm (Pan et al., 2006). Each measurement was performed in triplicate.

Phosphofructokinase was assayed according to procedure given by Andersen et al., 2001). The final concentrations of the components of the reaction mixture were 87 mM Tris-HCl (pH8.0), 1 mM ATP, 1 mM fructose-6-phosphate, 10mM $MgCl_2$, and 10 mM NH_4Cl, and 0.2 mM NADH; a mixture of 0.3 unit of triosephosphase isomerase, 1 unit of glycerol-3-phosphate dehydrogenase, 0.3 unit of aldolase, and 1 mM ATP was used to initiate the reaction.

Measurement of acetate kinase activity was determined at room temperature according to the protocol from Sigma Co (Sigma, St Louis, MO) which is based on the method described by Bergmeyer et al. (1983). The assay mixture contains in a final volume of 1 mL: 59.3 mM Triethanolamine Buffer (pH = 7.6), 200 mM NaOAc, 6.67 mM $MgCl_2$, 0.11 mM NADH, 6.07 mM ATP, 1.87 mM PEP, 11.67 unit Pyruvate Kinase, 16.67 unit Lactate Dehydrogenase and 16.67 unit Myokinase. One unit of acetate kinase activity was defined as the production of 1.0 µmole acetyl phosphate per minute at pH 7.6 at 25 degree C.

2.2.5 Measurement of the Concentration of Intracellular Metabolites

Cells were grown to the exponential growth stage in shake flasks, and cell extracts were prepared using the formic acid extraction method as described previously (Fry et al., 2000). Briefly, the mid-exponential culture was immediately chilled to 0~4°C by immersing and swirling the flask in liquid nitrogen. The nearly frozen liquid was then transferred to pre-cooled

centrifugation tube and the cells were harvested by centrifugation at 4°C for 5 minutes with a superspeed refrigerated centrifuge. The cell pellet was resuspended in 1 N cold formic acid and incubated at 4°C for 1 h. Cell debris was then removed by centrifugation. The supernatant was then lyophilized and resuspended in 0.2% of the original culture volume with distilled water. The assay of glucose-6-phosphate (G6P), phosphoenolpyruvate (PEP), pyruvate and fructose-1,6-biphosphate (FBP) was performed as described by Lowry and Passonneau (1972).

G6P is measured using an end-point enzymatic assay involving the following reactions:

$$G6P + NADP \xrightarrow{\quad G6PDH \quad} 6-P-Gluconolactone + NADPH$$

$$6-P-gluconolactone + H_2O \longrightarrow 6-P-gluconate$$
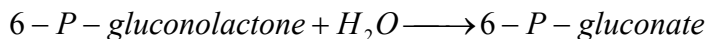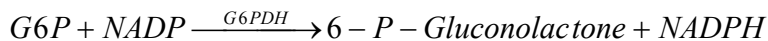
The formation of NADPH is proportional to the amount of G6P in the sample. NADPH formation is monitored by measuring absorbance at 340 nm. The first reaction is catalyzed by G6P dehydrogenase (G6PDH), and the second reaction is nonenzymatic. The assay mixture in the cuvette contained the sample, buffer (25 mM Tris, 25 mM Tris-HCl, pH7.5), 50 µM NADP, 0.1 mM ditiothreitol, 0.02 U/mL G6P dehydrogenase and up to 10^{-11} mM G6P (from sample or standard).

PEP was measured using an enzymatic assay involving the following two reactions:

$$PEP + ADP \xrightarrow{\quad PYK \quad} Pyruvate + ATP$$

$$Pyruvate + NADH \xrightarrow{\quad LDH \quad} Lactate + NAD$$
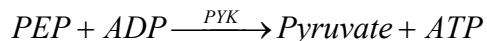
The decrease in NADH is proportional to the amount of PEP in the sample. NADH utilization is monitored by measuring absorbance at 340 nm. The first reaction is catalyzed by pyruvate kinase, and the second reaction is catalyzed by lactate dehydrogenase. The assay mixture contains 10 µM NADH, 10 mM

hydrazine HCl, 0.2 U/mL lactate dehydrogenase (LDH), 0.15 U/mL pyruvate kinase (PYK), 2 mM $MgCl_2$, 200 μM ADP and up to 10^{-11} mM PEP (from sample or standard). The reaction was started by adding lactate dehydrogenase. An initial reading is made, and then add pyruvate kinase.

Pyruvate is measured using the reaction:

$$Pyruvate + NADH \xrightarrow{\quad LDH \quad} Lactate + NAD$$
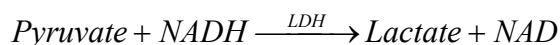
The reaction mixture contains 30 mM phosphate buffer (pH7.0), 10 mM NADH and 0.2 mg/mL lactic dehydrogenase. The reaction is started by adding the enzyme after the sample is in and an initial reading is made. The end point is reached in approximately 5 minutes.

FBP was measured by coupling aldolase, triose-phosphate isomerase, and glycerophosphate dehydrogenase and measuring the decrease in fluorescence of NADH after completion of the reaction.

$$FBP \xrightarrow{\quad aldolase \quad} dihydroxyacetone - P + glyceraldehyde - P$$

$$dihydroxyacetone - P \xrightarrow{\quad triose-P-isomerase \quad} glyceraldehyde - P$$

$$glyceraldehyde - P \xrightarrow{\quad GAPdehydrogenase \quad} 3 - P - glycerate + NADH + H^+$$
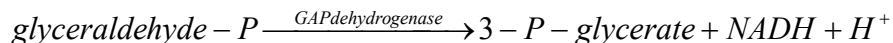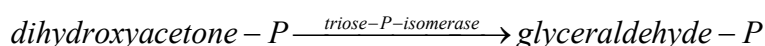
The reaction mixture contains 85 mM TEA buffer with 4.2 mM EDTA (pH7.6), 0.24 mM NADH, 0.331U/mL aldolase, 3.492 U/mL triosephosphate isomerase, 0.395 U/mL glycerophosphate dehydrogenase, and extract sample/standard in a final volume of 1 mL.

2.2.6   Folic Acid Measurement

Both extracellular and intracellular concentrations of folic acid were assayed. Samples taken at the intervals during the cultivation were centrifuged, and the supernatant was filtered with 0.02 μm syringe filter and diluted 10~100 times for the measurement of extracellular folic acid concentration. The cell pellet were resuspended and lysed with a French press, passed through a 0.02 μm filter, diluted 50 to 200 times for the measurement of intracellular folic acid concentration.

Microbial bioassay (Difco Manual, 11th edition) was then used to measure the folic acid concentration. A stock culture of the test strain ATCC 7469 which is an auxotroph of folic acid was prepared in a 15-mL tube with 10 mL Micro Inoculum Broth. These inocula were incubated at 37°C for 18 hr. Under aseptic conditions, the cultures were centrifuged to sediment the cells and then washed three times with the folic acid assay medium. The cells were then resuspended in folic acid free medium and incubated at 37°C for additional 5~8 hours. The cells were diluted 100-fold, and 10 μL of this suspension was used to inoculate each of the assay tubes (in a 2-mL microcentrifuge tube). To each tube, 1 mL double strength folic acid assay medium and 1 mL of sample were added. The optical density of the assay tubes was measured after 18 to 24 h of incubation at 37°C. It was essential that a standard curve be constructed for each separate assay. The standard curve was generated by using 0.0, 0.05, 0.1, 0.15, and 0.2 ng of folic acid per assay tube (2 ml). Optical density was measured using a Lambda 6 Perkin- Elmer spectrophotometer (Perkin-Elmer, Norwalk, CT) at 600 nm.

2.2.7 GFP Expression Measurement

Cells were sampled periodically along the culture, diluted with water to OD around 0.1 and used to measure the fluorescence. Fluorescence intensity was detected at room temperature using a Perkin Elmer luminescence spectrometer LS50B, with an excitation wavelength of 491 nm, an emission wavelength of 512 nm (Scholz et al., 2000), and a slit width of 5 nm. For the GFP+ measurement in the medium, the samples were centrifuged at 21,000g for 8~10 minutes, and the fluorescence of the supernatant was measured. Triplicate measurements were obtained for each sample, and average values are reported.

Flow Cytometry was also employed to measure fluorescence per cell. 1 mL culture was taken during the cultivation and cells were collected by centrifugation. The pellet was then washed once using cold PBS buffer before being applied to FACScan (Becton Dickinson, San Jose, CA) to analyze the expression of GFP+. The data analysis was performed with CellQuest Pro (Becton Dickinson, San Jose, CA) software.

2.2.8 Plasmid Purification and Plasmid Copy Number Measurement

To determine the copy number of different strains, cells were grown in flask cultures and same amount of cells from each culture was harvested in the mid-exponential phase. Plasmid DNA was then isolated using a Qiagen plasmid purification kit (Catalog No. 27106) according to the protocol specifically developed for *B. subtilis* (Appendix B). The pelleted cells were resuspended in 250μL Buffer P1 containing 1 mg/mL lysozyme and incubated at 37 $^{\circ}$C for 10 min. The rest steps followed the protocol provided with product. Plasmid concentration was

calculated based on the absorbance at 260 nm (A260nm), and purity was checked by absorbance ratio of A260nm/A280nm which should be around 1.8 and by agarose gel analysis. The plasmid copy number is defined as the number of plasmid copies per cell. Cell number was counted using a Spencer hemacytometer under a phase-contrast microscope. The calculation of plasmid copy number was based on the calculation of the molecular weight of the plasmid relative to the cell number. Average molecular weight of a base was assumed to be 309 g/mol (Neidharddt et al., 1990).

2.2.9   Gene Expression Measurement by Quantitative RT-PCR

mRNA was extracted from $1x10^7$ cells at mid-log phase using a mRNA capture kit from Qiagen (Catalog No. 70022). The RNA concentration of each sample was determined by absorbance at 260 nm using a Lambda-6 UV/Vis Perkin Elmer spectrophotometer. The purity was checked by absorbance ratio of A260nm/A280nm which should be around 1.8 and by agarose gel analysis. The pair of subcloning primer gfpF and gfpR was used to detect GFP+ mRNA using a one-step RT-PCR kit from Qiagen (Catalog No. 210210). A Kodak 1D imaging analysis system was utilized to semi-quantify the expression level of GFP+ mRNA in various samples.

2.2.10 Spore Counting

Sporulation was monitored under the phase-contrast microscope at a magnification of ×1000. Collected culture was diluted and cells and free spores were counted using a Spencer hemacytometer.

2.2.11 Measurement of Protein Using SDS-PAGE

Protein profile was determined using SDS-PAGE as described elswhere (Banerjee-Bhatnagar, 1998). 1 mL culture was centrifuged, and the pellets were resuspended in 10 mM Tris-HCl, pH 7.5 buffer containing 1 mM PMSF to same cell density, mixed with 2× solubilization buffer (Laemmli's sample buffer containing 8 M urea), boiled for 5 minutes and 25 µL was loaded on a 10-12% SDS-polyacrylamide gel.

2.3   CLONING

2.3.1   Construction of Inducible Pyruvate Kinase (iPYK) Mutant

The primers BspykF (5'-CC**GGATCC**GAAGATTTCAGAAGGAAGTG AACC-3') and BspykR (5'-CC**GGATCC**GGAATTTCCACACCTAAGTCTCC-3') were designed using the sequence of the *B. subtilis pyk* gene obtained from GenBank. These primers were designed to include *BamHI* restriction sites (shown in bold) to facilitate cloning, and used to amplify a 700-bp fragment from *B. subtilis* genomic DNA by PCR with 50 ng of genomic DNA in a final volume of 50 µL containing deoxyribonucleoside triphosphates (0. 5mM each), oligonucleotides (50 pM), and 1 U of Pfx polymerase (Invitrogen, Paisley, Great Britain). Amplification was performed in a GeneAmp PCR system 2400 (Perkin Elmer, Norwalk, CT) with 35 cycles of denaturation at 94 $^{\circ}$C for 30 s, annealing at 50-60 $^{\circ}$C for 30 s, and elongation at 68 $^{\circ}$C for 1 to 3 minutes. The PCR amplified fragment was then digested, purified and cloned into plasmid pMutin4 (Vagner, 1998) as shown in Figure 2.2, and the resulted recombinant plasmid

35

(pMTPYK) was purified again, and transformed into competent *E. coli* DH5a (Invitrogen, Paisley, Great Britain). Isolation of *E. coli* plasmid DNA was performed using Promega Wizard® SV Gel and PCR Clean-Up System. The purified recombinant Plasmid pMTPYK was then transformed into competent *B. subtilis* cells, and transformants were selected on antibiotic medium plates containing 0.3 mg/L erythromycin. The mutants were analyzed by PCR to confirm the integration of a single copy of the plasmid into the target gene on the chromosome, using a strategy similar to that described previously (Pragai and Harwood, 2000). Additionally, to identify colonies who respond to IPTG induction, the harvested colonies were further patched on two glycerol minimal medium plates, one without IPTG and the other contains 0.2 mM IPTG. The colonies that grew well on both plates were discarded. For an inducible *pyk* mutant, there shall be very little or no visible growth on the glycerol minimal medium plate without IPTG and good growth on the glycerol minimal medium plate with 0.2 mM IPTG. The very slow growth rate for the inducible *pyk* mutant without IPTG on glycerol minimal medium plate can be due to the action of phosphoenolpyruvate (PEP) carboxykinase, which can operate in the reverse direction from PEP to oxaloacetate upon knockout of pyruvate kinase in *B. subtilis* (Zamboni et al., 2004). Another possible reason for slow growth rate on glycerol in the absence of induction may be the leaky expression of *pyk*. Colonies were identified that showed very good growth with 0.2 mM IPTG (fully developed after two days) but grew on glycerol minimal medium at very slow rate (tiny colonies were observed in the glycerol minimal medium plate without IPTG after 5 days culture).

Inducible PFK mutant was constructed in a same way as inducible PYK mutant except that the primers BspfkF (5'-CC**GGATCC**GAAGATTTCAGAAGGAAGTG AACC-3') and BspfkR (5'-CC**GGATCC**GGAATTTCCACACCTAAGTCTCC-3') were used in the cloning.
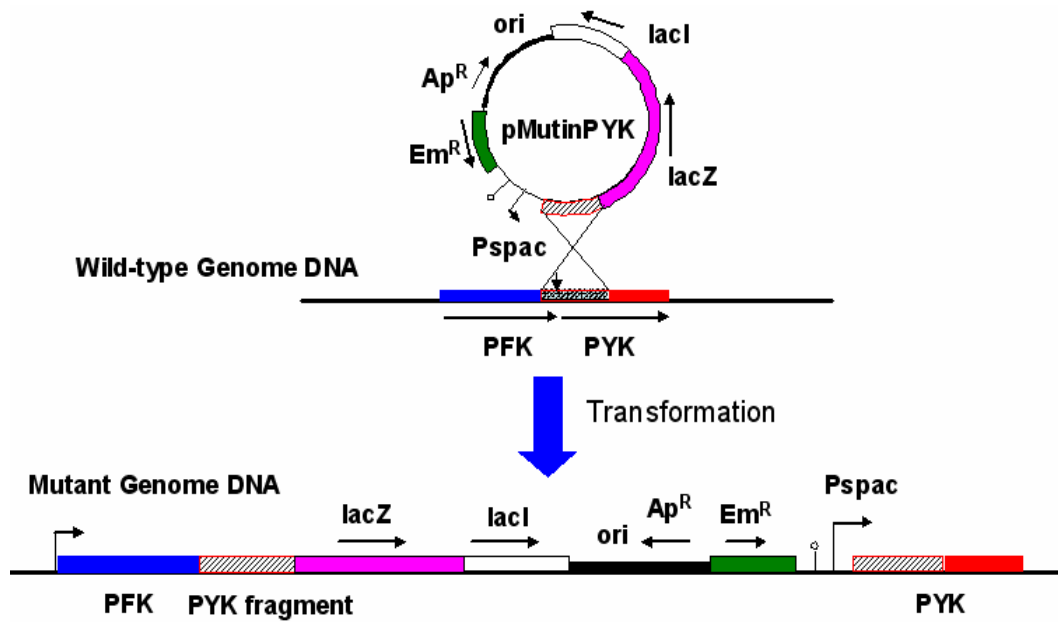
Figure 2.2. Construction of inducible *pyk* mutant.

The vector is integrated into *pyk* gene of wild type *B. subtilis* chromosome by a single crossing-over event. Arrows indicate direction of transcription, broken arrows denote the promoter of the *pfk-pyk* operon and Pspac, and the lollipop strand is for the transcription termination.

2.3.2   Construction of Plasmid with *gfp+*

B. subtilis plasmid pGFP10 was created by cloning *gfp+* gene from vector pMN402 (Bacillus Genomic Stock Center, Columbus, OH) to the shuttle vector pRB374 (Brückner, 1992), using primers gfpF (5'-GGC CAT **CTGCAG** GAA GGA GAT ATA CAT ATG GCT-3') and gfpR (5'-GGC CAT **GAA TTC** GCT CGA ATT CAT TAT TTG TAG-3'). These primers were designed to include Pst I and EcoR I restriction sites (shown in bold) to facilitate cloning. The recombinant plasmid was amplified in *E. coli* DH5a, isolated and transformed into competent *B.*

subtilis cells (wild-type 168 and inducible *pyk* mutant), and transformants were selected on antibiotic medium plates containing 10 mg/L kanamycin for wild-type 168 and 10 mg/L kanamycin plus 0.5 g/L erythromycin for the *pyk* mutant. The transformants were confirmed by restriction digestion of plasmid prepared from the culture, as well as the DNA sequencing.

3.0   CHARACTERIAZATION OF IPYK MUTANT OF *B. SUBTILIS*

3.1   INTRODUCTION

The gram positive bacterium *B. subtilis* has long been used for the chemical production. One common problem happened during fermentation is the production of acidic by-products which limits the product yield and overall productivity. Previous work in our group has identified Pyruvate kinase as a mutation target to reduce acids production (Goel et al., 1995 and 1999; Lee et al., 1997; Phalakornkule et al., 2000). The knockout of *pyk* gene in *B. subtilis* eliminated acetate formation; however, a dramatically reduced cell growth in the glucose minimal medium was observed (Fry et al., 2000). Addition of pyruvate in medium restored the cell growth rate back to that of wild-type level, which indicates that the complete abolishment of pyruvate kinase may result in limited supply of pyruvate to TCA cycle. These findings indicate that the expression level of *pyk* may affect both cell growth rate and acetate production. To obtain an insight of the metabolic responses upon a change in *pyk* expression, an inducible *pyk* mutant of *B. subtilis* was constructed (Zhu et al., 2005; Pan et al., 2006). The relationship among Pyruvate Kinase (PYK) activity, cell growth rate, and acetate formation of the inducible PYK (iPYK) mutant at different induction levels were examined in batch cultures. The results illustrated that a wide range of pyruvate kinase activities in the cultures of the iPYK mutant can be displayed by varying in vitro IPTG concentration. Measurements of cell growth rate and

acetate formation of the iPYK mutant at different induction levels revealed that a PYK activity of about 12% of wild-type allows for good growth rate (0.4 hr^{-1} versus 0.63 hr^{-1} of wild-type), low acetate production (0.26 g/L versus 1.05 g/L of wild-type).

3.2   RESULTS

3.2.1   Pyruvate Kinase Activities at Various Concentration of IPTG in Batch Cultures.

The PYK activities possessed by the wild-type and iPYK mutant at several concentrations of IPTG were measured in batch cultures. Samples were taken during the mid-exponential phase. As given in Table 2, the specific PYK activity exhibited by the iPYK mutant without IPTG present is 0.48 mmol/(g cell·hr), which is only about 3% of that of the wild-type. The PYK activity of iPYK mutant without IPTG present in the medium is similar to that of the *pyk* knockout mutant (data not shown), indicating the leaky expression of PYK in the iPYK mutant is very low. The low leakage concurs with the design of the iPYK mutant. A pMUTIN4 plasmid was used whose promoter Pspac was strongly repressed. Strong repression is provided by using an "oid" operator (Lehming et al., 1987) to facilitate the binding of LacI, and two additional strong terminators (t_1t_2 from *rrnB*) to minimize the transcriptional read-through. Both design elements greatly increased the repression of Pspac in the absence of IPTG (Vagner, 1998) as was confirmed by the nearly zero value of the pyruvate kinase activity without induction (Table 2).

The PYK activity increased significantly when the IPTG concentration was raised from 0.0 to 0.05 mM, and then from 0.05 to 0.2 mM. For the culture supplemented with 1.0 mM IPTG, the pyruvate kinase activity of iPYK mutant reached 18.24 mmol/(g cell·hr), which is similar to the wild-type activity (16.32 mmol/(g cell·hr)). Therefore, the iPYK mutant displays a wide-range of PYK activity to meet the need of this study.

Table 2. PYK activity, cell growth rate, acids of wild-type and inducible PYK of *B. subtilis*

	WT		iPYK Mutant		
IPTG (mM)	0	0	0.05	0.2	1
PYK activity (mmol/(g cell·hr))	16.32 ± 1.92	0.48 ± 0.048	5.02 ± 1.28	12.48 ± 1.25	18.24 ± 2.64
Growth rate (hr-1)	0.63 ± 0.022	0.14 ± 0.003	0.40 ± 0.036	0.58 ± 0.007	0.60 ± 0.165
Acetate (g/L)	1.05 ± 0.130	0.02 ± 0.015	0.26 ± 0.065	0.80 ± 0.018	1.21 ± 0.215
Pyruvate (g/L)	0.38 ± 0.023	0.00	0.06 ± 0.011	0.29 ± 0.017	0.45 ± 0.032
Lactate (g/L)	0.53 ± 0.028	0.00	0.12 ± 0.015	0.41 ± 0.021	0.67 ± 0.033

Both strains were cultivated in glucose minimal medium with 8g/L glucose and iPYK mutant cultures have various dosage of IPTG in the medium. The acetate concentration, PYK activity, and growth rate were measured in three independent experiments. The standard deviations are relatively small as given in the Table.

3.2.2 Cell Growth Rate & Acetate Production in Batch Cultures of Wild-type & iPYK Mutant at Different Induction Levels

The results of cell growth in batch cultures with 8 g/L glucose were shown in Figure 3.1A. The iPYK mutant in the absence of IPTG grew very slowly in the glucose minimal medium with a growth rate of about 0.14 hr^{-1}, which is comparable to the *pyk* knockout mutant (Fry et al., 2002). When the medium was supplemented with 0.05 mM IPTG, the growth rate was significantly increased to 0.42 hr^{-1}. With IPTG concentration of 0.2 mM, the iPYK mutant grew nearly as fast as wild-type (ca 0.63 hr^{-1}). Increasing the IPTG concentration from 0.2 to 1.0 mM did not increase the cellular growth rate, though the PYK activity increased by almost 50% (Table 2). In one experiment the wild type cells were grown in the presence of 1 mM IPTG as a control. As expected, there was no effect of IPTG on growth rate of wild type culture (data not shown).

The concentrations of acetate, lactate, and pyruvate were measured in the last three points on the growth curves of Figure 3.1A. In each case there was a point that displayed the highest concentrations of these by-products. The concentrations of acetate, lactate, and pyruvate found in the points corresponding to the maximum concentrations were given in Table 2. The results indicate that the level of PYK expression influences both cellular growth rate and acetate formation, but how acid formation and growth rate depend on PYK activity differs. Acetate production increases consistently with PYK activity. In contrast, the cellular growth rate reaches a plateau with respect to PYK expression. This disparate behavior provides an advantage because one may control the acetate production at a low level while still maintaining high cell growth rate. This is the case for the iPYK mutant cultured in the presence of 0.05 mM IPTG, which produced 83% less acetate than the wild-type yet maintained a growth rate that is only 30%

lower than the wild-type. In addition to acetate, the concentrations of secreted lactate and pyruvate were also substantially lower in the iPYK mutant grown with 0.05 mM IPTG than the wild-type (Table 2). The cell density of the iPYK mutant grown with 0.05 mM IPTG is about 20% higher than the wild type culture (Figure 3.1A).
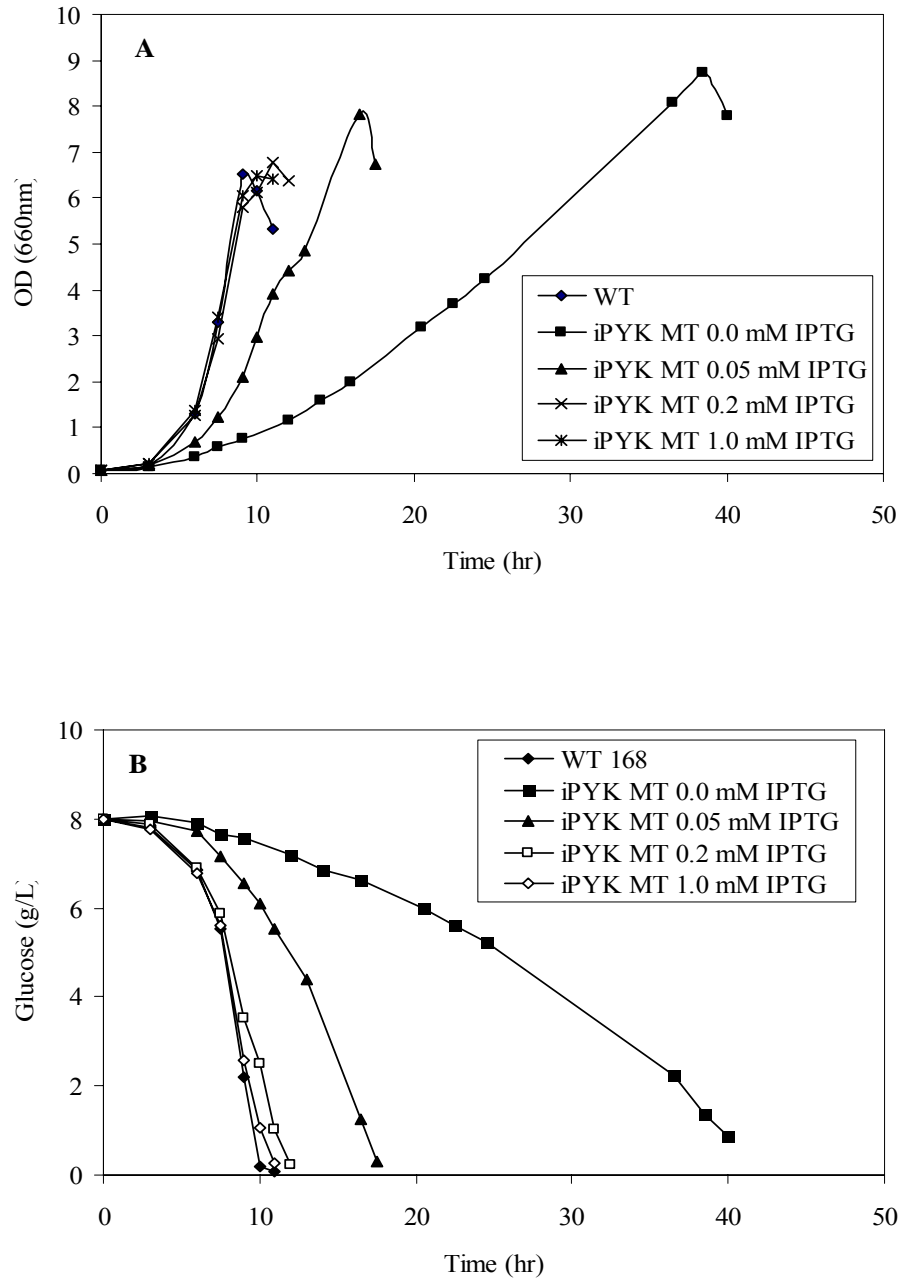
Figure 3.1. Cell growth of wild-type (WT 168) and inducible PYK mutant (iPYK MT) in glucose

minimal medium with 8g/L glucose.

The values are the average of three independent experiments, and the standard deviation is less than 15%. The residual glucose concentration at the end of growth phase was negligible.

3.2.3   Intracellular Metabolite Pools and Acetate Kinase Activity

Because glucose was completely consumed at the end of both cultures (iPYK mutant cultured in the presence of 0.05 mM IPTG and the wild-type) as shown in Figure 3.1B, the glucose consumption rate will be lower for the iPYK mutant with 0.05 mM IPTG than the wild type due to its lower growth rate. Thus, one factor contributing to the lower acetate formation will be the lower glycolytic flux. However, it is possible that regulatory effects of reduced PYK activity on the acetate synthesis pathway may also contribute to the lower acetate production. The measurements of several key metabolites and the acetate kinase activity indicate that low acetate formation in the iPYK mutant is primarily caused by reduced glycolytic flux and not by some regulatory effects on the acetate synthesis pathway due to reduced PYK activity.

The dependence of PEP and glucose-6-phosphate (G-6-P) concentrations on IPTG induction level is shown in Figure 3.2. The concentration of PEP increases as the induction level decreases. The PEP concentration is dramatically higher in iPYK mutant cultivated in the absence of IPTG than that of the wild-type as was the case for the *pyk* mutant (Fry et al., 2000). One important consequence of higher PEP concentration for the iPYK mutant than the wild type is that the PYK flux may not have reduced to the same extent as the PYK activity. Another important consequence of high PEP concentration is its potential effect on glucose uptake rate. Since PEP is an inhibitor of phosphofructose kinase (PFK) in bacteria (Blangy et al., 1968; Doelle et al., 1982; Evans and Hudson, 1979; Hansen et al., 2002), it is conceivable that a high PEP pool will inhibit PFK. PFK catalyzes fructose-6-Phosphate to form fructose-1, 6-biphosphate (FBP), thus the inhibition of PFK may result in high intracellular G-6-P concentrations, and consequently lower glucose uptake by the PTS system. Figure 3.2 shows that indeed G-6-P was significantly higher in the iPYK mutant induced with low levels of IPTG. For

the iPYK mutant in the absence of IPTG, the concentrations of PEP and G-6-P are very high leading to a very low glucose uptake rate as is evident from the low growth rate in the absence of IPTG. Induction of *pyk* expression with 0.05 mM IPTG, also led to higher concentrations of PEP and G-6-P, but the increase was much less pronounced than when there was no IPTG. In the case of induction with 0.05 mM IPTG, good growth rate, high cell yield, and low acetate production were achieved.
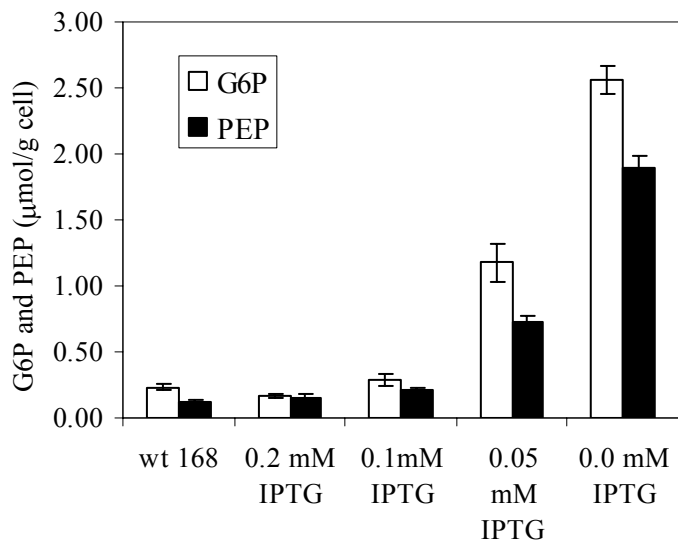
Figure 3.2. Intracellular concentrations of PEP and G6P in batch cultures of iPYK mutant at several IPTG concentrations.

The error bars represent the variations of three measurements. The black column represents the intracellular concentration of PEP and the white column represents intracellular G6P concentration in the exponential growth cells. The metabolites concentrations of wild-type (WT 168) and inducible PYK mutant (iPYK) of *B. subtilis* with various induction levels were presented.

The nil acetate production in iPYK mutant may also result from some regulatory effect on the acetate synthesis pathway. To elucidate if such a regulatory effect exists, the acetate kinase activity was measured in both wild type and iPYK mutant in the absence of IPTG. The measured activities were 0.2 and 0.16 units/mg protein, respectively. Additionally, the intracellular concentration of fructose-1,6-biphosphate (FBP) was measured (Figure 3.3). FBP is required for carbon catabolite activation of genes on the acetate synthesis pathway (Presecan-Siedel et al., 1999). The differences in the acetate kinase activities or the changes in FBP concentrations between the wild type and iPYK mutant are not significant enough to cause several fold reduction in acetate production. Thus, it is highly likely that the decrease in glycolysis flux is the key factor contributing to the decreased acetate formation. In addition, the intracellular of pyrvate is closely related to the induction level of pyruvate kinase, and figure 3.3 showed that pyruvate, a precursor for lactate and acetate, was very low when the induction level is low. The significant decrease in formation of other acidic products (lactate and pyruvate, Table 2) should also be caused by the lower glycolysis flux of the iPYK mutant.
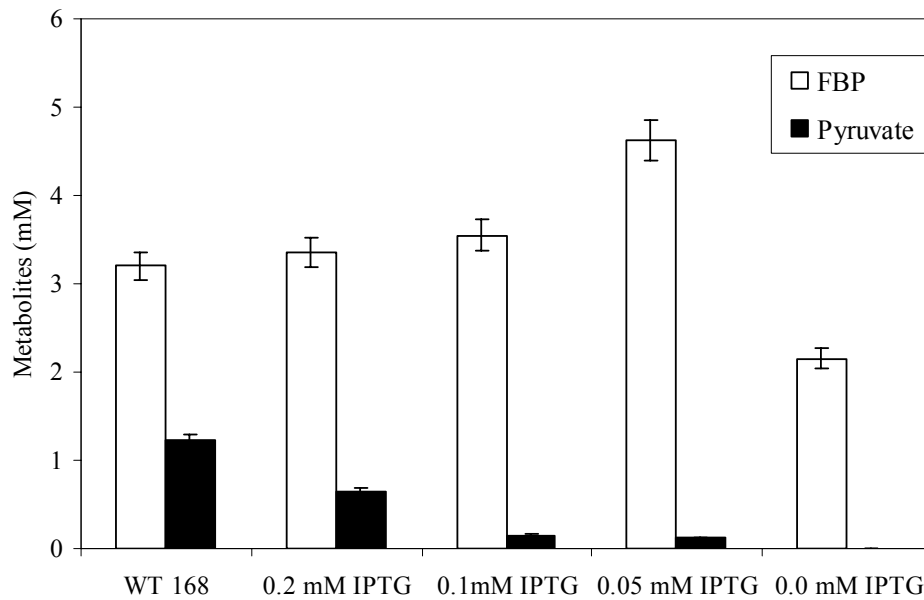
Figure 3.3. Intracellular concentrations of Pyruvate and FBP in batch cultures of iPYK mutant at several IPTG concentrations.

The error bars represent the variations of three measurements. The intracellular concentrations of fructose-1,6-biphosphate (FBP) and pyruvate of iPYK mutant at various induction levels represented by IPTG concentration were presented in the same figure with wild-type (WT 168) for comparison.

3.2.4 Metabolic Flux Analysis.

To calculate metabolic fluxes, a set of continuous cultures were carried out. The continuous culture data at dilution rate of 0.3 hr^{-1} were used to calculate the metabolic fluxes. Data for cell mass, glucose consumption, CO_2 and acids were collected after the cultures reached steady state at dilution rate of 0.3 hr^{-1}, as shown in Table 3. A detailed stoichiometric approach was used to calculate the carbon flux through the central carbon metabolic pathways (Goel et al., 1995; Zhu et al., 2003). All metabolic intermediates are assumed to be at the pseudo-steady-state (no accumulation of metabolic pools).

Infinite feasible solutions exist due to the degeneracy of problem. Using the MILP method or the convex analysis method (Zhu et al., 2003), extreme points of solution space at different culture conditions were found. Glucose consumption rate and acid formation rates were used in the calculation.

At different IPTG levels, two extreme solutions were obtained. The actual fluxes will be between these two values. A sample set of the metabolic fluxes of wild-type and iPYK mutant at three levels of induction is placed in Table 4. The PYK fluxes of iPYK mutant at 0.05 mM IPTG are quite lower than the iPYK mutant at higher level of induction (0.2 and 1.0 mM IPTG) and wild-type. This lower level of PYK flux for the iPYK mutant with 0.05 mM IPTG corresponds to lower pyruvate kinase and acetate production than the iPYK mutant at higher level of IPTG and the wild type.

Table 3. Continuous cultures of wild-type and iPYK mutant at different levels of IPTG in minimal medium

supplemented with 5 g/L glucose at dilution rate of 0.3 hr^{-1}

	Wild type	iPYK mutant		
IPTG	0	0.05	0.2	1
OD	2.23	2.64	2.43	2.27
Glucose consumed	2.65	2.36	2.75	2.88
Acetate	0.90	0.35	0.69	0.87
Pyruvate	0.12	0.04	0.22	0.29
Biomass yield*	0.37	0.49	0.39	0.34
Acids yield*	0.38	0.17	0.33	0.40
CO$_2$ yield*	0.28	0.41	0.30	0.33

* Biomass yield is defined as the carbon content in the cell mass divided by the carbon in consumed glucose. Acids yield is defined as the carbon content in acids (both acetate and organic acids) divided by the carbon in consumed glucose. CO$_2$ yield is defined as the carbon content in CO$_2$ divided by the carbon in consumed glucose.

Table 4. PYK fluxes of wild-type and inducible *pyk* mutant with different levels of induction

	WT		iPYK Mutant		
IPTG (mM)	0	0	0.05	0.2	1
PYK fluxes (mmol/(g.hr))	3.39-4.09		2.28-2.69	3.29-3.28	3.84-4.47

The data for the flux analysis was obtained from the continuous cultures for both wide-type (WT) and inducible PYK (iPYK) mutant at dilution rate of 0.3 hr^{-1}. The metabolic flux was calculated using the metabolic flux analysis software Metabologica (Zhu et al., 2003).

3.2.5 Inducible Phosphofructokinase (iPFK) Mutant of *B. subtilis*.

Our study with iPYK mutant of *B. subtilis* demonstrates that the PYK expression is closely related to glucose uptake, cell growth and acetate production. The PYK mutation reduces glucose uptake rate and glycolysis flux through a regulatory effect upon glycolysis pathway (Figure 3.4). Reduced PYK expression resulted in elevated intracellular PEP which inhibited the upstream enzyme PFK, and the inhibition of PFK resulted in the accumulation of G-6-P. G-6-P was reported to speed up the degradation of mRNA of *ptsG* (Morita et al., 2003) therefore reduce glucose uptake rate. Based on this hypothesis, the glucose uptake can be manipulated directly by modifying the expression level of PFK. Therefore, an inducible PFK mutant was constructed and its effect on glucose consumption, cell growth and acetate formation was investigated.
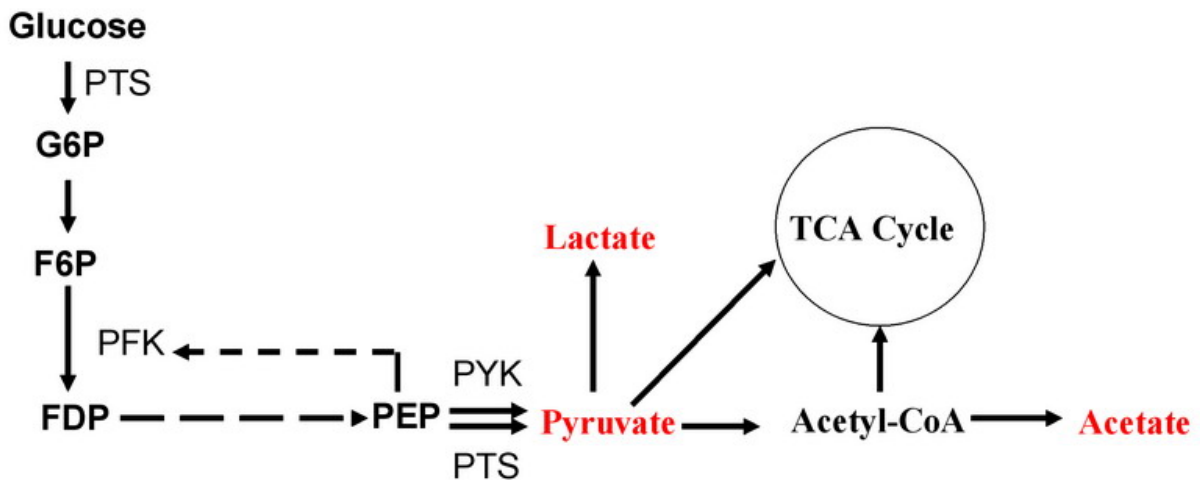
Figure 3.4. Regulatory effects of PYK mutation on glucose uptake and glycolysis flux.

iPFK mutant was grown in glucose(8g/L) minimal medium with various IPTG supply. Figure 3.5 shows PFK activity at each induction level and PYK activities for uninduced and fully induced cultures. Activity of PFK is closely related to IPTG concentration in the iPFK mutant, following a similar pattern as that of PYK activity to IPTG concentration in the iPYK mutant. When there is no IPTG, the iPFK mutant still has 60% activity of PYK compared to wild-type. It was surprising that PFK and PYK expression responded to IPTG differently as both genes are in the same operon. These results indicate that the coordination of expression of *pfk* and *pyk* is disrupted by replacing the wild-type promoter with inducible promoter P_{spac} (Andersen et al., 2001). The low concentration of PEP in iPFK mutant with different induction levels also supported that PYK was expressed in considerate amount at the absence of IPTG (Figure 3.6).
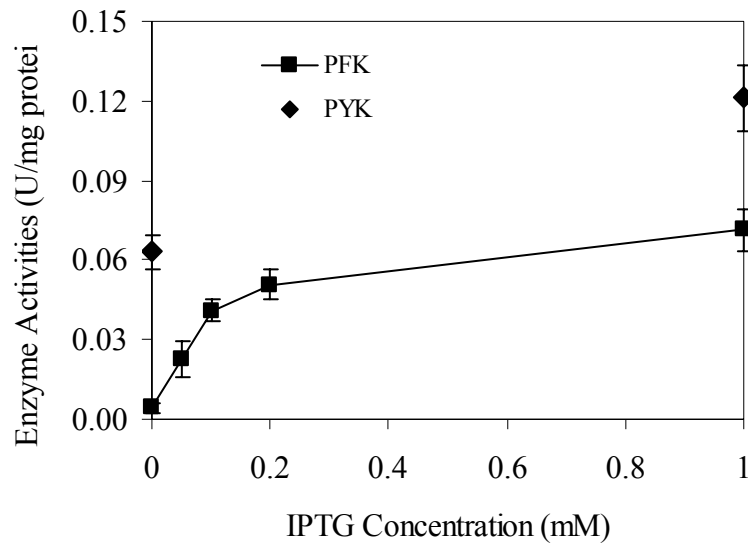
Figure 3.5. Specific activities of phosphofructokinase (PFK) and pyruvate kinase (PYK) in iPFK mutant

52
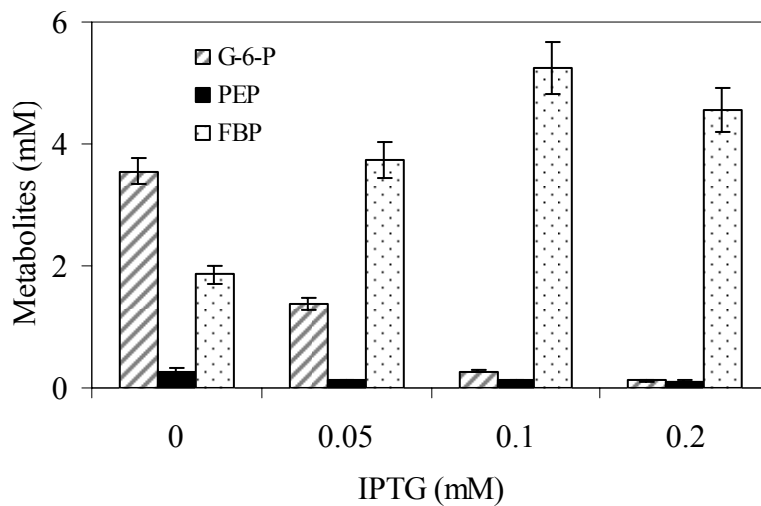
Figure 3.6. The concentrations of intracellular metabolites in iPFK mutant at various induction levels.

The intracellular metabolites were measured for exponential growth cells. G-6-P: Glucose-6-phosphate; PEP: Phosphoenolpyruvate; FBP: Fructose-1,6-biphosphate

The cell growth, glucose consumption and acetate production rates of iPFK mutant at various induction levels of PFK are shown in Figure 3.7. These results demonstrate that cell growth, glucose consumption, and acetate production rates are closely related to the expression level of PFK. Therefore, we can control glucose uptake rate by manipulating either PFK or PYK expression in *B. subtilis*. From the comparison of iPFK and iPYK mutants, we also found that it is G-6-P that determines the glucose uptake and cell growth rates. Though PEP may also have some regulatory effect on glucose transport, its effect is minor as compared to G-6-P.
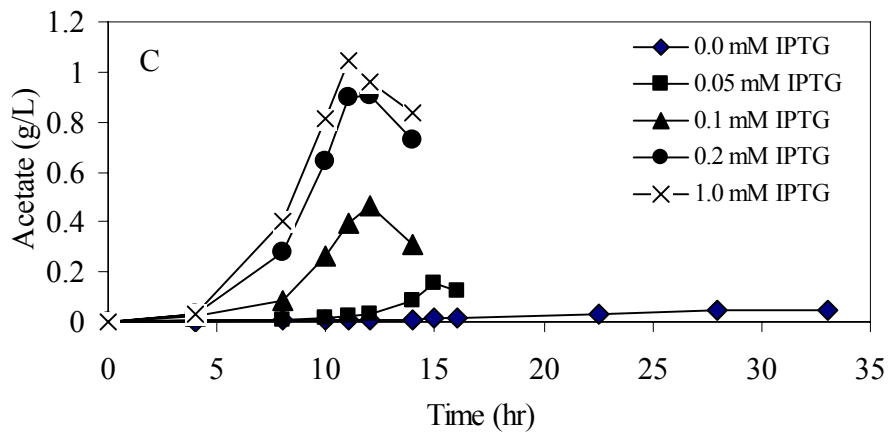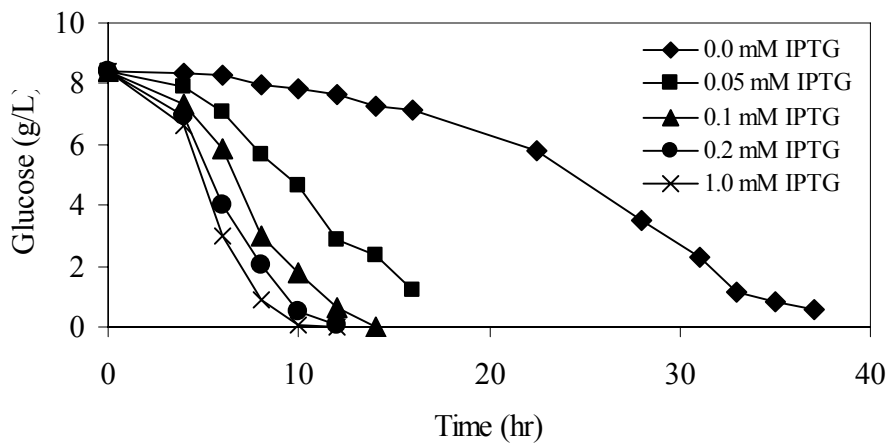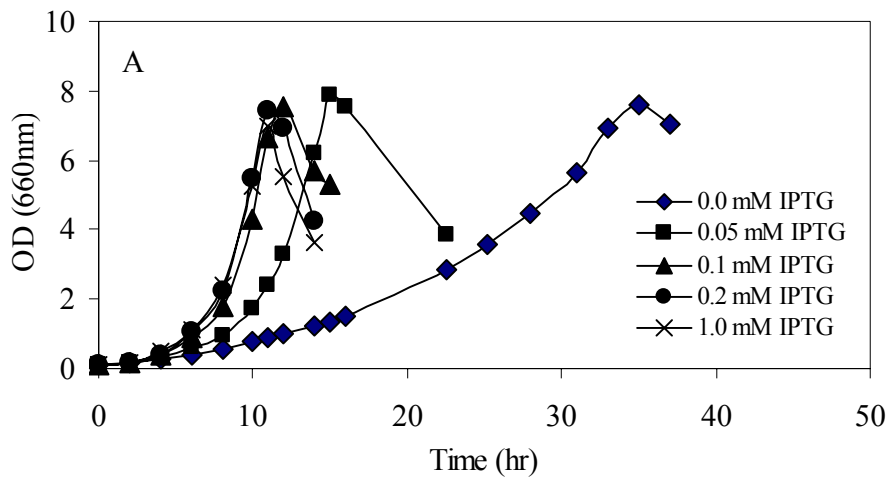
Figure 3.7. Batch cultures of iPFK mutant in minimal medium with 8 g/L glucose and various IPTG

concentrations.

(A) Cell growth, (B) glucose consumption, (C) acetate production.

54

4.0   RECOMBIANT PROTEIN PRUDUCTION

4.1   INTRODUCTION

Previous work has demonstrated that acetate production was eliminated after the *pyk* mutation in *B. subtilis*. The acetate production was frequently reported to have detrimental effect on recombinant protein production (George et al., 1992; Jensen and Carlsen, 1990; Hahm et al., 1994) and strategies led to reduced acetate formation usually resulted in improved recombinant protein production (Aristidou et al., 1995; Jaoon et al., 2003; March et al., 2002). Therefore, we investigated the impact of *pyk* mutation on recombinant protein production. GFP+ was selected as a model protein and constitutively expressed in both wild-type strain and inducible *pyk* mutant.

4.2   RESULTS

4.2.1   Comparison of GFP+ Production in Wild-type and Inducible PYK Mutant Grown in Glucose Minimal Medium

To investigate how the change of PYK flux affects recombinant protein production in *B. subtilis*, we introduced a plasmid bearing *gfp+* gene into both the inducible PYK mutant and the

wild-type *B. subtilis*, resulting in two GFP+ production strains, i.e., MTpGFP+ and WTpGFP+. The expression of GFP+ in these strains was under the control of the constitutive *B. subtilis vegII* promoter of pRB374. The production of GFP+ from each strain in batch cultures in minimal medium with 5 g/L glucose was compared. As shown in Figure 4.1, GFP+ was constitutively expressed during the cultivation in a partially growth related fashion. The growth rate of uninduced MTpGFP+ (0.15 hr^{-1}) was about 30% of the WTpGFP+ (0.51 hr^{-1}), but its total GFP+ production in the culture of MTpGFP+ is 3-fold higher than that of the wild-type culture (WTpGFP+). On a per cell basis, MTpGFP+ also produced 100% higher GFP+ as represented by the fluorescence intensity (Table 5). Additionally, uninduced WTpGFP+ produced about 0.72 g/L acetate while MTpGFP+ produced about 80% less acetate. As expected, the inclusion of 0.05 mM IPTG in the cultures of MTpGFP+ did not lead to significant increase in acetate production, but the GFP+ production was substantially lower than the uninduced culture.

Considering the specific GFP+ production rate (GFP+/(time·cell)) as it is represented as RFU/OD/hr in Table 5, it is 15% higher in MTpGFP+ cultures both uninduced or induced with 0.05mM IPTG than that in the WTpGFP+ culture. This analysis shows that despite significantly lower growth rate, the specific production rate of the mutant is similar to the wild-type. Assuming the turnaround time for a batch culture is 10 hour; the average production rate is 10 RFU/hour for WTpGFP+ and 17.8 RFU/hour for MTpGFP+. Thus, in terms of both volumetric production rate and product concentration, the uninduced MTpGFP+ is superior for protein production. Moreover, when high cell density fed-batch cultures are considered, the mutant performance may even be much more pronounced given that its low acetate production rate would limit total acetate production and hence minimize the inhibitory effect of acetate at high concentrations. Furthermore, it is likely that under conditions that very high levels of protein

expressions are examined the mutant could devote more biosynthetic resources to the recombinant protein production due to lower levels of acetate production.

The high GFP+ production in MTpGFP+ may be due to the following factors: (1) slower growth rate and longer culture time, leading to longer production time; (2) change of amino acid pools after down-regulating *pyk* as the *pyk* mutation leads to the redistribution of carbon and energy among central carbon metabolism pathways. (3) slower degradation of GFP+ by proteases considering the lower ATP flux/higher ATP yield in the *pyk* mutant; (4) lower acetate production, as it is widely accepted as a factor that limits recombinant protein production; (5) more stable plasmid in the iPYK mutant; (6) elevated intermediate metabolites (PEP and G6P) which may exert regulatory effect on GFP+ expression. Each factor will be elaborated in the following sections.

Table 5. Summary of batch cultures of wild-type (WTpGFP+) and iPYK mutant (MTpGFP+) bearing pGFP+ in minimal medium with 5 g/L glucose

	Maximal OD660nm	Acetate (g/L)	RFU/OD	μ hr^{-1}	RFU/OD/hr
WTpGFP	3.76	0.72	59	0.51	7.2
MTpGFP+ with 0.05mM IPTG	3.85	0.31	78	0.15	8.1
MTpGFP+	4.25	0.15	116	0.37	8.2

RFU: Relative Fluorescence Unit.
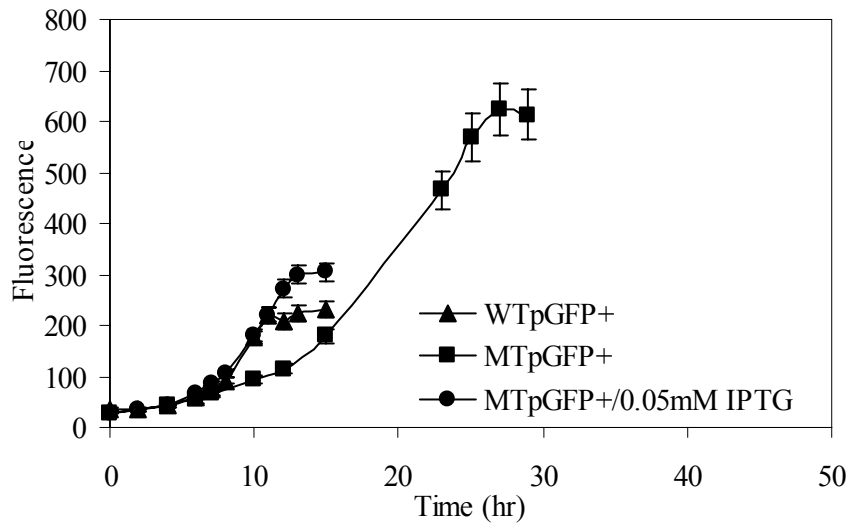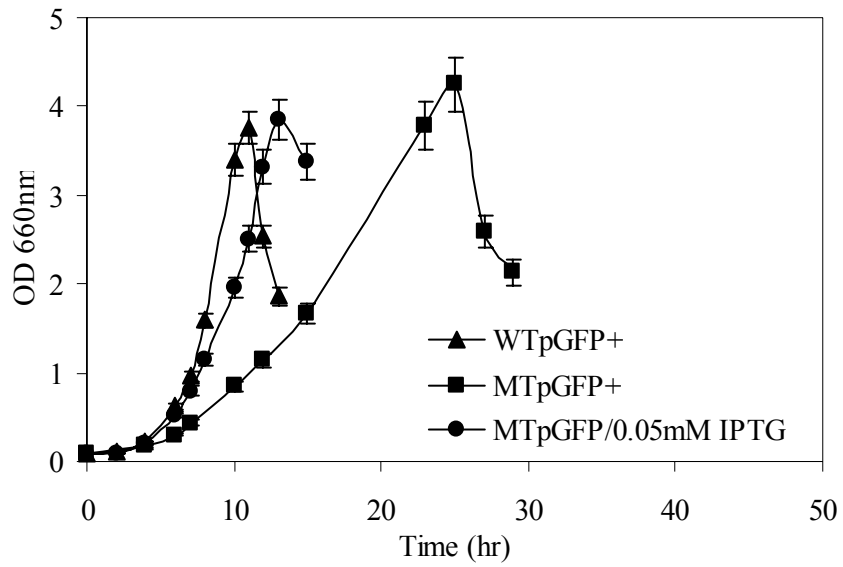
Figure 4.1. Cell growth and GFP+ production in batch cultures of wild-type strain (WTpGFP+) and inducible *pyk* mutant (MTpGFP+) in glucose (5 g/L) minimal medium.

MTpGFP+/0.05mM IPTG: 0.05mM IPTG was added in the medium at the beginning of MTpGFP+ culture.

4.2.2   GFP+ Stability

The difference of GFP+ production in WTpGFP+ and MTpGFP+ may result from both the synthesis side and/or degradation side. *B. subtilis* usually produces a lot of proteases which limit the yield of heterologous proteins. Many of these proteases are ATP-dependent (Nakano, et al., 2002; Wehrl et al., 2000). The iPYK mutant shows much higher ATP yield from the metabolic flux analysis, and the low energy level is favorable for the recombinant protein production since protein turnover via ATP-stimulated proteases is suppressed. To test if protein degradation is indeed a factor, we monitored the stability of GFP+ in the medium. 10 mL late-exponential phase cultures was filtered with 0.45 μm disposable filters, and the filtrate was kept at room temperature for a couple of days. No significant change of fluorescence in the cell-free medium was observed, indicating GFP+ is very stable and has strong resistance to protease-mediated degradation, which is consistent with other reports (Hoskins and Wickner, 2006; Roth and Ward, 1983). Therefore, higher recombinant protein production in MTpGFP+ more likely results from synthesis side factors.

4.2.3   Gene Expression Levels in WTpGFP+ and MTpGFP+

The accumulation of acetate is widely accepted to have inhibitory effect on recombinant protein production (Jensen and Carlsen, 1990; Hahm et al., 1994; Huang et al., 2004). However, the mechanism of the detrimental effect of acetate on cell growth and recombinant protein production remains unclear. Acetate may potentially affect transcription or translation processes or both of them. To better understanding this process, the gene expression levels of WTpGFP+ and MTpGFP+ was measured using quantitative RT-PCR. Figure 4.2 shows the relative mRNA

levels of *gfp+* in cells harvested in the exponential growth phase. The image analysis of band intensity shows that the mRNA levels for WTpGFP+ and MTpGFP+ are almost same. Therefore, the higher GFP+ production, which corresponds to lower acetate production, is probably due to the higher efficiency of translation based on our results in this study. Recent evidence showed that high glucose concentration which corresponds to acetate-forming conditions also activates the methyl glycoxalate pathway in bacteria (Weber et al., 2005). The methyl glyoxalate pathway, which converts dihydroxyacetone phosphate (DHAP) to pyruvate via methylglyoxal and D-lactate, may short-cut the glycolysis pathway and lead to limited energy (ATP) supply for biosynthesis. In addition, methyl glyoxalate itself is a highly toxic compound and may adversely react with deoxyribonucleic acid (DNA), ribonucleic acid (RNA) and proteins (Lo et al., 1994; Papoulis et al., 1995).
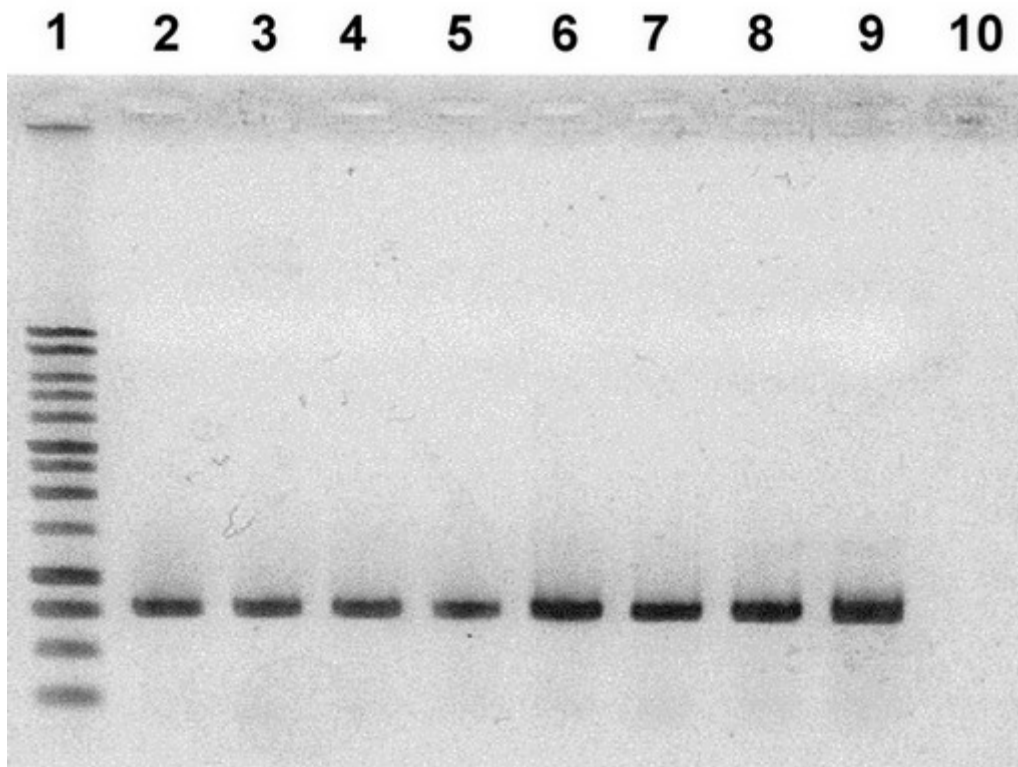
Figure 4.2. mRNA levels of WTpGFP+ and MTpGFP+.

From left to right: lane 1, Marker; lane 2&3, WTpGFP+; lane 4&5, MTpGFP+; lane 6&7, 2× WTpGFP+; lane 8&9, 2× MTpGFP+; lane 10, Control.

4.2.4 Effect of Acetate in the Medium on GFP+ Production

The inhibitory effect of acetate on cell growth and recombinant protein production in *E. coli* usually occurred in the range of 3 ~5 g/L (Aristidou et al., 1995; Luli and Strohl, 1990). For some species and proteins, the inhibitory concentration of acetate could be even lower. Huang et al. (2004) reported that addition of 1g/L acetate seriously inhibited cell growth and that concentrations as low as 0.1 g/L acetate in the medium could be sufficient to significantly repress amylase production in a recombinant *B. subtilis* strain. To investigate if the accumulation of acetate in the medium limited the protein production, WTpGFP+ was cultivated in glucose minimal medium supplied with varying amount of sodium acetate. The results show that the addition of acetate in the medium up to 2 g/L has no remarkable effect on both cell growth and recombinant protein production (Figure 4.3). In previous batch cultures, acetate never accumulated to more than 1 g/L in the medium, therefore, the lower GFP+ production in our wild-type strain WTpGFP+ was not due to a higher concentration of accumulated acetate in the medium. Instead, acetate production rate may be the key factor affecting protein synthesis which seems to be very sensitive to the redirection carbon flow from acetate production to protein synthesis (March et al., 2002).
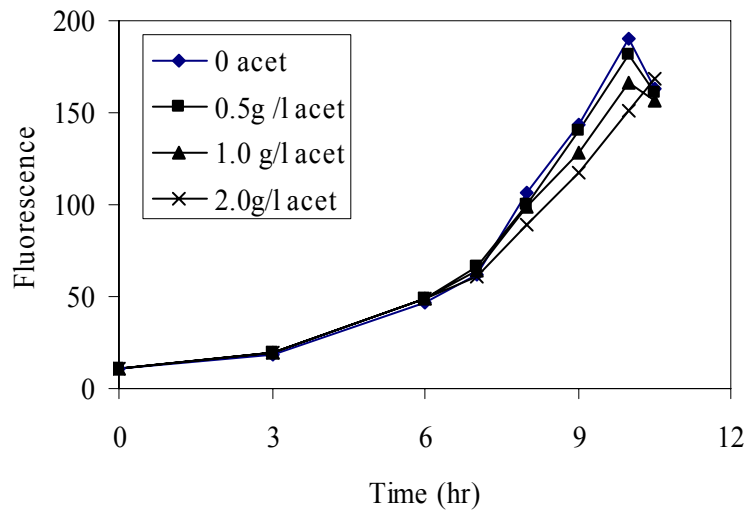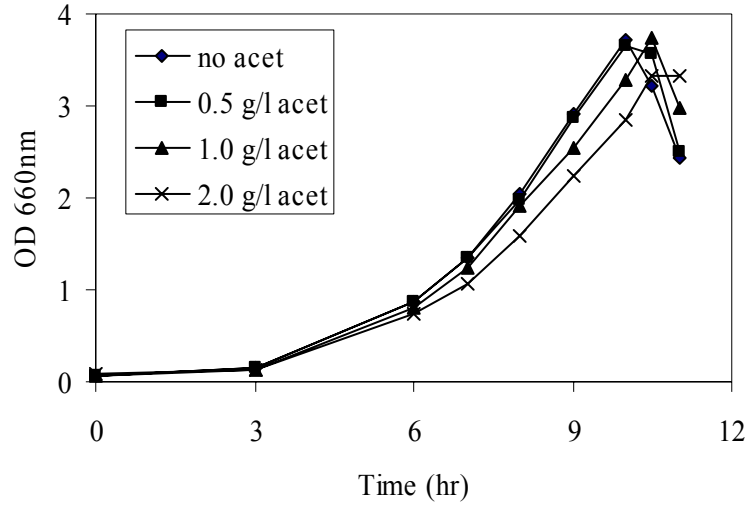
Figure 4.3. Effects of acetate in the medium on cell growth and protein production of WTpGFP+.

The glucose (30 mM) minimal medium was supplemented with 0.0, 0.5, 1.0, and 2.0 g/L sodium acetate.

4.2.5   Metabolic Modeling of Potential Recombinant Protein Production

Previous results implied that recombinant protein synthesis seems to be very sensitive to the acetate production rate. In MTpGFP+, less acetate was produced which could permit a greater surplus of metabolic resources to be directed toward protein synthesis. To explore this possibility, metabolic flux calculations were performed. A stoichiometric model of the central carbon metabolism of *B. sbutilis* was built using the software Metabologica (Zhu et al., 2003). Glucose was the sole source of carbon and energy, and carbon was allowed to exit the network through CO2 evolution, byproduct (acetate, lactate, pyruvate, succinate) formation, and biomass synthesis. The model assumes that all metabolic intermediates are at the pseudo-steady-state (no accumulation of metabolic pools). Additionally, constraints such as net NADPH formation for reductive biosynthesis and minimum ATP requirements are included in the model formulation. These constraints limit the metabolic trafficking alternatives as well as insure that a particular solution is physiologically feasible. Finally, a reaction for GFP+ synthesis was built to determine how sensitive GFP+ production is to the change of flux to acidic byproducts (Figure 4.4). The amino acid composition of GFP+ was determined from the translation table presented at open source NCBI (Accession No. CAH64882), and the overall stoichiometry of metabolic precursors for GFP+ synthesis was taken as that presented at Table 6. Information about metabolite and energy requirements for the production of each amino acid and peptide bond was obtained from the literature (Vijayasankaran et al., 2005). To find all feasible solutions, glucose uptake and CO_2 evolution rates, as well as by-product production rates were not constrained in the model. Then the software Metabologica was used to solve the model for all metabolic trafficking alternatives meeting the specific constraints and assuming a dilution rate of 0.3 hr^{-1}.

Table 6. Metabolic synthesis requirement for the production of GFP+

R5P, Ribose-5-phosphate; E4P, Erythrose-4-phosphate; PEP, Phosphoenol pyruvate; 3GP, 3-phosphoglycerate; AcCoA, Acetyl coenzyme A; α-KG, α-ketoglutarate; OAA, Oxaloacetate.

Amino Acid	Moles	R5P	E4P	PEP	3GP	Pyruvate	AcCoA	α-KG	OAA	ATP	NADH	NADPH
Alanine	9					9						9
Arginine	7							7		49	-7	28
Asparagine	13								13	39		13
Aspartate	18								18			18
Cysteine	2				2					8	-2	10
Glutamate	16							16				16
Glutamine	7							7		7		7
Glycerine	22				22						-22	22
Histidine	10	10								60	-30	10
Isoleucine	12					12			12	24		60
Leucine	20					40	20				-20	40
Lysine	20					20			20	40		80
Methionine	5								5	35		40
Phenylalanine	11		11	22						11		22
Proline	10							10		10		30
Serine	11				11						-10	10
Threonine	17								17	34		51
Tryptophan	1	1	1	1						5	-2	3
Tyrosine	11		11	22						11	-11	22
Valine	16					32						32
peptide bond										952		
GFP+	238	11	23	45	35	113	20	40	85	1285	-104	523

65
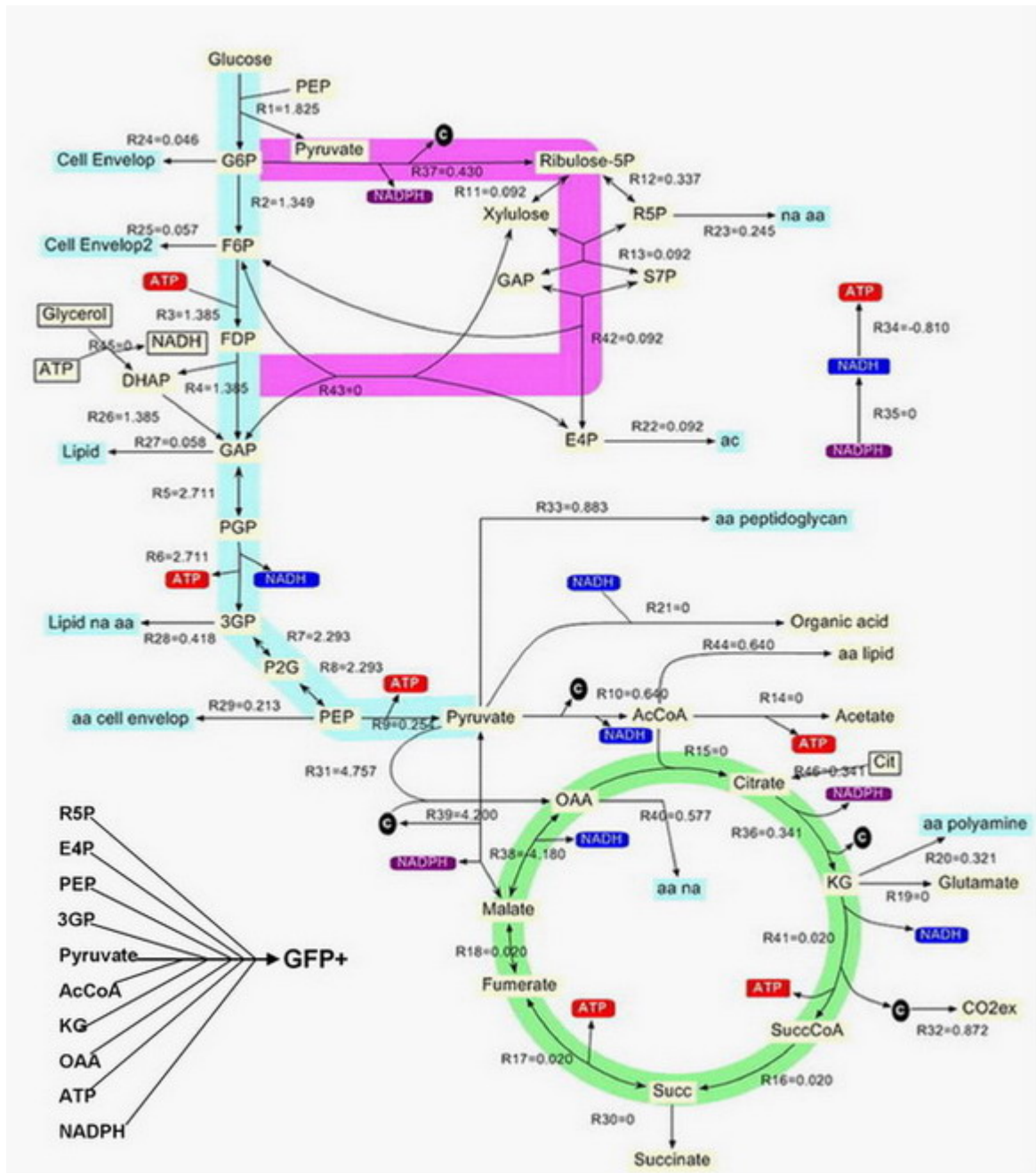
Figure 4.4. The metabolic reaction network of *B. subtilis* used for the modeling of potential recombinant protein synthesis

Twenty-eight different feasible solutions were found to exist. The GFP+ flux and corresponding acids flux (mmol/(g cell·hr)) for those solutions were plotted in the phase plane (Figure 4.5). Any point inside the bounded region is a feasible solution. Overall, the modeling determined what the maximum GFP+ production rate could be at each acid formation rate. Figure 4.5A demonstrates that the maximum GFP+ production rate is limited at high acetate formation rate. Perhaps the more interesting finding is the relationship between GFP+ flux and PYK flux. GFP+ production was limited at both the high and low end of PYK flux (Figure 4.5B), however, our experimental data showed that GFP+ production was higher at low levels of PYK activity. This discrepancy may be resulted from the assumptions we have made during the modeling. In this model, we have not included the reaction between phosphoenolpyruvate (PEP) and Oxaloacetate (OAA). When PYK activity is low, the phosphoenolpyruvate carboxykinase (PCK) may operate at the direction from PEP to OAA (Zamboni et al., 2004; Pan et al., 2006). When PCK is operative, our modeling results showed that the maximum GFP+ production capacity was attained at the low end of PYK flux (Figure 4.5C). The correlation of GFP+ flux versus acid flux with PCK included is similar to Figure 4.5A.
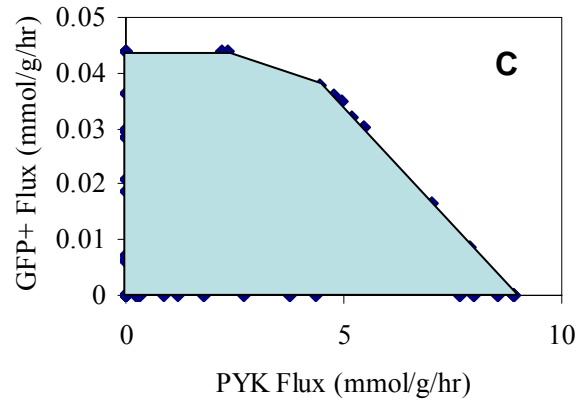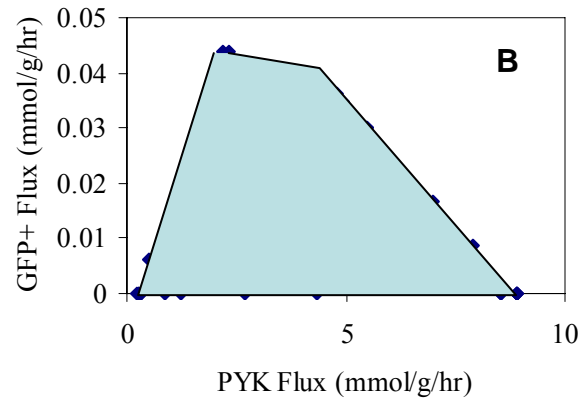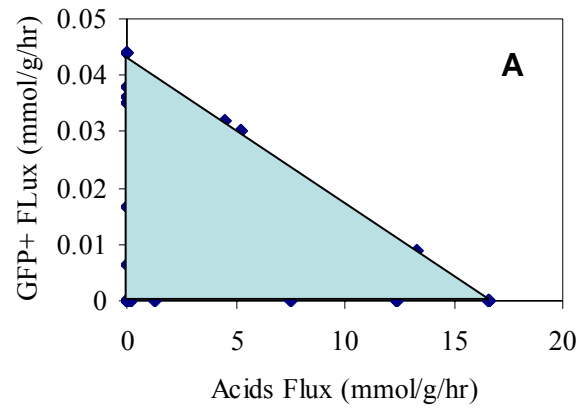
Figure 4.5. Solution spaces for GFP+ production.

A and B: the phosphoenolpyruvate carboxykinase (PCK) was not included; C: PCK catalyzed reaction was included.

4.2.6   GFP+ Production in Semi-Rich Medium

Given that the specific GFP+ production rate is similar between wild type and mutant despite the significant differences in growth rate, an interesting question is how the production rates will be affected in cultures supplemented with biosynthetic precursors. The recombinant GFP+ production of WTpGFP+ and uninduced MTpGFP+ cultures in glucose (5 g/L) minimal medium with 2 g/L LB was compared. LB is composed of 20% yeast extract, 40% tryptone and 40% sodium chloride. The amino acid components in LB should partially provide precursors for protein synthesis therefore lessen the burden of amino acids that need to be supply from glucose catabolism. As shown in Figure 4.6, the addition of LB increased both cell growth and GFP+ production rates, however, both WTpGFP+ and MTpGFP+ produced similar amount of protein to their counterparts in glucose minimal medium (Figure 4.1) at the end of growth period. These results may suggest that both WTpGFP+ and uninduced MTpGFP cultured with glucose as the only carbon source (Figure 4.1) are translating the *gfp+* transcripts at their maximum capacity and that it is the availability of biosynthetic precursors not the growth rate that determine the specific production rate of GFP+.
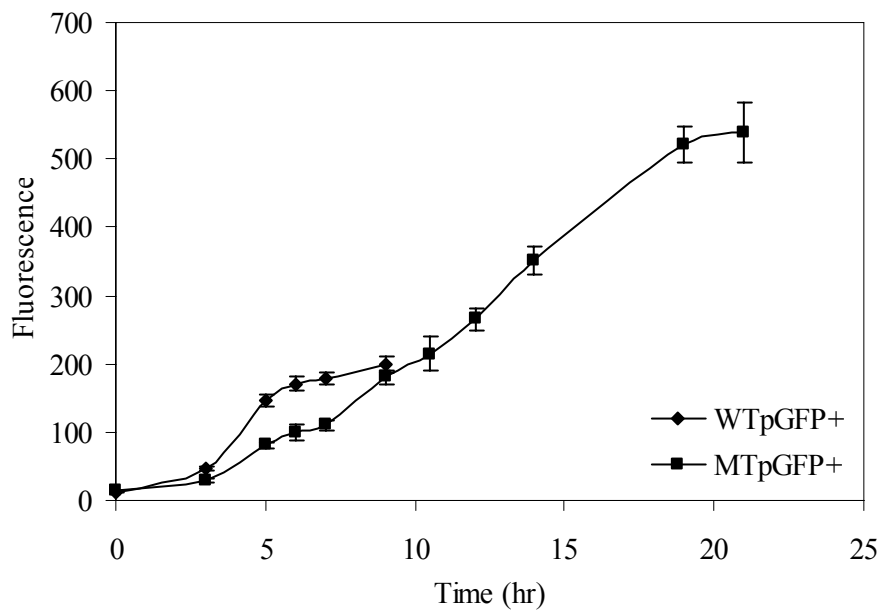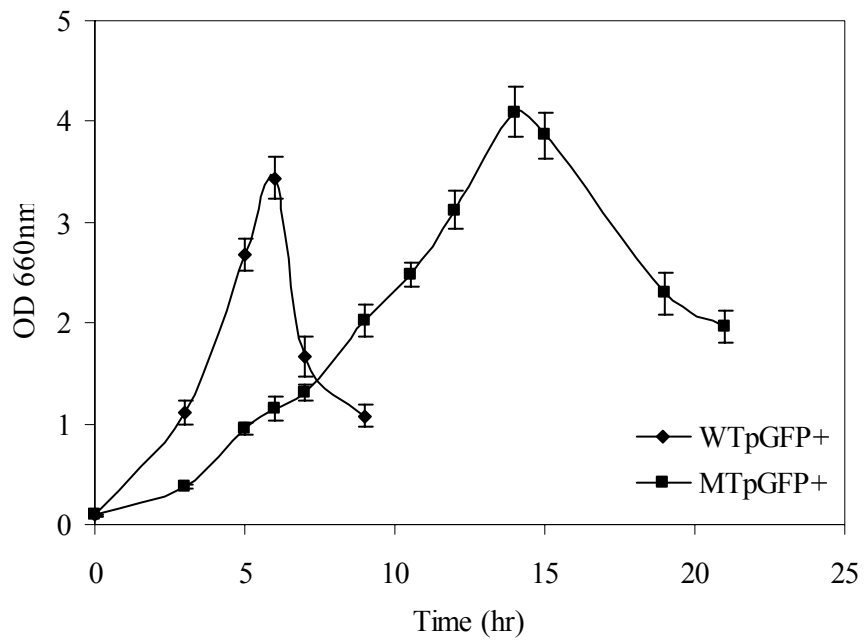
Figure 4.6. Cell growth and GFP+ production in batch cultures of WTpGFP+ and MTpGFP+ in semi-rich medium(C medium with 5 g/L glucose and 2 g/L LB).

4.2.7   Effect of Carbon Sources on Recombinant Protein Production in Batch Cultures of WTpGFP+

Pyruvate is supplied from both phosphoenolpyruvate (PEP)-sugar phosphotransferase system (PTS) and PYK when a PTS sugar such as glucose is employed as a carbon source. Besides PYK mutation, pyruvate supply can also be reduced by inactivating the PTS (Chen et al., 1997) or by using a non-PTS substrate as carbon source, which should potentially reduce acetate formation and improve recombinant protein production. To test this hypothesis, the GFP+ expression of WTpGFP+ cultivated with either glucose or glycerol as the sole carbon source was compared. WTpGFP+ was grown in minimal medium supplemented with 5g/L glucose or glycerol, and their respective cell growth rate, acetate accumulation and recombinant protein production were compared. As shown in Figure 4.7, the culture with glycerol grew as fast as the culture with glucose. In addition, the glycerol culture obtained a 35% higher maximum cell density and 60% less acetate. Moreover, the expression of recombinant protein GFP+ is 60% higher in the culture with glycerol as compared to that of the culture with glucose. The glycerol culture also showed higher GFP+ production per cell and higher productivity. The high GFP+ production in glycerol minimal medium may be due to lower acetate formation. In addition, the cells (*E. coli*) grown in glycerol medium may have greater tolerance to acetate than those grown in glucose (Lasko et al., 2000). The differences amongst carbon sources are even more prominent at high concentrations. Cultures of WTpGFP+ in minimal medium with 20 g/L glycerol produced 150% more GFP+ as compare to cultures with 20 g/L glucose (data not shown).
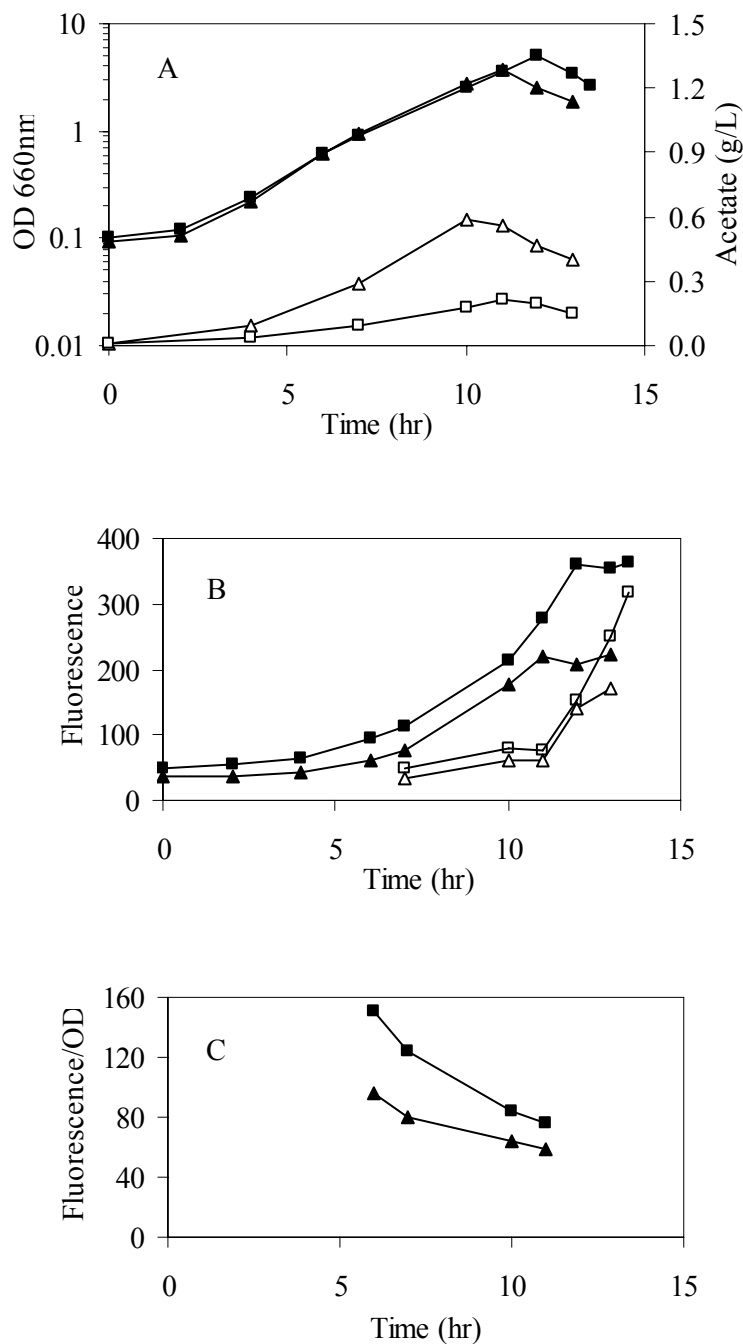
Figure 4.7. Cell growth, acetate formation and GFP+ production of WT168pGFP+ in C medium with 5g/L glucose (Triangle) or glycerol (Square).

(A) Cell density (solid symbols) and acetate (open symbols), (B) total fluorescence (solid symbols) and medium fluorescence (open symbols), (C) fluorescence per optical density.

5.0   FOLIC ACID PRODUCTION

5.1   INTRODUCTION

The bulk of commercially sold folic acid is currently produced via chemical synthesis due to the low yield of folic acid provided by current microbes. Several reasons, however, have prompted new exploration into using microbes for the commercial production of folic acid. First, the glutamated and reduced form of the natural vitamin produced by bacteria produce is what the digestive system designed to process. Secondly, a single-step fermentation route is more environmentally benign than a multi-stage chemical process. Thirdly, the yield of folic acid production could be dramatically improved by metabolic engineering the production strain. One of the potential production strains is *B. subtilis*. In addition to its "generally regarded as safe" status by FDA, *B. subtilis* has been successfully used to produce these products metabolically related to folic acid such as D-ribose (De Wulf and Vandamme, 1997) and riboflavin (Perkins et al., 1999). Two outcomes of PYK mutation in *B. subtilis*, low acetate and high PEP and G-6-P concentration, may potentially improve the productivity of folic acid. While low acetate formation may help reach high cell density, high PEP and G-6-P may improve folic acid synthesis by providing precursors. We hypothesis the PYK expression level will significantly affect folic acid production. Both metabolic flux prediction and experimental measurement will be conducted to test this hypothesis.

5.2   RESULTS

5.2.1   Network Model and Flux Predictions

A stoichiometric model of the central carbon metabolism with a lumped reaction leading to folic acid was built using the software Metabologica (Zhu et al., 2003). A reference specific growth rate of 0.4 h^{-1} was used to generate flux units (e.g. mmol g $cell^{-1}$ h^{-1}). The overall stoichiometry inputted into Metabologica for the lumped reaction that leads to folic acid (FA) production is

$$2PEP + E4P + 2\ 3\text{-}PG + KG + 11ATP + R5P + 4NADPH \rightarrow FA + PYR + CO_2$$
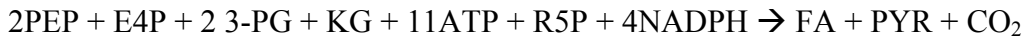
where PEP (phosphoenolpyruvate), E4P (erythrose-4-phosphate), 3-PG (3-phosphoglyceric acid), KG (oxoglutarate), R5P (ribose-5-phosphate), and PYR (pyruvate) are both FA precursors and intermediate metabolites present in central carbon metabolism. We found that 32 different feasible solutions exist for the growth of folic-acid producing *B. subtilis* in glucose minimal medium. The use of phase plane-like graphical displays provides a means for exploring the effect of *pyk* mutation (Figure 5.1), where PYK-catalyzed flux is the X dimension and folic acid flux is the Y dimension. Any point inside the bounded region is a feasible solution. The maximum folic acid synthesis rate increases linearly as the PYK catalyzed flux decreases to zero. The geometry of the phase plane boundary also suggests that as PYK flux decreases to zero, solutions that yield high folic acid productivity still exist.

These solutions indicate that highly attenuated PYK flux may be associated with a metabolically feasible and high folic acid-yielding scenario. The concentration of the folic acid precursors, PEP and 3-PG, may increase due to a downstream blockage in consumption, and this increase could stimulate folic acid synthesis. Accordingly, the modeling results and envisioned

74

mass action consequences suggest that a strategy based on decreasing PYK flux may work in *B. subtilis* (Zhu et al., 2005).
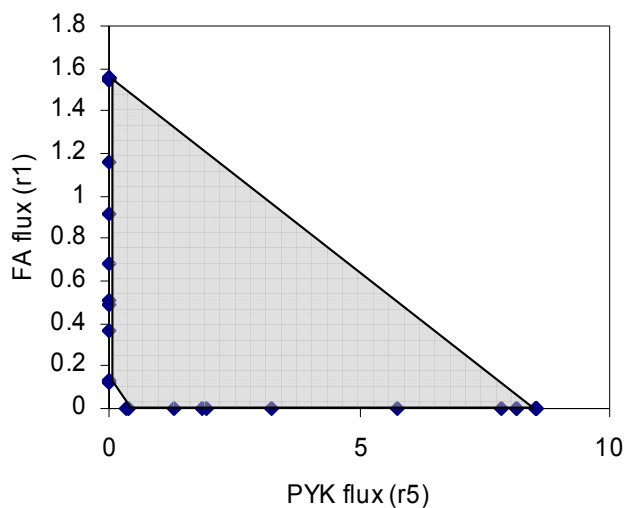
Figure 5.1. Phase planes for folic acid production.

Folic acid formation rate vs. PYK flux (Zhu et al., 2005).

5.2.2 Effect of *pyk* Expression on Productivity of Folic Acid in *B. subtilis*.

Prior results showed that the *pyk* mutant of *B. subtilis* has dramatically elevated PEP and G6P pool, both of which are precursors for folic acid biosynthesis. Our first experiment is to explore how the expression of *pyk* can change the folic acid yield as well as to investigate whether a high yielding (amount per cell) and productive strain (amount per time) could be developed.

Figure 5.2 shows the folic acid yield and doubling time exhibited by iPYK mutant of *B. subtilis* when different levels of IPTG are provided in glucose minimal medium. The yield and doubling time characteristics of iPYK mutant are also contrasted to those exhibited by *B. subtilis* 168 (*trpC2*). When 0.2 mM IPTG is present, the growth rate of iPYK mutant is essentially equal to that of *B. subtilis* 168 (*trpC2*), whereas the growth of iPYK mutant is very slow when no IPTG is added. Both this result and enzyme activity measurements indicate that significant control via IPTG induction exists over *pyk* expression in iPYK mutant.

The advantage of inducible control of *pyk* is evident in the case when the IPTG concentration was set to 0.02 mM. The several-fold enhancement in folic acid yield of iPYK mutant as compared to *B. subtilis* 168 (*trpC2*) is similar to that exhibited by the *pyk* knockout. However, the doubling time of iPYK mutant with 0.02 mM IPTG is several-fold smaller than the knockout mutant. Consequently, when *pyk* induction is controlled, a three-fold increase in folic acid yield can be obtained while sustaining 60% of the parent strain's growth rate. Reasonable growth rate, in turn, translates into increased bioprocess productivity.
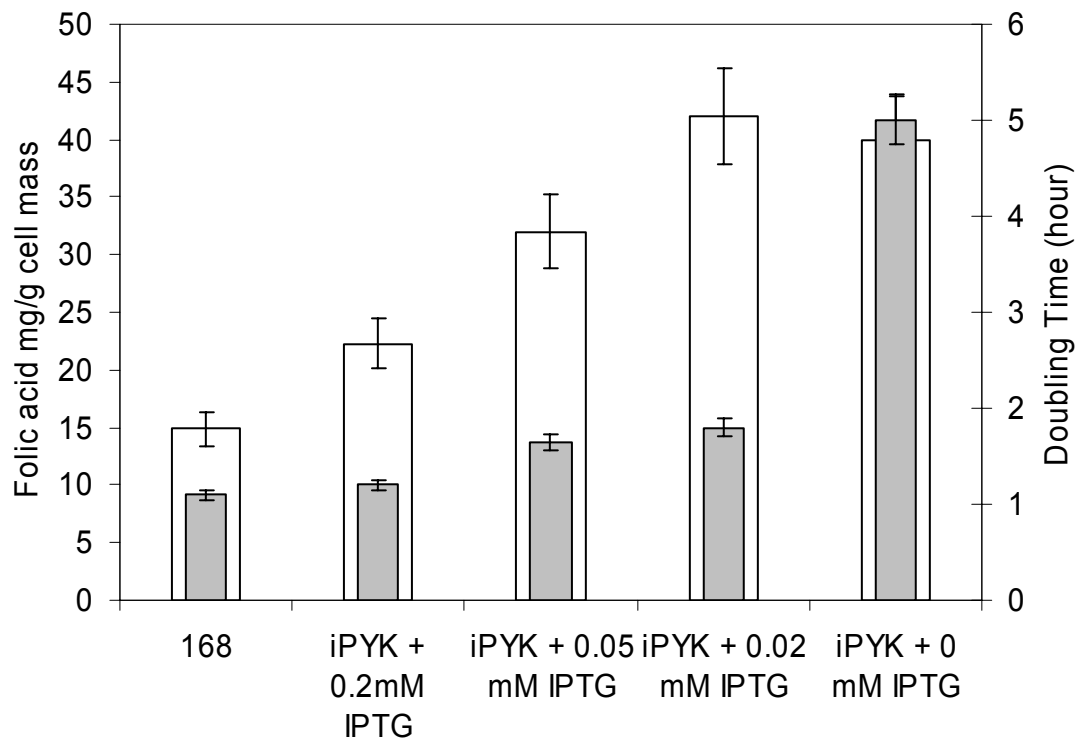
Figure 5.2. How folic acid yield (white bar) and doubling time (gray bar) depend on IPTG

concentration in strain iPYK mutant of *B. subtilis*.

The parent strain's (*B. subtilis* 168) folic acid yield and doubling time are included for comparison (Zhu et al., 2005).

5.2.3   Folic Acid Yield for Other *B. subtilis* Mutants

Para-aminobenzoic acid (PABA) pathway may be rate limiting for folic acid synthesis in *B. subtilis*, based on the experimental results that addition of PABA in the medium dramatically increased folic acid production (Miyata et al., 1999). Metabolic engineering approaches to enhance the flux to PAPA pathway may result in improved folic acid production. The folic acid

yields and growth rates exhibited by 1A96 (*pheA1*, *trpC2*), BSZT0410 (*trpC2*, *aroH*^{over}), BSZT0412 (*trpC2*, *aroH*^{over}, *tktA*^{over}), and BSZT0408 (*trpC2*, *mtrB::cm*) were measured in glucose minimal medium. The yields and growth rates are compared to each other and those of *B. subtilis* 168 (*trpC2*) in Table 7 (Zhu et al., 2005). The cell mass concentration at time of the sampling and the yield on the basis of total volume of cells and spent medium are also listed in Table 7. Amplifying *aroH* (BSZT0410) and disrupting *mtrB* (BSZT0408) both increase the folic acid yield by about 80%. Blocking phenylalanine production (1A96) increases the folic acid yield by about 100%. In contrast, amplifying the *tktA* gene (BSZT0412) reduced the folic acid yield by 46% as compared to the parent strain (BSZT0410).

5.2.4 Combinations of Mutation Strategies

The different mutation strategies that introduced inducible expression of *pyk*, *aroH* amplification, and *mtrB* disruption were combined to explore the synergistic effects. The folic acid yields of BSTZ0419 (*trpC2, mtrB::cm, pyk*^{ind}), BSTZ0425 (*trpC2, aroH, pyk*^{ind}), and BSTZ0437 (*trpC2, aroH*^{over}, *mtrB::cm, pyk*^{ind}) are listed in Table 7 along with doubling times, cell yields, and volumetric yields. The combination of the three mutations in BSTZ0437 resulted in an 8-fold increased yield of folic acid as compared to *B. subtilis* 168. Moreover, the growth rate and carbon yield of BSTZ0437 are both about 70% of the starting strain 168 when 0.05 mM IPTG is added to induce *pyk*.

Table 7. Folic acid yields of wild-type & engineered *B. subtilis* in glucose minimal medium (5g/l)

Strain Name	Description	Doubling Time (hour)	Folic Acid Mass Yield (mg /g cell)	Dry Cell Mass Concentration (g/L)	Volumetric Yield Folic (mg/L)
168	*trp2C*	1.08 ± 0.08	14.7 ± 0.7	1.95 ± 0.05	28.7
1A96	*trp2C, pheA*	1.08 ± 0.08	30.2 ± 2.0	1.98 ± 0.04	59.8
BSZT0410	*trpC2, aroH^{over}*	1.15 ± 0.08	26.8 ± 1.3	1.85 ± 0.05	49.6
BSZT0412	*trpC2, aroH^{over}, tktA^{over}*	1.40 ± 0.1	14.3 ± 0.7	1.60 ± 0.05	22.9
BSZT0408	*trpC2, mtrB::erm*	1.20 ± 0.1	26.3 ± 1.5	1.78 ± 0.05	46.8
BSZT0419	*trpC2, mtrB::cm, pyk^{ind}*	1.50 ± 0.1*	56.0 ± 4.0	1.75 ± 0.05	98
BSZT0425	*trpC2, aroH, pyk^{ind}*	1.25 ± 0.1*	60.0 ± 4.0	1.90 ± 0.06	114
BSZT0437	*trpC2, aroH^{over}, mtrB::cm, pyk^{ind}*	1.60 ± 0.2*	113 ± 11.0	1.45 ± 0.05	163

* 0.05 mM IPTG was added in the culture at time 0 (Zhu et al., 2005).

6.0   *BACILLUS THURINGIENSIS*

6.1   INTRODUCTION

Bacillus thuringiensis (Bt) is a gram-positive and spore-forming microorganism. It is widely used in agriculture and forests as an efficient pest control method because it can produce crystal proteins (endotoxins) in the cells during sporulation, which are toxic to many insect species (Schnepf et al., 1998). The low toxicity of *Bt* toxin to humans makes it desirable to improve the production of these alternatives to synthetic organic pesticides.

Many studies have shown that improving cell yield, toxin production, and sporulation is dependent on glucose concentration (Kuppusamy and Balaraman, 1991; Liu et al., 1994). Recent evidence shows that some of the toxin genes are repressed in the presence of glucose by catabolic repression (Banerjee-Bhatmagar, 1998) and a mutation in the catabolic repression site of HPr released the *cry4A* expression from the repression of glucose and resulted in higher transcripts (Khan and Banerjee-Bhatnagar, 2002), which implies that the central metabolic process plays an important role in the regulation of crystal toxin synthesis in *Bt*. Another study showed that the growth rate had a significant effect on the distribution of the consumed glucose (Mignone and Avignone-Rossa, 1996). The fraction of glucose consumed for biomass synthesis decreases with the growth rate, while the glucose flux through the TCA cycle reduces after a threshold value. The decrease of glucose flux through the TCA cycle is compensated by an

increase in the fraction of glucose being converted into acids. These results indicate that there is a mismatch between glycolysis and TCA cycle capacity, depending on the growth rate.

Although extensive work has been done to reduce acetate accumulation in *E. coli* and *B. subtilis* culture systems, the extension of these findings to *B. thuringiensis* cultures has received little attention. Based on our knowledge of *B. subtilis*, we hypothesized that the feeding of citrate would reduce acetate formation and improve the production of the toxin protein. In batch cultures, the inclusion of citrate in the growth medium was not as effective during the early exponential phase when the growth rate is high due to the presence of LB and low concentration of inhibitory by-products. However, production of acetate was significantly reduced and biomass yield substantially increased in the presence of citrate in continuous cultures operating at intermediate growth rates. Based on these results, it is conceivable that citrate will prove effective in reducing acid formation in fed-batch cultures where the growth rate is maintained below the maximum growth rate. Analysis of metabolic fluxes in continuous culture revealed that the glycolytic flux was significantly lower in the presence of citrate, and similar to *B. subtilis* cultures, pyruvate kinase flux was substantially attenuated. Thus, mutation of the pyruvate kinase gene in *Bt* may be a worthwhile metabolic engineering strategy to be tested for reducing acetate production and improve biomass yield.

6.2   RESULTS

6.2.1   Nutrition Requirements for *Bacillus thuringiensis* (*Bt*)

The *Bt* strain used in this study was unable to grow in glucose minimal medium (BGM + glucose). Additionally, supplementation of glucose minimal medium with glutamate, aspartate, citrate, or EDTA did not support cell growth as previously reported for other *Bt* strains (Nickerson and Bulla., 1974a). Addition of LB or yeast extract to glucose minimal medium enables good growth of the *Bt* strain. Batch experiments in basic growth medium (BGM) supplemented with glucose and either LB or yeast extract (10g/L glucose and 10g/L LB or yeast extract) revealed that LB is better for sporulation and toxin production than the more commonly used yeast extract. As shown in Figure 6.1, spores and crystal inclusion bodies are more prevalent in cells cultured with LB in the medium than when yeast extract is used. This improvement could be due to the positive effect of NaCl on spore formation in LB (Ghribi et al., 2005). Thus, in all our subsequent experiments, LB was added to the glucose minimal medium.

A
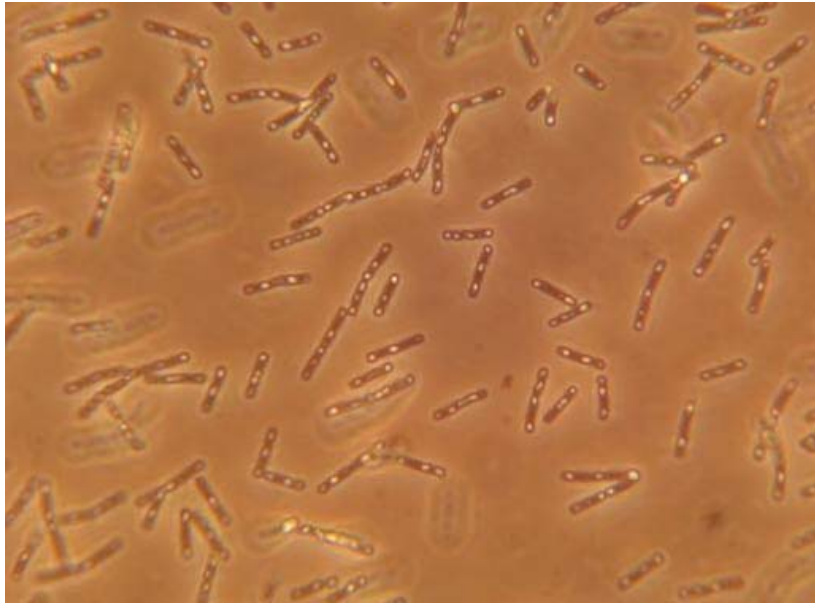
B
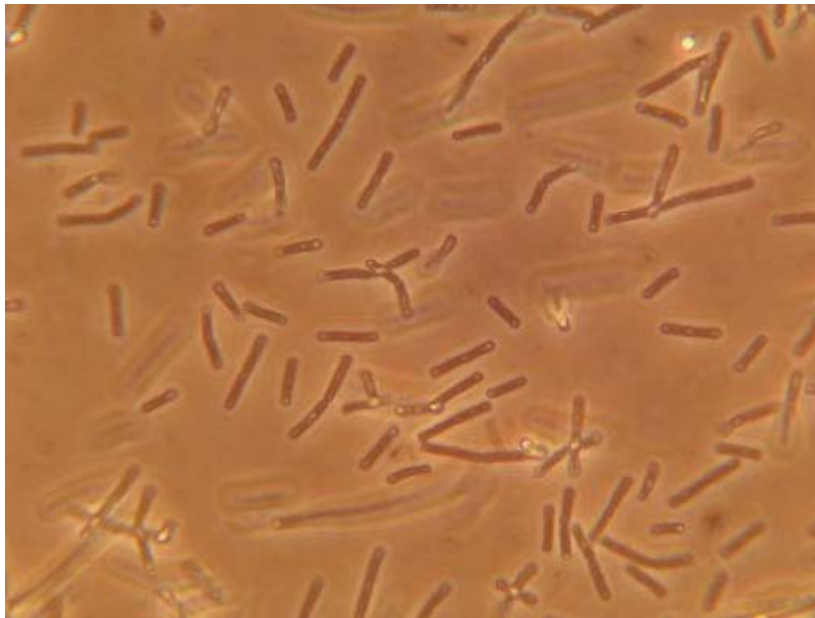
Figure 6.1. Morphology of *Bt* after 24 hour cultivation in BGM supplemented with 10g/L glucose and either 10g/L LB (A) or yeast extract (B).

Note that both spores and toxin protein crystals appear as phase bright inclusions in cells. A cell with two inclusions, as is the case for most cells in the LB culture, contains both a spore and a toxin crystal.

6.2.2   Effect of the Ratio of LB/Glucose in Batch Cultures

The glucose minimal medium (BGM) with a glucose concentration of 10 g/l was supplemented with different amounts of LB. The results of these batch experiments are shown in Figure 6.2 and summarized in Table 8. The maximum optical density (OD) increased as the LB concentration was raised from 1 to 7 g/L, but further increasing the LB concentration to 20 g/L did not increase the cell density. Table 8 shows that glucose was fully utilized in cultures with LB concentrations of 5 g/l corresponding to an LB/glucose ratio of 1:2 or higher, but not in cultures with LB concentrations below 3 g/L. Moreover, higher levels of sporulation were reached at LB/glucose ratios between 5:10 and 10:10. For LB/glucose ratios above 10:10, cell density did not increase and there was an adverse effect on sporulation. The carbon/nitrogen (C/N) ratio of mixtures of LB and glucose was calculated based on 10% nitrogen content in the yeast extract and tryptone components of the LB. Glucose/LB ratios between 10:5 and 10:10 correspond to C/N ratios of 6.8 to 4.5. This observation is consistent with a report indicating that sporulation was either initiated or enhanced by reducing the nitrogen source in several *Bt* production media (Pearson and Ward, 1988). The best C:N ratio may be strain-dependent, but the highest relative crystal protein production was reported to occur with a C: N of 7:1 in *Bt* var. *kurstaki* HD-73 (Farrea et al., 1998). In summary, the results of Table 8 show that a LB/glucose ratio of 1:2 will be sufficient to achieve full glucose utilization and high sporulation efficiency.

Table 8. Effect of LB concentration on cell growth and sporulation in shake flask cultures with 10 g/L glucose

Exp No	LB (g/L)	C:N	Residue Glucose (g/L)	Max OD (660nm)	Spore Counts (24 hr) ($\times 10^8$/mL)
1	3	8.5	3.12	8.6	1.1
2	5	6.8	0	14.2	6.5
3	7	5.6	0	21.4	7.8
4	10	4.5	0	23.5	7.9
5	20	2.7	0	22.4	2.0
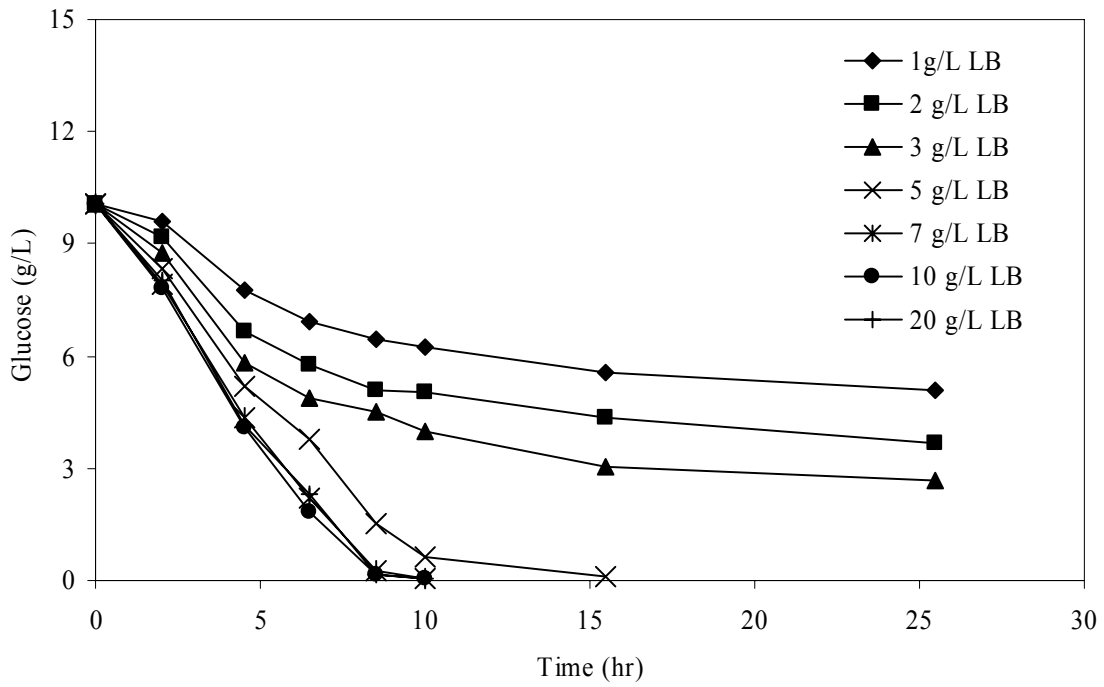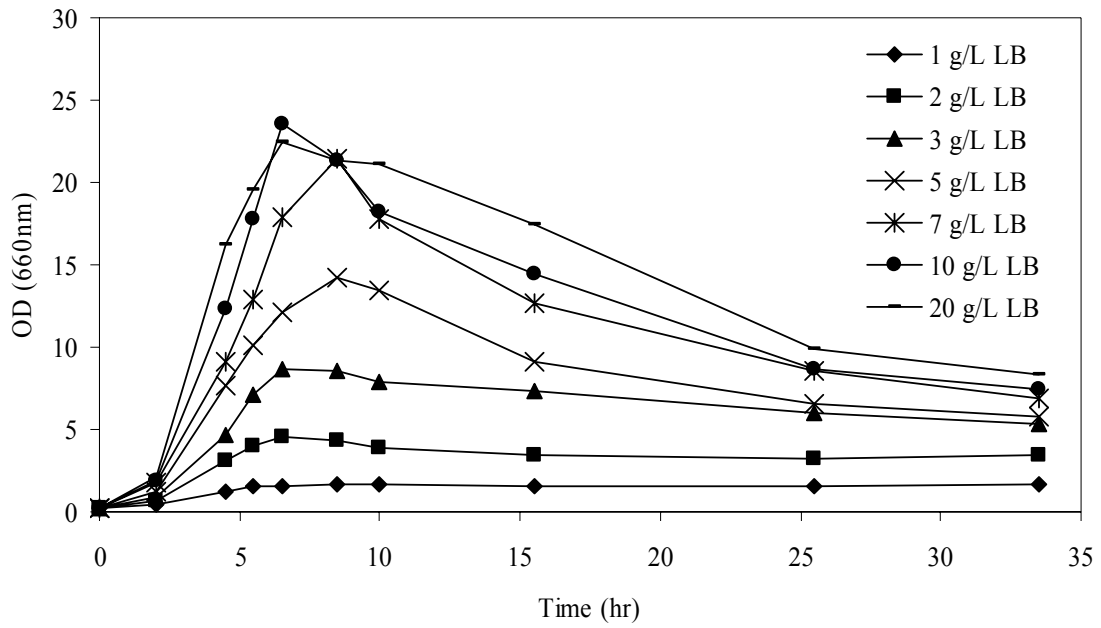
Figure 6.2. Cell growth and glucose utilization of *Bt* under different LB supplements in BGM with 10g/L glucose.

6.2.3 Effect of Citrate on Growth and Acids Formation in Batch Cultures with High Initial Glucose Concentration

The effect of citrate on growth and acid formation in batch cultures of *Bt* was investigated with an LB/glucose ratio of about 1:2. The medium was comprised of BGM, 10.8 g/L glucose, 5g/L LB, and 1.8 g/L sodium citrate or no citrate. As shown in Figure 6.3, cultures with and without citrate grew at the same rate, produced similar amounts of acetate, and consumed about same amount of glucose. Acetate accumulated in the culture broth over the first few hours during the exponential growth phase followed by a decrease in cell growth rate and rapid consumption of acetate. Thus, citrate was not effective in either enhancing cell density or reducing acetate production in this batch growth experiment. As shown in Figure 6.3B, citrate was not consumed in the first 3 hours when glucose concentration in the medium was still high and most of acetate was produced, indicating possible catabolite repression of citrate utilization by glucose (Warner et al., 2000; Meyer et al., 2001).
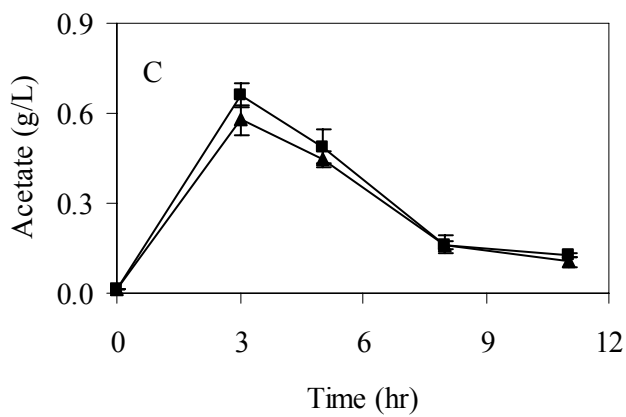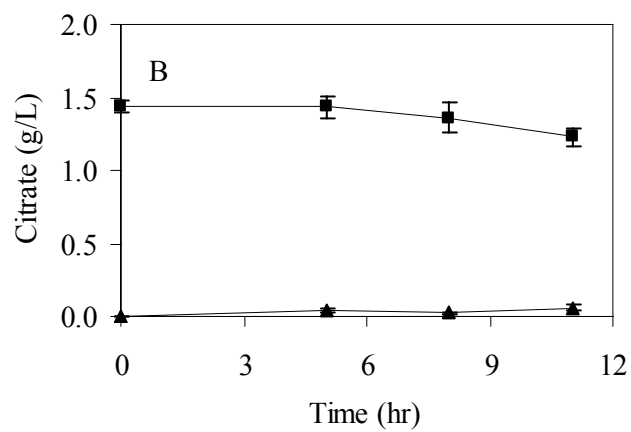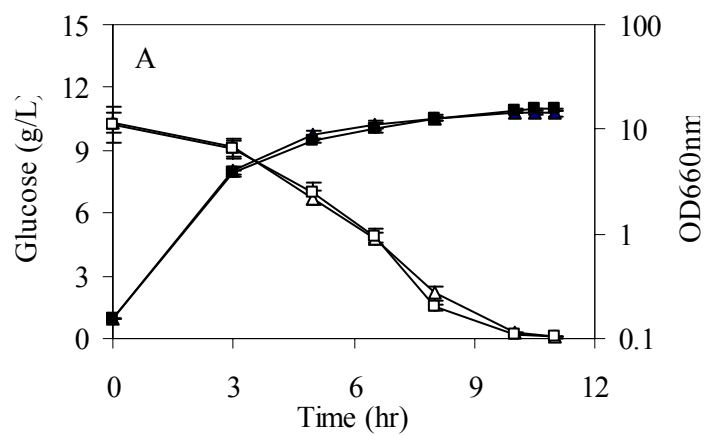
Figure 6.3. Effect of citrate on cell growth and acetate production in batch culture of *Bt* in BGM with

5 g/L LB and glucose: 10.8 g/L; Citrate: 1.8 g/L.

6.2.4 Citrate Uptake in *Bt* at Different Initial Glucose Concentrations

To investigate the catabolic effect of glucose concentration on citrate utilization, a set of experiments with various initial glucose concentrations were conducted in shake flask cultures. The culture medium contained 0.9 g/L citrate and 5 g/L LB. The cell growth, glucose consumption, citrate utilization, and acetate production are shown in Figure 6.4. For the culture with an initial glucose concentration of 10.8 g/L, citrate was not consumed initially until glucose concentration dropped below 5 g/L. Citrate consumption was also evident in the culture with an initial glucose concentration of 5.4 g/l at the early stage of growth. For the culture with initial glucose concentration of 1.8g/L, citrate was consumed from the beginning of growth phase and was quickly consumed in the first 2 hours. It is of interest to note the pattern of acetate concentration (Figure 6.4D). Acetate is only produced during early exponential growth. Moreover, results with initial glucose concentrations of 10.8 and 5.4 g/l reveal that acetate uptake becomes significant at about 6 and 3 hours of growth, respectively, corresponding to glucose concentration of about 3 g/l. Overall, results of Figure 6.4 indicate that citrate can be metabolized at glucose concentration below 5g/L and that acetate uptake becomes significant when glucose concentration drops below 3 g/l.

The above experiments were conducted with fixed LB concentration, and the LB/Glucose ratio changed with various initial glucose concentrations. In another set of experiments where glucose/LB ratio was fixed at 2/1, the culture with 2 g/L initial glucose produced much less acetate as compared to cultures with 5.4 g/L and 10.8 g/L glucose (data not shown). The specific citrate uptake rates decline with increasing glucose concentration and its trend is similar to that of previous set of experiments.
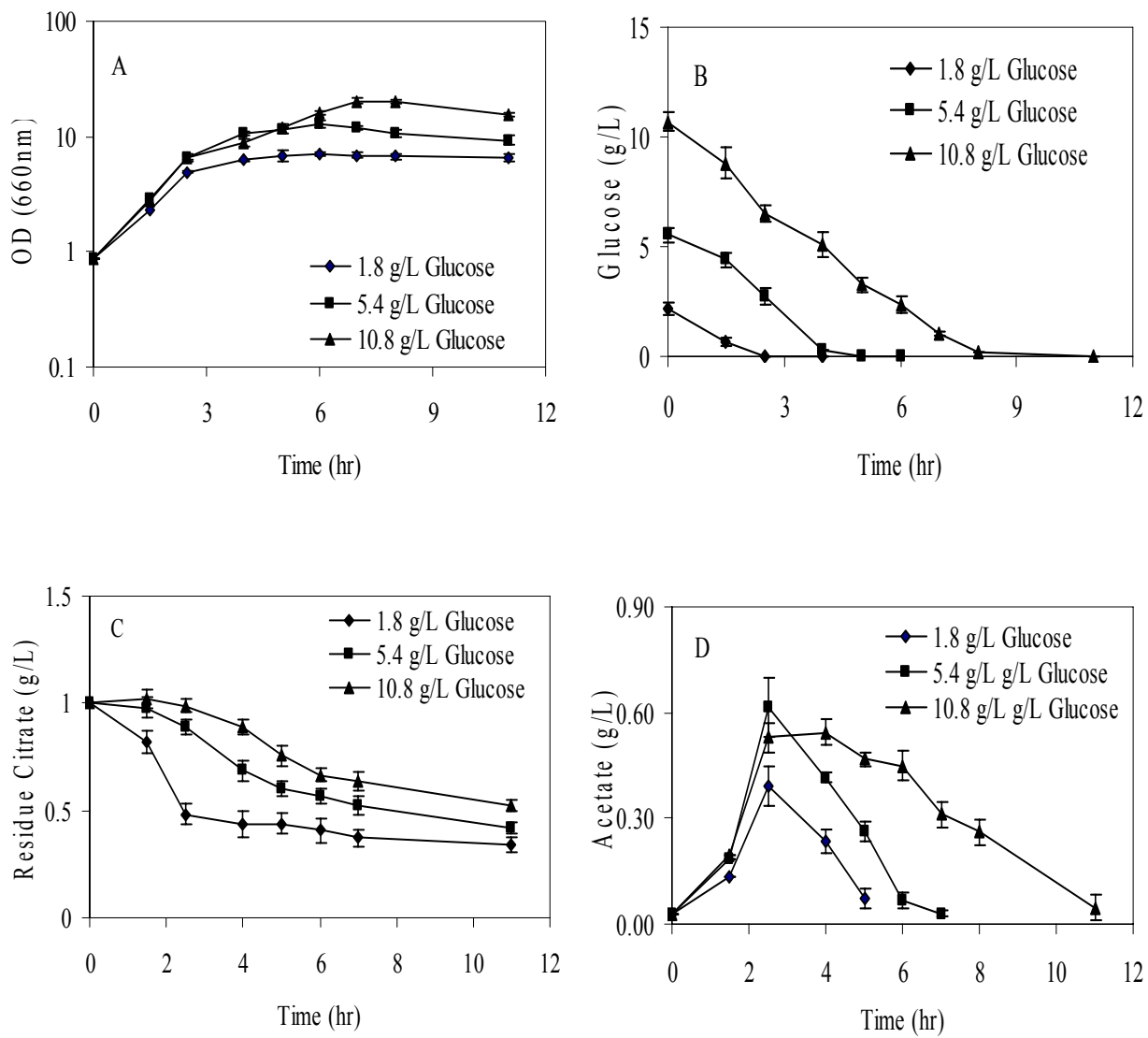
Figure 6.4. Batch cultures of *Bt* in BGM with 5g/L LB and 0.9 g/L citrate and variable initial glucose concentrations.

6.2.5 Effect of Citrate on Growth and Acids Formation in Batch Cultures with Low Initial Glucose Concentration

To investigate the effect of citrate on growth and acid formation in batch cultures of *Bt*, an initial glucose concentration of 3 g/l was used to ensure that citrate transport would not be inhibited. The LB concentration of 1.5 g/l corresponding to LB/glucose ratio of ½, significantly lower than the amount used for experiments reported in Figure 6.4, was used in this experiment. As shown in Figure 6.5, cultures with and without citrate grew at same rates, produced similar peak concentrations of acetate, and consumed about same amount of glucose in the first three hours of growth period. The key difference between the two cultures appears to be that in cultures provided with citrate, acetate was produced during the initial growth period (as was the case in Figure 6.4), while acetate production continued throughout most of the growth period in the culture lacking citrate. We hypothesized that this difference indicates that citrate is effective at moderate growth rates and/or lower LB concentrations. To test this hypothesis, and to gain some insight into possible regulatory role of citrate, continuous cultures at several dilution rates (growth rates) were conducted.

.
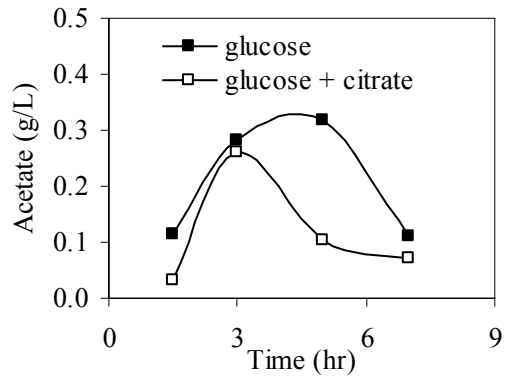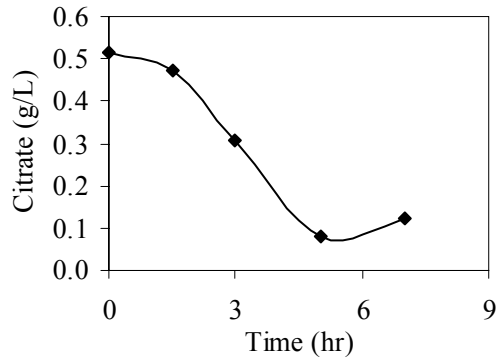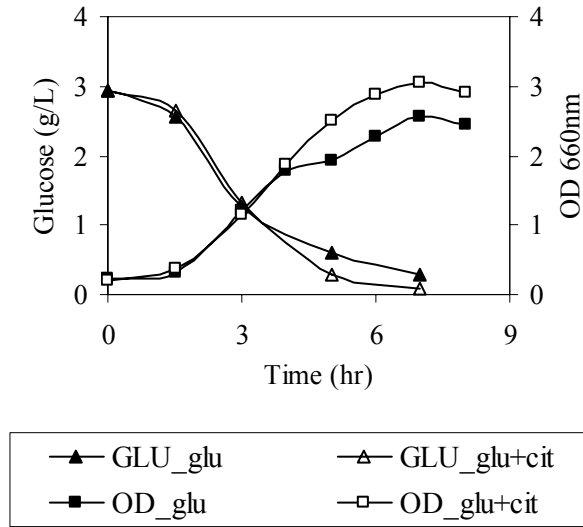
Figure 6.5. Effect of citrate on cell growth and acetate production in batch culture of *Bt* in BGM with 1.5 g/L LB and glucose: 3 g/L; Citrate: 0.6 g/L.

6.2.6   Effect of Citrate in Continuous Cultures at Various Dilution Rates.

Continuous culture experiments at various dilution rates from 0.1 to 0.4 hr^{-1} were performed to test the effect of citrate on cell and acetate production at different growth rates. Cells were grown in BGM (containing 3 g/l glucose) plus 1 g/L LB with and without citrate. As shown in Table 9, at dilution rate of 0.1 h^{-1}, no acetate was detected in the presence or absence of citrate (runs 1 and 2). Glucose was completely utilized in both cultures.

At higher dilution rates of 0.2 and 0.3 h^{-1} (runs 3-6), acetate was present in the cultures without citrate, but not in cultures with citrate. Moreover, the glucose utilization was improved in the presence of citrate. The remarkable difference was the enhancement in cell density in the presence of small amount of citrate. To assess whether the cell density enhancement is only due to higher levels of substrate utilization (higher glucose consumption and utilization of citrate), the values of cell yield based on total carbon consumed were calculated. The significantly higher values of cell yield exhibited in presence of citrate for dilution rates of 0.2 and 0.3 h^{-1} indicates that citrate has shifted the carbon metabolism more towards biosynthetic reactions. Finally, for a dilution rate of 0.4 h^{-1} (run 7 and 8), the culture without citrate was unstable in that the cell density continually decreased after the onset of the continuous medium flow. The maximum growth rate in batch cultures with the same medium is 0.49 h^{-1}. Thus, the culture washout is not due to dilution rate being larger than the maximum growth rate in batch culture. Rather, washout may be due to excessive acid formation or other metabolic factors repressing cell growth. Indeed, one sample taken 18 hours after the initiation of continuous culture showed OD660nm = 0.58 and acetic acid concentration of 0.32 g/l.

Table 9. Biomass yields and acetate production in continuous cultures of *Bacillus thuringiensis* at different levels of dilution rates (3 g/L glucose)

Exp No	D (h⁻¹)	Citrate (g/L)	Residue Glucose (g/L)	Residue Citrate (g/L)	OD (660nm)	Biomass Yieldᵃ (%)	Acetate (g/L)
1	0.1	0	0	0	4.18	61	0
2	0.1	0.5	0	0	5.58	81	0
3	0.2	0	0.93	0	2.45	52	0.33
4	0.2	0.5	0	0	5.28	77	0
5	0.3	0	1.41	0	1.81	50	0.42
6	0.3	0.5	0.63	0	3.53	65	0
7	0.4	0	Washout				
8	0.4	0.5	1.68	0	1.95	65	0.05

[a] Biomass yield is defined as gram of carbon in the cell/gram of carbon consumed from glucose, assuming the carbon content in biomass is 50%.

[b] 1.0 g/L LB was fed in the medium.

6.2.7   Glucose Utilization in Continuous Cultures of *Bt*.

Table 10 shows the glucose utilization, biomass synthesis, and acetate production in continuous cultures of *Bt* at dilution rate of 0.2 h⁻¹ with varying glucose concentration. The citrate concentration was set at 0.5 g/L, while 2, 3, and 5 g/L glucose concentration were investigated. Glucose was completely utilized and no remarkable acetate formation occurred for both single feeding and dual feeding cultures when 2 g/L glucose was initially supplied (run 1 and 2 in Table 10). In this situation, the glucose consumption rate was limited by the low glucose feeding rate; therefore, the glycolysis flux was under well control and no overflow of glycolysis would happen.

The feeding glucose concentration was then increased from 2 g/L to 3 g/L (run 3 and 4 in Table 10), accompanied by a decrease in the ratio of Citrate/Glucose. All glucose was utilized in the culture with citrate, while there is still some amount of glucose left unconsumed in the single feeding. Considering the consumption of glucose, it is obvious that citrate is beneficial to the catabolism of glucose. The higher glucose catabolism in dual feeding culture was rather due to the higher cell concentration than higher specific glucose uptake rate, as the glucose uptake rate per cell is much lower in the dual feeding cultures. Accompanied with the higher specific glucose uptake rate, more acetate was produced for the single feeding, while the specific glucose uptake rate for the dual feeding is still low and no acetate is produced.

Glucose utilization was incomplete for both single feeding and dual feeding cultures when 5 g/L glucose was initially supplied (run 5 and 6 in Table 10), with more than 50% feeding glucose left unconsumed after the system reached steady state. Compared with run 3 and 4, less glucose was consumed for the single feeding and dual feeding respectively. This was probably due to the lower citrate/glucose and LB/glucose ratio in run 5 and 6. As we keep the same ratios of citrate/glucose and LB/glucose in the culture with 5 g/L glucose as that in the cultures with 3 g/L glucose, more glucose was consumed (run 7 and 8). When 1 g/L LB was fed into the continuous culture, about 2 g/L glucose would be consumed, which is very consistent with our previous batch results.

The results of Table 9 and Table 10 indicated that, with citrate addition, acid formation was diminished and the cell yield increased remarkably. Furthermore, the differences of cell density, biomass yield and acetate production between single feeding and dual feeding are most significant for the cultures with moderate feeding ratio of citrate/glucose (0.5/3) as shown in Table 10. It was reported that the effect of citrate is at regulatory level in *B. subtilis* by altering

95

the metabolic fluxes in the central carbon metabolic pathways, not due to the fact that citrate is a TCA cycle metabolite (Goel et al, 1995). Metabolic flux analysis was then carried out to check the changes of metabolic fluxes in the *Bt* culture after it was exposed to citrate.

Table 10. Biomass yields and acetate production in continuous cultures of *Bacillus thuringiensis* supplemented with different amount of glucose at dilution rate of 0.2 h^{-1}

Exp No	Initial Glucose (g/L)	Feeding Citrate (g/L)	Residue Glucose (g/L)	Residue Citrate (g/L)	OD (660nm)	Biomass Yield[*] (%)	Acetate (g/L)	Glucose uptake rate mmol/(g.hr)
1	2	0	0	0	3.02	0.53	0.04	2.10
2	2	0.5	0	0	3.44	0.60	0	1.85
3	3	0	0.93	0	2.45	41	0.33	2.68
4	3	0.5	0	0	5.28	62	0	1.80
5	5	0	3.43±0.11	0	2.25±0.21	50±0.95	0.11±0.02	2.22
6	5	0.5	2.67±0.10	0	4.35±0.08	65±1.5	0	1.70
7**	5	0	2.33	0	3.98	52	0.15	2.13
8**	5	0.85	2.02	0.06	5.01	59	0	1.89

*Biomass yield is the carbon yield on glucose.
** Run #7 and run # 8 were fed with 1.67 g/L LB; run #1 to #6 were fed with 1.0 g/L LB

6.2.8   Network Model for Metabolic Flux Prediction and Calculation

We have previously reported that the effect of citrate in *B. subtilis* is not due to augmenting the abundance of a TCA cycle metabolite. Instead, the effect is at the regulatory level resulting in the alteration of the fluxes in the central metabolic pathways (Goel et al, 1996, Lee et al., 1997; Phalakornkule et al., 2000). Metabolic fluxes (mmol/(g cell ·h)) for glucose and glucose plus citrate fed cultures of *Bt* (run 3 and 4 in Table 9) were calculated using a stoichiometric model as described elsewhere (Zhu et al., 2003).

Bt has an incomplete TCA cycle owing to the absence of the α-ketoglutarate dehydrogenase (Nickerson et al., 1974b; Yousten et al., 1974; Aronson et al., 1975). However, there is an ancillary pathway that allows for glutamate and α-ketoglutarate metabolism via the γ-aminobutyric acid pathway (Aronson et al., 1975). Figure 6.6 depicts the metabolic pathways included in our flux model. A stoichiometric model of the central carbon metabolism of *Bt* was built using the software Metabologica (Zhu et al., 2003). The model assumes that all metabolic intermediates are at the pseudo-steady-state (no accumulation of metabolic pools). Additionally, constraints such as net NADPH formation for reductive biosynthesis and minimum ATP requirements are included in the model formulation. These constraints limit the metabolite trafficking alternatives as well as insure that a particular solution is physiologically feasible. Biomass composition data was adopted from *B. subtilis* (Sauer et al., 1996). We have reported that slight variations in cell composition do not significantly affect the relative distribution of key fluxes between glycolysis and TCA cycle (Goel et al., 1995).
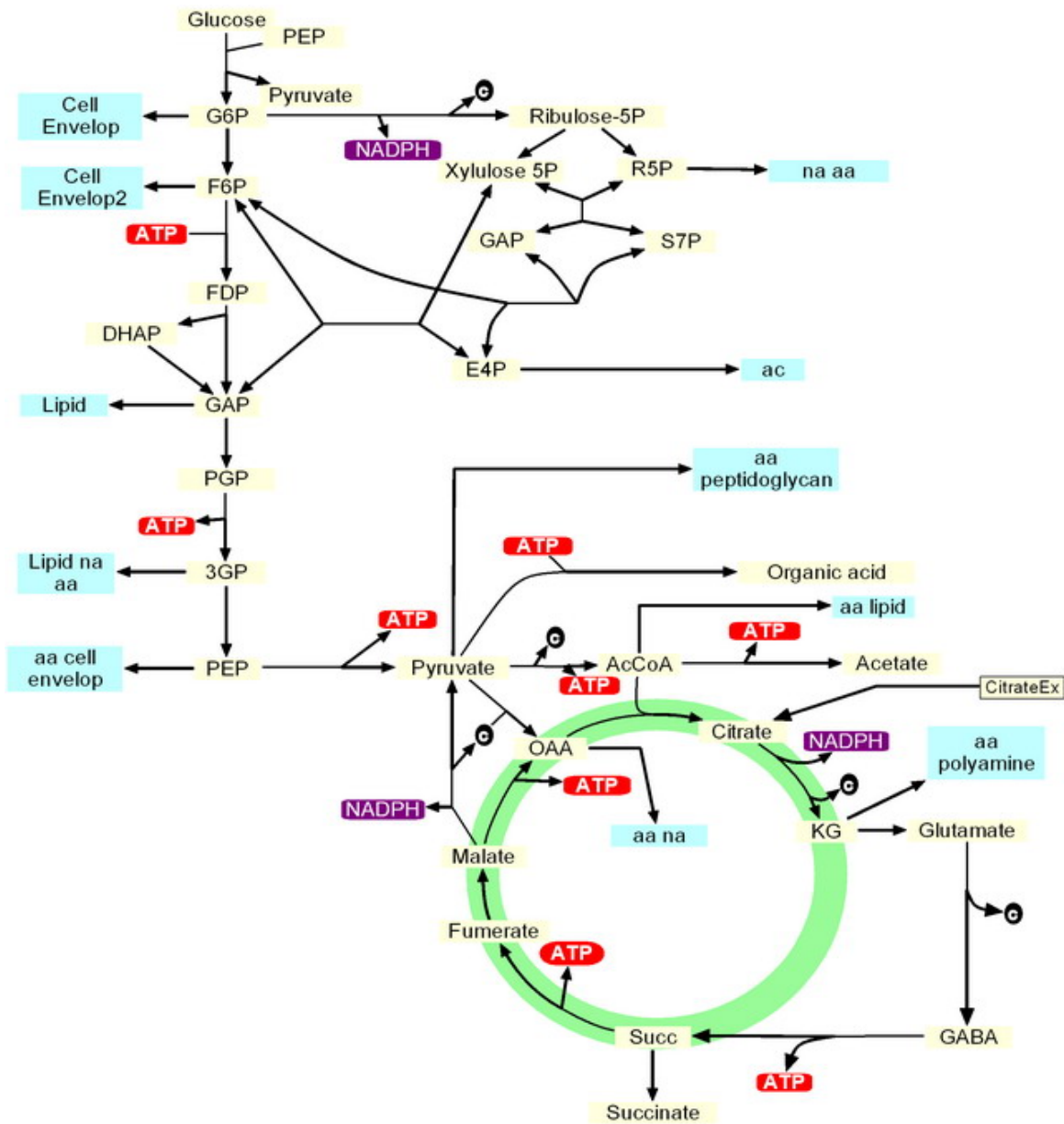
Figure 6.6. Scheme of central carbon metabolism pathways for flux modeling in *Bt*.

Abbreviations: aa (amino acids); na (nucleic acids); G6P (glucose-6-phosphate); F6P (fructose-6-phosphate); R5P (ribose-5-phosphate); E4P (erythrose-4-phosphate); FDP (Fructose-1,6-biphosphate); DHAP (dihydroxyacetone-phosphate); GAP (Glyceraldehyde-3-phosphate); S7P (sedoheptulose-7-P); PGP (1,3-biphosphoglycerate); 3GP (3-phosphoglycerate); PEP (phosphoenolpyruvate); AcCoA (acetyl-CoA); CitrateEx (Citrate External); KG (α-ketoglutarate); GABA (4-aminobutanote); Succ (succinate); OAA(oxaloacetate).

First, the effect of LB on fluxes was neglected and the cultures were treated as they were grown on glucose or glucose plus citrate. Two feasible solutions were found for cultures grown on glucose (3 g/l glucose) and four for cultures grown on glucose and citrate (3 g/l glucose and 0.5 g/l citrate). The actual solution is a linear combination of these solutions. The possible solutions of HMP pathway and pyruvate kinase (PYK) fluxes at dilution rate of 0.2 h^{-1} are shown in Figure 6.7. For the entire solution space, PYK pathway flux of glucose plus citrate-fed culture is lower than that when citrate is absent. High HMP flux is always accompanied by low PYK flux, and vice versa. It has been reported that most strains of *Bt* and other bacteria use primarily the EMP pathway for glucose catabolism, and the use of HMP pathway is not significant (Nickerson et al, 1974c). Therefore, the solution for glucose fed culture (without citrate) is most likely to be around the maximum PYK flux as point A in Figure 6.7.
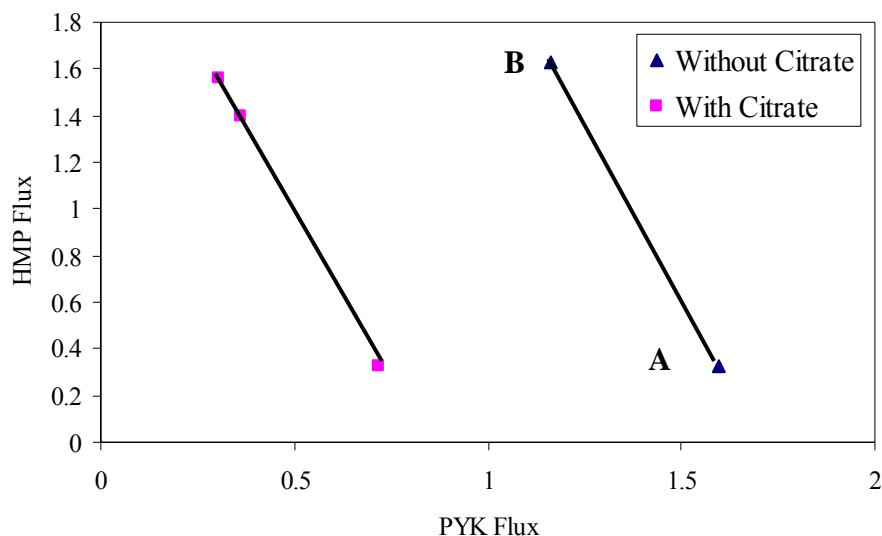
Figure 6.7. The solution space of HMP pathway flux and PYK flux for single feeding (3 g/L glucose) and dual feeding (3 g/L glucose and 0.5 g/L citrate) at dilution rate of 0.2 h^{-1}.

Note that two of solutions are the same (as far as HMP and PYK flux) for glucose with citrate case.

The average of main pathway fluxes for the glucose and glucose plus citrate-fed cultures for a dilution rate of 0.2 h^{-1} are given in Figure 6.8. Glycolytic fluxes were significantly lower for cells grown in the presence of citrate than its absence, while the fluxes through the TCA cycle were similar in the presence or absence of citrate indicating a possible saturation of TCA cycle. The most significant difference between the two cases was in flux of pyruvate kinase-catalyzed reaction; its value for the culture grown in the presence of citrate is about 33% of the value for the culture grown without citrate. It is reported that citrate transport is coupled with the uptake of divalent metal ions like Ca2+, which is a strong inhibitor of PYK (Willecke and Pardee, 1971; Boiteux et al., 1983). PYK inhibition can elevate PEP pool, which can further inhibit phosphofructokinase (PFK) (Fry, et al., 2000; Doelle et al., 1982) and lower glycolysis flux.

As noted in evaluation of metabolic fluxes of Figures 6.7 and 6.8, the contribution of LB to metabolic fluxes was neglected. To account for some of the effects of LB, the flux model was modified such that amino acids were provided by the LB and thus no biosynthetic precursors were used for amino acid synthesis. The ATP and NADPH constraints of the flux model were also modified by taking into account that no ATP and reducing power (NADPH) was used for amino acid synthesis. Five feasible solutions were obtained for glucose plus citrate grown cells with PYK flux value of 0.833, 1.048, 1.086, 1.181, 1.181 mmol/ (g cell.h). Four were found for glucose-fed cultures: the PYK flux values equal 1.823, 2.029, 2.061, and 2.061 mmol/(g cell h). Similar to the first case where the effect of LB was completely neglected, PYK fluxes are significantly lower for the glucose plus citrate fed culture than the culture without citrate.
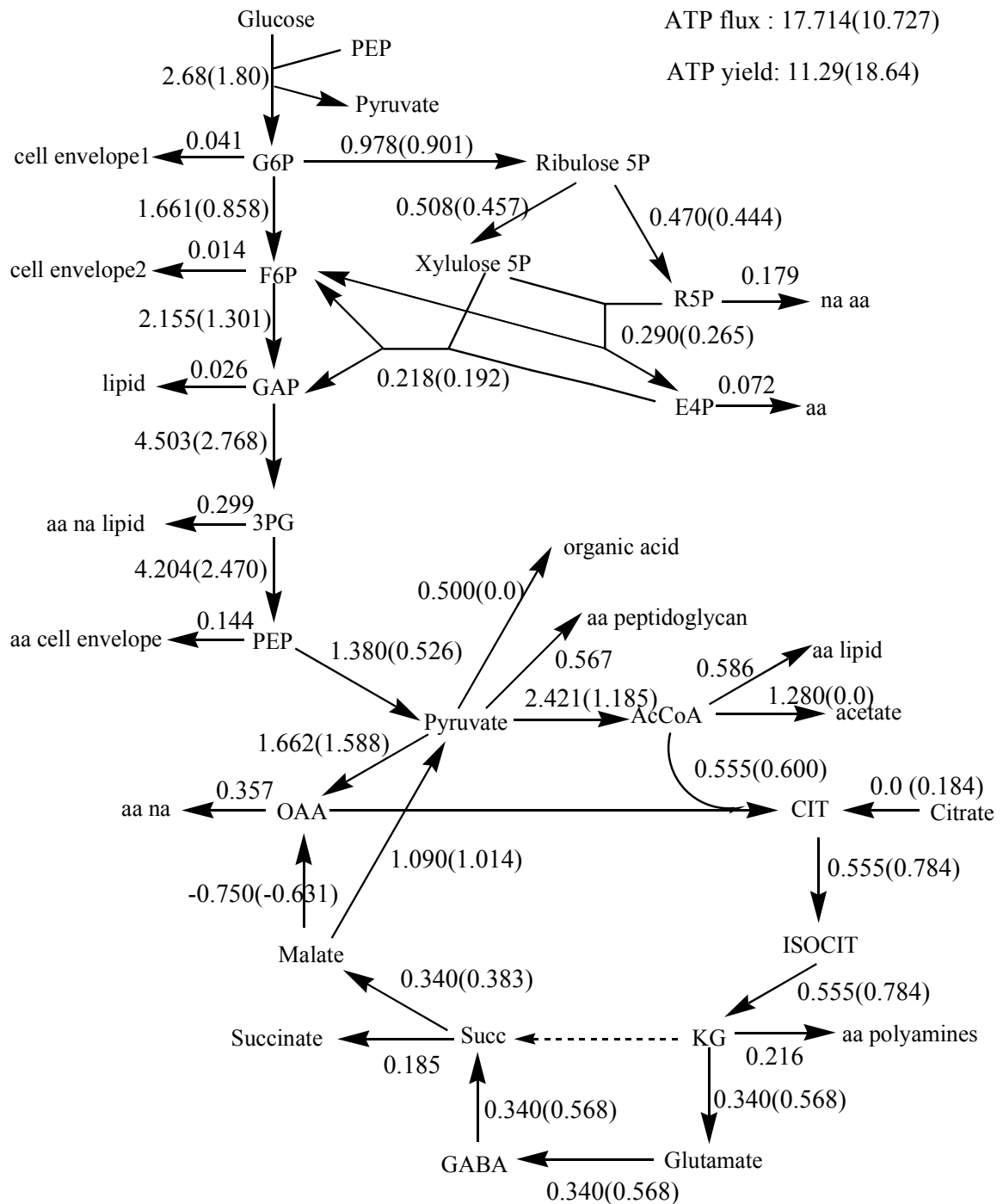
Figure 6.8. Metabolic fluxes of continuous culture of *Bt* at dilution rate of 0.2 h-1 for glucose fed (3 g/L glucose) (first number) and glucose plus citrate (3 g/L glucose + 0.5 g/L citrate) (number in parenthesis).

Finally, using the Metabologica (Zhu et al., 2003), possible flux distribution scenarios for the growth of *Bt* in glucose minimal medium was investigated. Sixteen different feasible solutions exist. The acids flux versus PYK flux (mmol/(g cell·hr)) is shown in the phase plane (Figure 6.9A). Any point inside the bounded region is a feasible solution. The maximum and minimum acids production rate decreases linearly as the PYK flux decreases. The geometry of the phase plane boundary also indicates that solutions that yield zero acids exist as the PYK flux decreases to a low range of values. Figures 6.9A and B show that higher biomass yield is correlated to lower acids and PYK flux. Thus, both the modeling and experimental results indicate that PYK may be a possible metabolic engineering site to reduce acetate production and improve biomass yield.
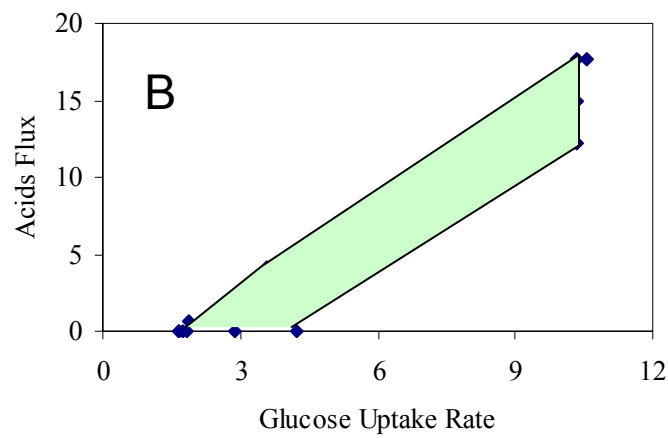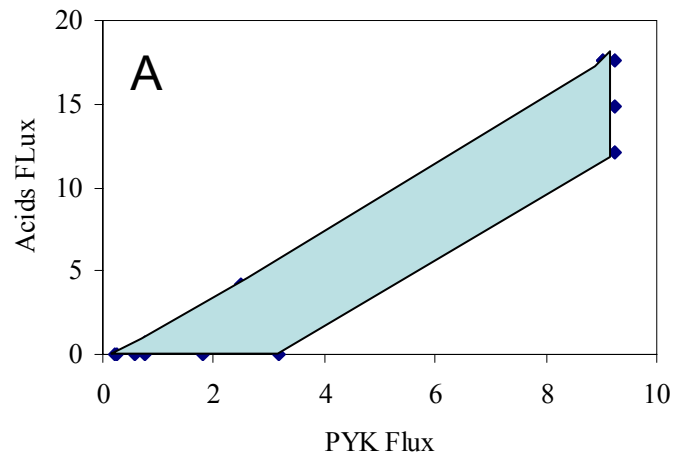
Figure 6.9. Phase plane for acids flux vs. PYK flux (A), acids flux vs. Glucose Uptake Rate (B).

The fluxes were generated with the modeling software at dilution rate of 0.2 hr-1.

These results demonstrated that citrate was very effective in reducing acid formation and enhancing cell density in continuous cultures operated at moderate to relatively high growth rates. Citrate was not as effective in batch cultures particularly during the early exponential phase when the growth rate is high due to the presence of LB and low concentration of inhibitory by-products. Based on these results, it is likely that citrate will be effective in reducing acid production in fed-batch cultures where the growth rate is sustained below the maximum growth rate.

We have reported that in *B. subtilis,* citrate attenuates the activities of pyruvate kinase and phosphofructose kinase, both of which are known to exert significant control over glycolysis (Goel et al., 1999). Since the observed redistribution of fluxes due to addition of citrate is similar in *B. subtilis* and *Bt,* the same mechanism may be operative in both microorganisms. This implication suggests that as was the case for *B. subtilis*, abolishing pyruvate kinase activity (Fry et al., 2000) or inducing expression at a low level (Pan et al., 2006) may prove beneficial for reducing acetic acid and enhancing product (e.g. crystal protein) production in *Bt* cultures.

7.0   CONCLUSIONS

The poor coordination between glucose consumption and precursor synthesis in the Krebs cycle often results in carbon overflow and excess acetate production. The acetate formation during microbial fermentation inhibits cell growth and recombinant protein production, and causes the instability of fermentation process. Here, we have demonstrated that the efficiency of carbon utilization can be markedly increased by regulating pyruvate kinase (PYK) expression in *B. subtilis* and by cofeeding citrate in *B. thuringiensis*. Outcomes of this study can be summarized as following.

1. Good growth and low acetate formation in *B. subtilis* can be attained by controlling either PYK or Phosphofructokinase (PFK) at an intermediate expression level.

2. Down-regulating *pyk* expression resulted in elevated concentrations of intracellular PEP and G6P therefore enhanced folic acid production.

3. Recombinant protein production is improved by down-regulating *pyk* expression.

4. Glycerol is a better carbon source for recombinant protein production as compare to glucose. In addition to higher protein productivity, cultures with glycerol also result in less acetate formation and higher biomass yield.

5. Feeding of citrate in the continuous cultures of *Bacillus thuringiensis* is very effective in reducing acetate formation, which results in improved cellular yield.

8.0   FUTURE WORK

Although the strain of *B. subtilis* with regulated PYK activity shows promise, the need for an external inducer supplied in the media is cumbersome and can increase the difficulty and cost of downstream processing. Based on the results presented in this study, a strain with a weaker promoter whose PYK expression level is equal or close to the induction level of iPYK mutant with 0.05 mM IPTG may have potential applications.

Down-regulating *pyk* expression reduced acetate formation but increased carbon dioxide evolution in *B. subtilis*. Modeling results indicate a solution maximizing carbon yield also corresponds to low PYK and α-Ketoglutarate dehydrogenase (α-KDH) activities. A double mutation of PYK and α-KDH may give low rates of acetate formation and CO_2 evolution thereby further increases biomass yield.

Citrate is very effective in reducing acetate formation and improving cellular yield in continuous cultures of *B. thuringiensis*. However, the effectiveness of citrate in batch cultures is limited due to the catabolic repression of citrate transport by glucose. In *B. subtilis*, citrate is proposed to attenuate PYK. Same mechanism may be operative in both microorganisms. As was the case for *B. subtilis*, abolishing pyruvate kinase activity (Fry et al., 2000) or inducing expression at a low level (Pan et al., 2006) may prove beneficial for reducing acetate and enhancing product (e.g. crystal protein) production in *B. thuringiensis* cultures.

APPENDIX A

PREPARE COMPETENT B. SUBTILIS AND TRANSFORMATION

1. Grow one loop of *B. subtilis* in LB overnight.

2. 1 ml overnight culture was then inoculated into 20mL growth medium GM1, and optical density was measured for every hour.

3. Record the time of cessation of logarithmic growth T_0.

4. Continue culture in GM1 for 90 minutes (T_{90}).

5. Dilute the culture 10-fold into GM2, and incubated at 37 °C and 250 rpm for 60 minutes.

6. Add DNA (1 to 5 μg/mL), and continue incubation for 30 minutes.

7. Terminate the reaction by adding 100 μg/mL of deoxyribonuclease (DNase) and incubate at 37 °C for 5 minutes.

8. Spread 0.1 mL onto LB agar plate with appropriate antibiotics and incubate for 24 hours.

Reagents:

10× Salts (/L):

 140 g K2HPO4

  60 g KH2PO4

 20 g (NH4)2SO4

 10 g sodium citrate

 2.0 g MgSO4·7H2O

1× GM1:

 22mM glucose

 0.02% acid hydrolyzed casein

 0.1% yeast extract

 10% 10× Salts

1× GM2:

 1× GM1

 0.5 mM CaCl$_2$

 2.5 mM MgCl$_2$

APPENDIX B

ISOLATION OF PLASMID DNA FROM BACILLUS SUBTILIS USING THE QIAGEN® PLASMID MIDI KIT

This procedure has been adapted from the QIAGEN® Plasmid Midi Kit Protocol. It has been used successfully for isolation of low-copy-number plasmids from various *Bacillus subtilis* strains.

Procedure

1. Take 2~5 ml sample during the mid-exponential stage culture.

2. Harvest the cells by centrifugation at 10000 x *g* for 5 min at 4°C.

3. Resuspend the bacterial pellet in 4 ml Buffer P1 containing 5 mg/ml lysozyme. Ensure that RNase A (100 µg/ml) has been added to Buffer P1.

4. Incubate at 37°C for 30 min.

5. Add 4 ml Buffer P2, and mix gently but thoroughly by inverting 4~6 times, and incubate at room temperature for 5 min. (Check Buffer P2 before use for SDS precipitation due to low storage temperatures. If necessary, dissolve the SDS by warming to 37°C).

6. Add 4 ml chilled Buffer P3, mix immediately but gently by inverting 4~6 times, and incubate on ice for 15 min.

7. Centrifuge at 14,000 × *g* for 10 min at 4°C. Remove supernatant containing plasmid DNA promptly.

8. Apply the supernatant from step 7 to the QIAGEN-tip and centrifuge for 1 minute.

9. Wash the QIAGEN-tip with 2 × 10 ml Buffer QC.

13. Elute DNA with 5 ml Buffer QF.

14. Precipitate DNA by adding 3.5 ml room-temperature isopropanol to the eluted DNA. Mix and centrifuge immediately at ≥15,000 x g for 30 min at 4°C. Carefully decant the supernatant.

15. Wash the DNA pellet with 2 ml of room-temperature 70% ethanol and centrifuge at ≥15,000 x g for 10 min. Carefully decant the supernatant without disturbing the pellet.

16. Air-dry the pellet for 5.10 min, and redissolve the DNA in a suitable volume of buffer (e.g., TE, pH 8.0, or 10 mM Tris·Cl, pH 8.5).

APPENDIX C

AGAROSE GEL ELECTROPHORESIS

Procedure:

1. Weight 0.7 to 1.0 g agarose and dissolve in 1× running buffer (TBE) by heating in microwave for 1 to 2 minutes.

2. Cool down the hot agarose solution to 60~70 °C, pour the warm agarose solution into mould with comb inserted, cool for 30 to 60 minutes.

3. Remove comb. With gel in electrophoresis chamber, add 1× TBE buffer till the gel is submerged completely.

4. Mix 9 parts DNA sample with 1 part dye with a total volume of 10~20 µl, and load the samples and DNA marker into wells of gel.

5. Place lid on top of chamber.

6. Set and turn on the power supply at 90 voltage, and let it run for 1~3 hour.

7. Turn off power supply.

8. Carefully remove gel from mold and stained in bath of 1 µg/ml ethidium bromide for about 30 minutes.

9. Remove gel from the staining container, and rinse in bath of water for 30 minutes.

10. Examine gel on UV light talbe.

Reagents:

20×TBE Buffer (stock solution)

      216 g   Tris base

      110 g   Boric acid

      80 mL 0.5M EDTA, pH 8.0

Adjust to final volume of 1 L with distilled water.

Dilute to 1× for use in electrophorisis.

BIBLIOGRAPHY

Alper, H., J. Moxley, E. Nevoigt, G. R. Fink, and G. Stephanopoulos. 2006. Engineering yeast transcription machinery for improved ethanol tolerance and production. Science **314:**1565-8.

Andersen, K. B., and K. von Meyenburg. 1980. Are growth rates of Escherichia coli in batch cultures limited by respiration? J Bacteriol **144:**114-23.

Andersen, H. W., C. Solem, K. Hammer, and P. R. Jensen. 2001. Twofold reduction of phosphofructokinase activity in Lactococcus lactis results in strong decreases in growth rate and in glycolytic flux. J Bacteriol **183:**3458-67.

Aristidou, A. A., K. Y. San, and G. N. Bennett. 1995. Metabolic engineering of Escherichia coli to enhance recombinant protein production through acetate reduction. Biotechnol Prog **11:**475-8.

Aymerich, S., G. Gonzy-Treboul, and M. Steinmetz. 1986. 5'-noncoding region sacR is the target of all identified regulation affecting the levansucrase gene in Bacillus subtilis. J Bacteriol **166:**993-8.

Bailey, J. E. 1991. Toward a science of metabolic engineering. Science **252:**1668-75.

Banerjee-Bhatnagar, N. 1998. Modulation of Cry IV A toxin protein expression by glucose in Bacillus thuringiensis israelensis. Biochem Biophys Res Commun **252:**402-6.

Beppu, T. 2000. Development of applied microbiology to modern biotechnology in Japan. Adv Biochem Eng Biotechnol **69:**41-70.

Bergmeyer, H. U. 1983. Methods of Enzymatic Analysis, 3rd ed.

Blangy, D., H. Buc, and J. Monod. 1968. Kinetics of the allosteric interactions of phosphofructokinase from Escherichia coli. J Mol Biol **31:**13-35.

Blattner, F. R., G. Plunkett, 3rd, C. A. Bloch, N. T. Perna, V. Burland, M. Riley, J. Collado-Vides, J. D. Glasner, C. K. Rode, G. F. Mayhew, J. Gregor, N. W. Davis, H. A. Kirkpatrick, M. A. Goeden, D. J. Rose, B. Mau, and Y. Shao. 1997. The complete genome sequence of Escherichia coli K-12. Science **277:**1453-74.

Bruckner, R. 1992. A series of shuttle vectors for Bacillus subtilis and Escherichia coli. Gene **122:**187-92.

Buhler, B., B. Witholt, B. Hauer, and A. Schmid. 2002. Characterization and application of xylene monooxygenase for multistep biocatalysis. Appl Environ Microbiol **68:**560-8.

Chen, R., V. Hatzimanikatis, W. M. Yap, P. W. Postma, and J. E. Bailey. 1997. Metabolic consequences of phosphotransferase (PTS) mutation in a phenylalanine-producing recombinant Escherichia coli. Biotechnol Prog **13:**768-75.

Chou, C. H., G. N. Bennett, and K. Y. San. 1994. Effect of modified glucose uptake using genetic engieering techniques on high-level recombinant protein production in *Escherichia coli* dense cultures. Biotechnol Bioeng **44:**952-960.

De Anda, R., A. R. Lara, V. Hernandez, V. Hernandez-Montalvo, G. Gosset, F. Bolivar, and O. T. Ramirez. 2006. Replacement of the glucose phosphotransferase transport system by galactose permease reduces acetate accumulation and improves process performance of Escherichia coli for recombinant protein production without impairment of growth rate. Metab Eng **8:**281-90.

Dedhia, N. N., T. Hottiger, and J. E. Baily. 1994. Overexproduction of glycogen in *E. coli* blocked in the acetate pathway improves cell growth. Biotechnol Bioeng **44:**132-139.

Demain, A. L., and J. Birnbaum. 1968. Alteration of permeability for the release of metabolites from the microbial cell. Curr Top Microbiol Immunol **46:**1-25.

De Wulf, P., and E. J. Vandamme. 1997. Production of D-ribose by fermentation. Appl Microbiol Biotechnol **48:**141-8.

Diaz-Ricci, J. C., L. Regan, and J. E. Bailey. 1991. Effect of alteration of acetic acid biosynthesis pathway in the fermentation pattern of E. coli. Biotechnol Bioeng **38:**1318-1324.

Doelle, H. W., K. N. Ewings, and N. W. Hollywood. 1982. Regulation of glucose metabolism in bacterial systems. Adv Biochem Eng **23:**1-35.

Eichler, K., C. Vockler, R. Carballido-Lopez, and A. P. G. M. van Loon. 1997. Investigation of the biotechnological potential of folic acid biosynthesis in Bacillus subtilis. 9th international conference on Bacilli., Lausanne, Switzerland.

Evans, P. R., and P. J. Hudson. 1979. Structure and control of phosphofructokinase from Bacillus stearothermophilus. Nature **279:**500-4.

Farmer, W. R., and J. C. Liao. 1997. Reduction of aerobic acetate production by Escherichia coli. Appl Environ Microbiol **63:**3205-10.

Fieschko, J., and T. Ritch. 1986. Production of Human Alpha Consensus Interferon in Recombinant Escherichia coli. Chem. Eng. Comm. **45:**229-240.

Fisher, S. H., and B. Magasanik. 1984. Synthesis of oxaloacetate in Bacillus subtilis mutants lacking the 2-ketoglutarate dehydrogenase enzymatic complex. J Bacteriol **158:**55-62.

114

Fry, B., T. Zhu, M. M. Domach, R. R. Koepsel, C. Phalakornkule, and M. M. Ataai. 2000. Characterization of growth and acid formation in a Bacillus subtilis pyruvate kinase mutant. Appl Environ Microbiol **66:**4045-9.

Gerigk, M., R. Bujnicki, E. Ganpo-Nkwenkwa, J. Bongaerts, G. Sprenger, and R. Takors. 2002. Process control for enhanced L-phenylalanine production using different recombinant Escherichia coli strains. Biotechnol Bioeng **80:**746-54.

Giovannucci, E., M. J. Stampfer, G. A. Colditz, D. J. Hunter, C. Fuchs, B. A. Rosner, F. E. Speizer, and W. C. Willett. 1998. Multivitamin use, folate, and colon cancer in women in the Nurses' Health Study. Ann Intern Med **129:**517-24.

Goel, A., J. Ferrance, and M. M. Ataai. 1993. Suppressed acid formation by cofeeding of glucose and citrate in Bacillus cultures: Emergence of pyruvate kinase as a potential metabolic engineering site. Biotechnol Bioeng **80:**746-754.

Goel, A., J. Lee, M. M. Domach, and M. M. Ataai. 1995. Suppressed acid formation by cofeeding of glucose and citrate in Bacillus cultures: emergence of pyruvate kinase as a potential metabolic engineering site. Biotechnol Prog **11:**380-5.

Goel, A., M. M. Domach, W. Hanley, J. W. Lee, and M. M. Ataai. 1996. Coordination of glycolysis and TCA cycle reaction networks. Citrate-glucose cometabolism eliminates acids and reveals potential metabolic engineering strategies. Ann N Y Acad Sci **782:**1-16.

Goel, A., J. Lee, M. M. Domach, and M. M. Ataai. 1999. Metabolic fluxes, pools, and enzyme measurements suggest a tighter coupling of energetics and biosynthetic reactions associated with reduced pyruvate kinase flux. Biotechnol Bioeng **64:**129-34.

Gottschalk, G. 1985. Bacterial Metabolism, Second ed. Springer Verlag.

Gray, C. T., J. W. Wimpenny, and M. R. Mossman. 1966. Regulation of metabolism in facultative bacteria II. Effects of aerobiosis, anaerobiosis and nutrition on the formation of Krebs cycle enzymes in E. coli. Biochem. Biophys. Acta **117:**33-41.

Hahm, D. H., J. Pan, and J. S. Rhee. 1994. Characterization and evaluation of a pta (phosphotransacetylase) negative mutant of Escherichia coli HB101 as production host of foreign lipase. Appl Microbiol Biotechnol **42:**100-7.

Han, C. S., G. Xie, J. F. Challacombe, M. R. Altherr, S. S. Bhotika, N. Brown, D. Bruce, C. S. Campbell, M. L. Campbell, J. Chen, O. Chertkov, C. Cleland, M. Dimitrijevic, N. A. Doggett, J. J. Fawcett, T. Glavina, L. A. Goodwin, L. D. Green, K. K. Hill, P. Hitchcock, P. J. Jackson, P. Keim, A. R. Kewalramani, J. Longmire, S. Lucas, S. Malfatti, K. McMurry, L. J. Meincke, M. Misra, B. L. Moseman, M. Mundt, A. C. Munk, R. T. Okinaka, B. Parson-Quintana, L. P. Reilly, P. Richardson, D. L. Robinson, E. Rubin, E. Saunders, R. Tapia, J. G. Tesmer, N. Thayer, L. S. Thompson, H. Tice, L. O. Ticknor, P. L. Wills, T. S. Brettin, and P. Gilna. 2006. Pathogenomic sequence analysis of Bacillus cereus and Bacillus thuringiensis isolates closely related to Bacillus anthracis. J Bacteriol **188:**3382-90.

Han, K., H. C. Lim, and J. Hong. 1992. Acetic acid formation in Escherichia coli fermentation. Biotechnol Bioeng **39:**663-671.

Hanson, R. S., and D. P. Cox. 1967. Effect of different nutritional conditions on the synthesis of tricarboxylic acid cycle enzymes. J Bacteriol **93:**1777-87.

Hansen, T., M. Musfeldt, and P. Schonheit. 2002. ATP-dependent 6-phosphofructokinase from the hyperthermophilic bacterium Thermotoga maritima: characterization of an extremely thermophilic, allosterically regulated enzyme. Arch Microbiol **177:**401-9.

Hatakeyama, K., K. Hohama, A. A. Vertes, M. Kobayashi, Y. Kurusu, and H. Yukawa. 1993. Genomic organization of the biotin biosynthetic genes of coryneform bacteria: cloning and sequencing of the bioA-bioD genes from Brevibacterium flavum. DNA Seq **4:**177-84.

Hatakeyama, K., K. Kohama, A. A. Vertes, M. Kobayashi, Y. Kurusu, and H. Yukawa. 1993. Analysis of the biotin biosynthesis pathway in coryneform bacteria: cloning and sequencing of the bioB gene from Brevibacterium flavum. DNA Seq **4:**87-93.

Hayashi, T., K. Makino, M. Ohnishi, K. Kurokawa, K. Ishii, K. Yokoyama, C. G. Han, E. Ohtsubo, K. Nakayama, T. Murata, M. Tanaka, T. Tobe, T. Iida, H. Takami, T. Honda, C. Sasakawa, N. Ogasawara, T. Yasunaga, S. Kuhara, T. Shiba, M. Hattori, and H. Shinagawa. 2001. Complete genome sequence of enterohemorrhagic Escherichia coli O157:H7 and genomic comparison with a laboratory strain K-12. DNA Res **8:**11-22.

Hintze, D. N., and J. L. Farmer. 1975. Identification of poly-gamma-glutamyl chain lengths in folates of Bacillus subtilis. J Bacteriol **124:**1236-9.

Hoischen, C., and R. Kramer. 1990. Membrane alteration is necessary but not sufficient for effective glutamate secretion in Corynebacterium glutamicum. J Bacteriol **172:**3409-16.

Hoskins, J. R., and S. Wickner. 2006. Two peptide sequences can function cooperatively to facilitate binding and unfolding by ClpA and degradation by ClpAP. Proc Natl Acad Sci U S A **103:**909-14.

Huang, H., D. Ridgway, T. Gu, and M. Moo-Young. 2004. Enhanced amylase production by Bacillus subtilis using a dual exponential feeding strategy. Bioprocess Biosyst Eng **27:**63-9.

Ingledew, W. J., and R. K. Poole. 1984. The respiratory chains of Escherichia coli. Microbiol Rev **48:**222-71.

Iwai, K., M. Kobashi, and H. Fujisawa. 1970. Occurrence of Crithidia factors and folic acid in various bacteria. J Bacteriol **104:**197-201.

Jensen, E. B., and S. Carlsen. 1990. Production of recombinant human growth hormone in Escherichia coli: Expression of different precursors and physiological effects of glucose, acetate, and salts. Biotechnol Bioeng **36:**1-11.

Jetten, M. S., and A. J. Sinskey. 1995. Purification and properties of oxaloacetate decarboxylase from Corynebacterium glutamicum. Antonie Van Leeuwenhoek **67:**221-7.

Johnston, W. A., M. Stewart, P. Lee, and M. J. Cooney. 2003. Tracking the acetate threshold using DO-transient control during medium and high cell density cultivation of recombinant Escherichia coli in complex media. Biotechnol Bioeng **84:**314-23.

Kinoshita, S., and K. Nakayama. 1978. Amino acids., vol. 2. Academic Press, London.

Kinoshita, S., S. Udaka, and M. Shimono. 1957a. Studies on the amino acid fermentations, part 1. Production of L-Glu. acid by various microorganisms. J. Gen. Appl. Micro. **3:**193-205.

Landwall, P., and T. Holme. 1977. Removal of inhibitors of bacterial growth by dialysis culture. J Gen Microbiol **103:**345-52.

Lardy, H. A., and R. Peanasky. 1953. Metabolic functions of biotin. Physiol Rev **33:**560-5.

Lasko, D. R., N. Zamboni, and U. Sauer. 2000. Bacterial response to acetate challenge: a comparison of tolerance among species. Appl Microbiol Biotechnol **54:**243-7.

Lee, J., A. Goel, M. M. Ataai, and M. M. Domach. 1997. Supply-side analysis of growth of Bacillus subtilis on glucose-citrate medium: feasible network alternatives and yield optimality. Appl Environ Microbiol **63:**710-718.

Lehming, N., J. Sartorius, M. Niemoller, G. Genenger, B. v Wilcken-Bergmann, and B. Muller-Hill. 1987. The interaction of the recognition helix of lac repressor with lac operator. Embo J **6:**3145-53.

Lo, T. W., M. E. Westwood, A. C. McLellan, T. Selwood, and P. J. Thornalley. 1994. Binding and modification of proteins by methylglyoxal under physiological conditions. A kinetic and mechanistic study with N alpha-acetylarginine, N alpha-acetylcysteine, and N alpha-acetyllysine, and bovine serum albumin. J Biol Chem **269:**32299-305.

Lowry, O. H., and J. V. Passonneau. 1972. A flexible system of enzymatic analysis. Academic Press, NY.

Luli, G. W., and W. R. Strohl. 1990. Comparison of growth, acetate production, and acetate inhibition of Escherichia coli strains in batch and fed-batch fermentations. Appl Environ Microbiol **56:**1004-11.

Lynen, F., J. Knappe, E. Lorch, G. Juetting, E. Ringelmann, and J. P. Lachance. 1961. [On the biochemical function of biotin. II. Purification and mode of action of beta-methyl-crotonyl-carboxylase.]. Biochem Z **335:**123-67.

Majewski, R. A., and M. M. Domach. 1990. Simple constrained-optimization view of acetate overflow in E. coli. Biotechnol Bioeng **35:**732-738.

March, J. C., M. A. Eiteman, and E. Altman. 2002. Expression of an anaplerotic enzyme, pyruvate carboxylase, improves recombinant protein production in Escherichia coli. Appl Environ Microbiol **68:**5620-4.

Martin, V. J., D. J. Pitera, S. T. Withers, J. D. Newman, and J. D. Keasling. 2003. Engineering a mevalonate pathway in Escherichia coli for production of terpenoids. Nat Biotechnol **21:**796-802.

McMahon, R. J. 2002. Biotin in metabolism and molecular biology. Annu Rev Nutr **22:**221-39.

Miyata, Reiko, Yonehara, and Tetsu. 1999. Method for producing folic acid. patent 5968788.

Morita, T., W. El-Kazzaz, Y. Tanaka, T. Inada, and H. Aiba. 2003. Accumulation of glucose 6-phosphate or fructose 6-phosphate is responsible for destabilization of glucose transporter mRNA in Escherichia coli. J Biol Chem 278:15608-14.

Nakamura, C. E., and G. M. Whited. 2003. Metabolic engineering for the microbial production of 1,3-propanediol. Curr Opin Biotechnol **14:**454-9.

Nakano, S., G. Zheng, M. M. Nakano, and P. Zuber. 2002. Multiple pathways of Spx (YjbD) proteolysis in Bacillus subtilis. J Bacteriol **184:**3664-70.

Nakao, Y., T. Kanamaru, M. Kikuchi, and S. Yamatodani. 1973. Extracellular accumulation of phospholipids, UDP-N-acetylhexosamine derivatives and L-glutamic acid by penicillin treated *Corynebacrerium alkanolyticum*. Agri. Biol. Chem. **37:**2399-2404.

Nakao, Y., M. Kikuchi, M. Suzuki, and M. Dio. 1972. Microbial production of L-glutamic acid by glycerol auxotrophs and production of L-glutamic acid from n-paraffins. Agri. Biol. Chem. **36:**490-496.

Neidhardt, F. C., J. L. Ingraham, and M. Schaechter. 1990. Physiology of the bacterial cell: a molecular approach. Sinauer Associates Inc., Sunderland, MA.

Nielsen, J. 2001. Metabolic engineering. Appl Microbiol Biotechnol **55:**263-83.

Oh, M. K., and J. C. Liao. 2000. Gene expression profiling by DNA microarrays and metabolic fluxes in Escherichia coli. Biotechnol Prog **16:**278-86.

Paalme, T., K. Tiisma, A. Kahru, K. Vanatalu, and R. Vilu. 1990. Glucose-limited fed-batch cultivation of *Escherichia coli* with computer-controlled fixed growth rate. Biotechnol Bioeng **35:**312-319.

Papoulis, A., Y. al-Abed, and R. Bucala. 1995. Identification of N2-(1-carboxyethyl)guanine (CEG) as a guanine advanced glycosylation end product. Biochemistry **34:**648-55.

Perkins, J. B., S. Bower, C. L. Howitt, R. R. Yocum, and J. Pero. 1996. Identification and characterization of transcripts from the biotin biosynthetic operon of Bacillus subtilis. J Bacteriol **178:**6361-5.1.

Perkins, J. B., A. Sloma, T. Hermann, K. Theriault, E. Zachgo, T. Erdenberger, N. Hammett, N. P. Chatterjeel, V. Williams, I. I., G. A. Rufo, R. Hatch, and J. Perol. 1999. Genetic engineering of *Bacillus subtilis* for the commercial production of riboflavin. J. Ind. Microbiol. Biotech. **22:**8-18.

Phalakornkule, C., B. Fry, T. Zhu, R. Kopesel, M. M. Ataai, and M. M. Domach. 2000. 13C NMR evidence for pyruvate kinase flux attenuation underlying suppressed acid formation in Bacillus subtilis. Biotechnol Prog **16:**169-75.

Pitera, D. J., C. J. Paddon, J. D. Newman, and J. D. Keasling. 2006. Balancing a heterologous mevalonate pathway for improved isoprenoid production in Escherichia coli. Metab Eng.

Pragai, Z., and C. R. Harwood. 2000. YsxC, a putative GTP-binding protein essential for growth of Bacillus subtilis 168. J Bacteriol **182:**6819-23.

Presecan-Siedel, E., A. Galinier, R. Longin, J. Deutscher, A. Danchin, P. Glaser, and I. Martin-Verstraete. 1999. Catabolite regulation of the pta gene as part of carbon flow pathways in Bacillus subtilis. J Bacteriol **181:**6889-97.

Roth, A. F., and W. W. Ward. 1983. Conformational stability after protease treatment in Aequorea GFP. Photochem Photobiol **37S**.

Sauer, U., D. C. Cameron, and J. E. Bailey. 1998. Metabolic capacity of Bacillus subtilis for the production of purine nucleosides, riboflavin, and folic acid. Biotechnol Bioeng **59:**227-38.

Scholz, O., A. Thiel, W. Hillen, and M. Niederweis. 2000. Quantitative analysis of gene expression with an improved green fluorescent protein. p6. Eur J Biochem **267:**1565-70.

Shuler, M. L., and F. Kargi. 2001. Bioprocess Engineering: Basic Concepts, 2nd edition ed. Prentic Hall.

Stephanopoulos, G. 1999. Metabolic fluxes and metabolic engineering. Metab Eng **1:**1-11.

Sybesma, W., M. Starrenburg, M. Kleerebezem, I. Mierau, W. M. de Vos, and J. Hugenholtz. 2003. Increased production of folate by metabolic engineering of Lactococcus lactis. Appl Environ Microbiol **69:**3069-76.

Udagawa, K., S. Abe, and S. Kinoshita. 1962. J. Ferment. Technol. **40:**614.

Vagner, V., E. Dervyn, and S. D. Ehrlich. 1998. A vector for systematic gene inactivation in Bacillus subtilis. Microbiology **144:**3097-3104.

van de Walle, M., and J. Shiloach. 1998. Proposed mechanism of acetate accumulation in two recombinant Escherichia coli strains during high density fermentation. Biotechnol Bioeng **57:**71-8.

Vemuri, G. N., E. Altman, D. P. Sangurdekar, A. B. Khodursky, and M. A. Eiteman. 2006. Overflow metabolism in Escherichia coli during steady-state growth: transcriptional regulation and effect of the redox ratio. Appl Environ Microbiol **72:**3653-61.

Vemuri, G. N., M. A. Eiteman, J. E. McEwen, L. Olsson, and J. Nielsen. 2007. Increasing NADH oxidation reduces overflow metabolism in Saccharomyces cerevisiae. Proc Natl Acad Sci U S A **104:**2402-7.

Vierheller, C., A. Goel, M. Peterson, M. M. Domach, and M. M. Ataai. 1995. Sustained and constitutive high levels of protein production in continuous cultures of *bacillus subtilis*. Biotechnol Bioeng **47:**520-524.

Vijayasankaran, N., R. Carlson, and F. Srienc. 2005. Metabolic pathway structures for recombinant protein synthesis in Escherichia coli. Appl Microbiol Biotechnol **68:**737-46.

Wang, D. I. C., C. L. Cooney, A. L. Demain, P. Dunnill, A. E. Humphrey, and M. D. Lilly. 1979. Fermentation and Enzyme Technology. Wiley-Interscience, New York.

Warner, J. B., B. P. Krom, C. Magni, W. N. Konings, and J. S. Lolkema. 2000. Catabolite repression and induction of the Mg(2+)-citrate transporter CitM of Bacillus subtilis. J Bacteriol **182:**6099-105.

Weber, J., A. Kayser, and U. Rinas. 2005. Metabolic flux analysis of Escherichia coli in glucose-limited continuous culture. II. Dynamic response to famine and feast, activation of the methylglyoxal pathway and oscillatory behaviour. Microbiology **151:**707-16.

Wehrl, W., M. Niederweis, and W. Schumann. 2000. The FtsH protein accumulates at the septum of Bacillus subtilis during cell division and sporulation. J Bacteriol **182:**3870-3.

Wessman, G. E., and C. H. Werkman. 1950. Biotin in the assimilation of heavy carbon in Oxalacetate. Arch Biochem **26:**214-8.

Westers, L., H. Westers, and W. J. Quax. 2004. Bacillus subtilis as cell factory for pharmaceutical proteins: a biotechnological approach to optimize the host organism. Biochim Biophys Acta **1694:**299-310.

Willecke, K., and A. B. Pardee. 1971. Inducible transport of citrate in a Gram-positive bacterium, Bacillus subtilis. J Biol Chem **246:**1032-40.

Wong, S. L. 1995. Advances in the use of Bacillus subtilis for the expression and secretion of heterologous proteins. Curr Opin Biotechnol **6:**517-22.

Yamamoto, H., M. Murata, and J. Sekiguchi. 2000. The CitST two-component system regulates the expression of the Mg-citrate transporter in Bacillus subtilis. Mol Microbiol **37:**898-912.

Yang, Y. T., A. A. Aristidou, K. Y. San, and G. N. Bennett. 1999. Metabolic flux analysis of Escherichia coli deficient in the acetate production pathway and expressing the Bacillus subtilis acetolactate synthase. Metab Eng **1:**26-34.

Yang, Y. T., G. N. Bennett, and K. Y. San. 1999. Effect of inactivation of nuo and ackA-pta on redistribution of metabolic fluxes in Escherichia coli. Biotechnol Bioeng **65:**291-7.

Yang, M., A. de Saizieu, A. P. van Loon, and P. Gollnick. 1995. Translation of trpG in Bacillus subtilis is regulated by the trp RNA-binding attenuation protein (TRAP). J Bacteriol **177:**4272-8.

Yoon, S. K., W. K. Kang, and T. H. Park. 1994. Fed-batch operation of recombinant *Escherichia coli* containing trp promoter with controlled specific growth rate. Biotechnol Bioeng **43:**995-999.

Zamboni, N., H. Maaheimo, T. Szyperski, H. P. Hohmann, and U. Sauer. 2004. The phosphoenolpyruvate carboxykinase also catalyzes C3 carboxylation at the interface of glycolysis and the TCA cycle of Bacillus subtilis. Metab Eng **6:**277-84.

Zhu, T., C. Phalakornkule, R. R. Koepsel, M. M. Domach, and M. M. Ataai. 2001. Cell growth and by-product formation in a pyruvate kinase mutant of E. coli. Biotechnol Prog **17:**624-8.

Zhu, T., C. Phalakornkule, S. Ghosh, I. E. Grossmann, R. R. Koepsel, M. M. Ataai, and M. M. Domach. 2003. A metabolic network analysis & NMR experiment design tool with user interface-driven model construction for depth-first search analysis. Metab Eng **5:**74-85.

Zhu, T., Z. Pan, N. Domagalski, R. Koepsel, M. M. Ataai, and M. M. Domach. 2005. Engineering of Bacillus subtilis for enhanced total synthesis of folic acid. Appl Environ Microbiol **71:**7122-9.